34336

National Library of Canada / Bibliothèque nationale du Canada

CANADIAN THESES ON MICROFICHE / THÈSES CANADIENNES SUR MICROFICHE

NAME OF AUTHOR/NOM DE L'AUTEUR BRIAN PATRICK ERNO

TITLE OF THESIS/TITRE DE LA THÈSE KINETIC STUDIES OF THE FORMATION AND DECOMPOSITION OF MULTIDENTATE TRANSITION METAL COMPLEXES

UNIVERSITY/UNIVERSITÉ UNIVERSITY OF ALBERTA

DEGREE FOR WHICH THESIS WAS PRESENTED/ GRADE POUR LEQUEL CETTE THÈSE FUT PRÉSENTÉE Ph. D.

YEAR THIS DEGREE CONFERRED/ANNÉE D'OBTENTION DE CE GRADE 1977

NAME OF SUPERVISOR/NOM DU DIRECTEUR DE THÈSE DR. R. B. JORDAN

Permission is hereby granted to the NATIONAL LIBRARY OF CANADA to microfilm this thesis and to lend or sell copies of the film.

The author reserves other publication rights, and neither the thesis nor extensive extracts from it may be printed or otherwise reproduced without the author's written permission.

L'autorisation est, par la présente, accordée à la BIBLIOTHÈQUE NATIONALE DU CANADA de microfilmer cette thèse et de prêter ou de vendre des exemplaires du film.

L'auteur se réserve les autres droits de publication; ni la thèse ni de longs extraits de celle-ci ne doivent être imprimés ou autrement reproduits sans l'autorisation écrite de l'auteur.

DATED/DATÉ May 20 1977 SIGNED/SIGNÉ Brian Erno

PERMANENT ADDRESS/RÉSIDENCE FIXÉ #18 - 125 COLUMBIA BLVD.
LETHBRIDGE ALBERTA

NL-91 (3-74)

National Library of Canada

Cataloguing Branch
Canadian Theses Division

Ottawa, Canada
K1A 0N4

Bibliothèque nationale du Canada

Direction du catalogage
Division des thèses canadiennes

NOTICE

The quality of this microfiche is heavily dependent upon the quality of the original thesis submitted for microfilming. Every effort has been made to ensure the highest quality of reproduction possible.

If pages are missing, contact the university which granted the degree.

Some pages may have indistinct print especially if the original pages were typed with a poor typewriter ribbon or if the university sent us a poor photocopy.

Previously copyrighted materials (journal articles, published tests, etc.) are not filmed.

Reproduction in full or in part of this film is governed by the Canadian Copyright Act, R.S.C. 1970, c. C-30. Please read the authorization forms which accompany this thesis.

THIS DISSERTATION
HAS BEEN MICROFILMED
EXACTLY AS RECEIVED

AVIS

La qualité de cette microfiche dépend grandement de la qualité de la thèse soumise au microfilmage. Nous avons tout fait pour assurer une qualité supérieure de reproduction.

S'il manque des pages, veuillez communiquer avec l'université qui a conféré le grade.

La qualité d'impression de certaines pages peut laisser à désirer, surtout si les pages originales ont été dactylographiées à l'aide d'un ruban usé ou si l'université nous a fait parvenir une photocopie de mauvaise qualité.

Les documents qui font déjà l'objet d'un droit d'auteur (articles de revue, examens publiés, etc.) ne sont pas microfilmés.

La reproduction, même partielle, de ce microfilm est soumise à la Loi canadienne sur le droit d'auteur, SRC 1970, c. C-30. Veuillez prendre connaissance des formules d'autorisation qui accompagnent cette thèse.

LA THÈSE A ÉTÉ
MICROFILMÉE TELLE QUE
NOUS L'AVONS REÇUE

THE UNIVERSITY OF ALBERTA

KINETIC STUDIES OF THE FORMATION AND DECOMPOSITION OF MULTIDENTATE TRANSITION METAL COMPLEXES

by

© BRIAN PATRICK ERNO

A THESIS

SUBMITTED TO THE FACULTY OF GRADUATE STUDIES

IN PARTIAL FULFILMENT OF THE REQUIREMENTS FOR THE DEGREE

OF DOCTOR OF PHILOSOPHY

DEPARTMENT OF CHEMISTRY

EDMONTON, ALBERTA

FALL 1977

UNIVERSITY OF ALBERTA

FACULTY OF GRADUATE STUDIES

The undersigned certify that they have read, and recommend to the Faculty of Graduate Studies for acceptance a thesis entitled

"KINETIC STUDIES OF THE FORMATION AND DECOMPOSITION OF MULTIDENTATE TRANSITION METAL COMPLEXES"

submitted by Brian Patrick Erno in partial fulfilment of the requirements for the degree of Doctor of Philosophy.

Roland B Jordan
.....
Supervisor

Joel Tobias
.....

H B Dunford
.....

Lloyd Kotowycz
.....

W Mansfield
.....

F W Wardlaw
.....
External Examiner

May 18 1977.

To Marianne

ABSTRACT

The rates of formation and decomposition of *cis*-$(en)_2Co(OH_2)(CO_3H)^{+2}$ and its conjugate bases have been investigated in the pH range 1-7 by the stopped-flow method. Loss of CO_2 occurs predominantly through the fully protonated species, *cis*-$(en)_2Co(OH_2)(CO_3H)^{+2}$, and the rate constant and activation parameters of this process are indicative of C-O rather than Co-O bond-breaking. Ring-closure of the monodentate complexes to form $(en)_2CoCO_3^+$ has also been studied. Only *cis*-$(en)_2Co(OH_2)(CO_3)^+$ undergoes chelate ring-closure at a measurable rate, and the rate constant is indicative of C-O bond-making. The monodentate carbonato complexes are formed mainly by the reaction of CO_2 with *cis*-$(en)_2Co(OH_2)(OH)^{+2}$. The pH dependence of the rates allowed the acid dissociation constants of *cis*-$(en)_2Co(OH_2)(CO_3H)^{+2}$ to be determined.

It was found that histidine reacts with a stable tridentate Schiff base complex of nickel(II) ($NiTRI(OH_2)_3^{+2}$) in a stereoselective way. This reaction was used to resolve the optical isomers of $NiTRI(OH_2)_3^{+2}$.

Kinetic studies of the reactions of $NiTRI(OH_2)_3^{+2}$ with histidine, 3-methylhistidine, histamine, and histidine methyl ester indicate that initial complexing occurs

with the imidazole nitrogen followed by ring-closure of the deprotonated amine nitrogen to give a bidentate complex. The rate constants for formation of the monodentate complexes were determined as well as rate constants for ring-opening of the bidentate complexes. The rate of reaction with histidine appears to be independent of the optical isomer used despite the stereoselectivity of the reaction products. This indicates that the stereoselectivity results from interactions after the rate-determining step in complex formation.

Studies of the reactions of $NiTRI(OH_2)_3^{+2}$ with glycine and 1-methylhistidine gave overall rate constants for the formation and decomposition processes. The rate constants could not be reduced to values for specific reaction paths in an unequivocal way. The rates of the reactions of $Ni(OH_2)_6^{+2}$ with histidine and α-N,N,N-trimethylhistidine were studied.

Several mechanisms are proposed for bidentate chelation to a metal ion, and these are discussed and analysed in detail. The restrictions imposed by the ion pair dissociative mechanism are emphasized. The interpretation of the rate laws indicates that the rate-determining step for the process of chelate formation changes from ring-closure

to initial bond formation as the pH is increased.

The denticity of several multidentate ligands coordinated to $NiTRI^{+2}$ was investigated by an nmr titration method. There is evidence of incomplete ring-closure in the histamine complex with $NiTRI(OH_2)_3^{+2}$ in the region of pH = 6.2.

A comparison of the rate constants for analogous $NiTRI(OH_2)_3^{+2}$ and $Ni(OH_2)_6^{+2}$ systems shows that the formation rate constants are quite similar but dissociation rate constants are larger for the TRI complexes. These observations are consistent with a dissociative formation mechanism and steric acceleration by TRI in the dissociative steps.

ACKNOWLEDGMENTS

I wish to express my gratitude to Dr. Robert B. Jordan for his encouragement and excellent guidance during this work.

I want to thank my parents, Pat and Dick Erno, for their love and support throughout my years of study.

To my wife, Marianne, I would like to express my most sincere thanks for her love and continual encouragement. I also thank my children, Jennifer, Catherine, and our new baby, Michelle, for giving up time which was rightfully theirs, particularly in these last months.

Financial assistance from the University of Alberta and the National Research Council of Canada is gratefully acknowledged.

TABLE OF CONTENTS

Page

Abstract v

Acknowledgements viii

List of Tables xii

List of Figures xv

CHAPTER I The Formation and Decomposition of carbonato-aquo-*bis*-(ethylenediamine)cobalt(III) ion

INTRODUCTION 1

EXPERIMENTAL 6

Materials 6

Kinetic Instrumentation 8

Kinetic Measurement of the Rate of Decarboxylation 10

Kinetic Measurement of the Rate of Isomerization 10

Kinetic Measurement of Carboxylation and Ring-Closure 11

Treatment of Kinetic Data 12

RESULTS AND DISCUSSION 17

Decarboxylation 17

Isomerization 31

Page

Carboxylation and Chelate Ring-Closure 37

Chelate Ring-Closure 47

CONCLUSION 53

Decarboxylation 53

Isomerization 56

Carboxylation 57

Chelate Ring-Closure 61

CHAPTER II Complex Formation Reactions of Nickel(II)

INTRODUCTION 65

EXPERIMENTAL 76

Materials 76

Resolution of $NiTRI(OH_2)_3^{+2}$ 81

-Ion Exchange Method 81

-Precipitation Method 82

Determination of the Acid Dissociation Constant of Hercynine 84

Kinetic Measurements 84

NMR Measurements 86

RESULTS AND DISCUSSION 89

Resolution of $NiTRI(OH_2)_3^{+2}$ 89

Acid Dissociation Constants 98

Page

Kinetics and Mechanisms 100

- The reaction of $NiTRI(OH_2)_3^{+2}$ with histidine 100

- The reaction of $NiTRI(OH_2)_3^{+2}$ with 3-methylhistidine 127

- The reaction of $NiTRI(OH_2)_3^{+2}$ with histamine 131

- The reaction of $NiTRI(OH_2)_3^{+2}$ with histidine methyl ester 134

- The reaction of $Ni(OH_2)_6^{+2}$ with histidine . 139

- The reaction of $Ni(OH_2)_6^{+2}$ with hercynine . 143

- The reaction of $NiTRI(OH_2)_3^{+2}$ with glycine 147

- The reaction of $NiTRI(OH_2)_3^{+2}$ with 1-methylhistidine 154

Nuclear Magnetic Resonance Measurements 161

CONCLUSION 168

REFERENCES 193

APPENDIX A The Method of Linear Least-Squares using Relative Residuals 199

APPENDIX B Derivations of the Rate Laws for the Mechanisms in Chapter I 205

APPENDIX C Derivations of the Rate Laws for the Mechanisms in Chapter II 211

LIST OF TABLES

Table		Page
1.	Molar Absorptivity of $(en)_2CoCO_3^+$	7
2.	Acid Dissociation Constants of Buffers	8
3.	Observed Rate Coefficients for the Decarboxylation Reaction	24
4.	Observed Rate Coefficients for *cis-trans* Isomerization	32
5.	Rate and Equilibrium Constants for aquo Cobalt(III) Species	34
6.	Observed Rate Coefficients for Carboxylation	40
7.	A Summary of the Results of Computer Fits of the Carboxylation Data	45
8.	A Comparison of the Observed and Calculated Rate Coefficients for Carboxylation	46
9.	Observed Rate Coefficients for Chelate Ring-Closure	49
10.	A Summary of the Results of Computer Fits of the Ring-Closure Data	52

Table		Page
11.	A Comparison of the Kinetic Parameters for Decarboxylation of Monodentate Carbonato Complexes	54
12.	Rate Constants for Ring-Closure of Cobalt(III) Complexes	62
13.	Apparent Optical Rotations of Eluent Fractions	91
14.	Observed Molecular Rotations of $NiTRI(OH_2)_3^{+2}$ Isomers	93
15.	Molecular Rotations of Resolved $NiTRI(OH_2)_3^{+2}$	94
16.	Analytical Results for the Precipitate	97
17.	Acid Dissociation Constants of the Ligands	99
18.	Observed Rate Coefficients for the Reaction of $NiTRI(OH_2)_3^{+2}$ with Histidine	102
19.	A Summary of the Data Fits for the Reaction of $NiTRI(OH_2)_3^{+2}$ with Histidine	113
20.	Observed Rate Coefficients for the Reaction of $NiTRI(OH_2)_3^{+2}$ with 3-methylhistidine	128
21.	Observed Rate Coefficients for the Reaction of $NiTRI(OH_2)_3^{+2}$ with Histamine	132

Table		Page
22.	Observed Rate Coefficients for the Reaction of $NiTRI(OH_2)_3^{+2}$ with Histidine Methyl Ester	135
23.	Observed Rate Coefficients for the Reaction of $Ni(OH_2)_6^{+2}$ with Histidine	140
24.	Observed Rate Coefficients for the Reaction of $Ni(OH_2)_6^{+2}$ with Hercynine	144
25.	Observed Rate Coefficients for the Reaction of $NiTRI(OH_2)_3^{+2}$ with Glycine	148
26.	Observed Rate Coefficients for the Reaction of $NiTRI(OH_2)_3^{+2}$ with 1-methylhistidine	156
27.	Results of nmr Titration of $NiTRI(OH_2)_3^{+2}$ with *L*-Histidine	163
28.	A Summary of nmr Titration Results for $NiTRI(OH_2)_3^{+2}$	166
29.	Kinetic Results for the Reactions of $NiTRI(OH_2)_3^{+2}$	172
30.	Kinetic Results for the Reactions of $Ni(OH_2)_6^{+2}$	176
31.	Kinetic Results for the Reactions of Several α-Amino acids with Nickel(II)	181
32.	Formation Constants for Nickel(II) Complexes	190

LIST OF FIGURES

Figure		Page
1.	Analysis of transmittance-time data.	14
2.	Consecutive scans of the electronic spectrum of 5 x 10^{-3}M $(en)_2CoCO_3^+$ in 0.20 M NaOH.	18
3.	Transmittance changes observed at 520 nm upon rapid neutralization of a solution of 10^{-3}M *cis*-$(en)_2Co(OH)(CO_3)$ and 10^{-3}M $NaHCO_3$ to pH 6.5.	20
4.	A comparison of the transmittance changes observed at 520 nm and 320 nm upon decarboxylation of *cis*-$(en)_2Co(OH_2)(CO_3H)^{+2}$.	21
5.	The pH dependence of k_{exp} for the decarboxylation of *cis*-$(en)_2Co(OH_2)(CO_3H)^{+2}$.	29
6.	A plot of k_{exp} *versus* $K_{a3}/(K_{a3} + (H^+))$ for the isomerization of *cis*-$(en)_2Co(OH_2)(OH)^{+2}$.	36
7.	Transmittance changes observed at 320 nm upon rapid neutralization of a solution of CO_2 and *cis*-$(en)_2Co(OH_2)_2^{+3}$ to pH 6.52.	38
8.	The pH dependence of k_{exp} for carboxylate chelate ring-closure.	48

Figure		Page
9.	The structure of the Schiff base complex $NiTRI(OH_2)_3^{+2}$.	73
10.	Electronic absorption spectra of solutions of $NiTRI(OH_2)_3^{+2}$ and *L*-histidine.	90
11.	ORD spectrum of $(+)_{436}$ $NiTRI(OH_2)_3^{+2}$.	95
12.	ORD spectrum of $(-)_{436}$ $NiTRI(OH_2)_3^{+2}$.	96
13.	Variation of k_{exp} with ligand concentration for the reaction of $NiTRI(OH_2)_3^{+2}$ with histidine at pH = 6.15.	105
14.	A plot of k_{exp} *versus* $L_t/(K_{a1} + (H^+))$ for the reaction of $Ni(OH_2)_6^{+2}$ with histidine.	141
15.	A plot of k_{exp} *versus* $[Ni(OH_2)_6^{+2}]/(K_{a1} + (H^+))$ for the reaction of $Ni(OH_2)_6^{+2}$ with hercynine.	145
16.	A plot of k_{exp} *versus* $L_t/(K_{a2} + (H^+))$ for the reaction of $NiTRI(OH_2)_3^{+2}$ with glycine.	150
17.	A plot of k_{exp} *versus* $L_t/(K_{a1} + (H^+))(K_{a2} + (H^+))$ for the reaction of $NiTRI(OH_2)_3^{+2}$ with 1-methylhistidine.	158
18.	Reaction coordinate diagrams illustrating the mechanism of chelation of a bidentate ligand.	185

CHAPTER I

INTRODUCTION

Carbon dioxide and its conjugate bases, the bicarbonate and carbonate ions, are among the simplest and most widely distributed chemical species found in nature. They are of fundamental importance to both the physical makeup of the earth and to the existence of life. As a result, they have been the subject of much study and discussion in the scientific literature.[1-7]

In recent years, the binding of carbon dioxide to metal ions has been a subject of some interest. Much of this interest centers around the function of the metal ion in the enzyme carbonic anhydrase,[2,3,4] which increases the rate of hydration of CO_2 by a factor of about 10^9. Zinc(II) is found in the native enzyme, but replacement by other metal ions has been accomplished, and the cobalt(II) enzyme also shows catalytic activity.[2]

Most of what is known about the binding of CO_2 with metal ions results from studies of carbonato complexes of cobalt(III). Because of their kinetic inertness, it has been possible to prepare a wide variety of these complexes, in which the carbonate ligand is either monodentate (e.g. carbonatopentaamminecobalt(III) ion, $(NH_3)_5CoCO_3^+$) or bidentate (e.g. carbonato-*bis*-(ethylenediamine)cobalt(III) ion, $(en)_2CoCO_3^+$).

Two reviews of the chemistry of carbonato complexes give a detailed survey of the work up to 1968.[6,7]

The hydrolysis of carbonatoaminecobalt(III) complexes has been the subject of a number of studies. For the monodentate complex, $(NH_3)_5CoCO_3^+$, in the pH region 1 to 8, the following mechanism has been proposed.[8]

$$(NH_3)_5CoCO_3H^{+2} + H_2O \underset{}{\overset{K_a}{\rightleftharpoons}} (NH_3)_5CoCO_3^+ + H_3O^+ \qquad (1.1)$$

$$(NH_3)_5CoCO_3H^{+2} \xrightarrow{k} (NH_3)_5CoOH^{+2} + CO_2 \qquad (1.2)$$

If the total reactant concentration is represented by

$$T = [(NH_3)_5CoCO_3H^{+2}] + [(NH_3)_5CoCO_3^+] \qquad (1.3)$$

and K_a[9] is assumed to be a rapid pre-equilibrium, then reactions (1.1) and (1.2) lead to the rate law

$$-\frac{dT}{dt} = \frac{k(H^+)\,T}{K_a + (H^+)} \qquad (1.4)$$

where (H^+) refers to the activity of the hydrogen ion. The values of K_a and k are 4×10^{-7} M and 1.25 s^{-1} respectively, at 25° and an ionic strength of 0.5 M($NaClO_4$).

Other monodentate carbonato complexes ($(NH_3)_5RhCO_3^+$ $(NH_3)_5IrCO_3^+$, $(en)_2(NH_3)CoCO_3^+$) appear to undergo hydrolysis in a similar manner, since they are found to have the same rate law, and their rate constants are similar.[10,11] Oxygen(18) labelling experiments have shown[12] that reaction (1.2) involves C-O bond-breaking, and therefore it is best described as a decarboxylation reaction.

In contrast with the results obtained for the monodentate complexes, the rate law for acid hydrolysis of bidentate carbonato complexes contains two terms, one independent of and the other first order in hydrogen ion concentration. The following reactions have been proposed to explain the kinetic results for the hydrolysis of $(en)_2CoCO_3^+$ [13,14] in the pH region 1-5.

$$(en)_2CoCO_3^+ + H_3O^+ \xrightarrow{k_1} cis\text{-}(en)_2Co(OH_2)(CO_3H)^{+2} \quad (1.5)$$

$$(en)_2CoCO_3^+ + H_2O \xrightarrow{k_{-3}} cis\text{-}(en)_2Co(OH)(CO_3H)^+ \quad (1.6)$$

$$cis\text{-}(en)_2Co(OH_2)(CO_3H)^{+2} + H_2O \xrightleftharpoons{K_{a1}} cis\text{-}(en)_2Co(OH)(CO_3H)^+ + H_3O^+ \quad (1.7)$$

$$cis\text{-}(en)_2Co(OH_2)(CO_3H)^{+2} \xrightarrow{k_2} cis\text{-}(en)_2Co(OH_2)(OH)^{+2} + CO_2 \quad (1.8)$$

$$cis\text{-}(en)_2Co(OH_2)_2^{+3} + H_2O \xrightleftharpoons{K_{a3}} cis\text{-}(en)_2Co(OH_2)(OH)^{+2} + H_3O^+ \quad (1.9)$$

The rate constants are numbered so as to be consistent with the later discussion. Harris and Sastri[14] assumed that the rate of ring-opening, by reactions (1.5) and (1.6), is slow relative to the rate of (1.8). With this assumption, and if it is assumed that the equilibria governed by K_{a1} and K_{a3} are rapidly maintained, then the

rate law is given by

$$\frac{-d[(en)_2CoCO_3^+]}{dt} = \{k_1(H^+) + k_{-3}\}[(en)_2CoCO_3^+] \qquad (1.10)$$

Values of $0.6M^{-1}s^{-1}$ and $1.2 \times 10^{-4}s^{-1}$ were reported for k_1 and k_{-3} respectively, at 25^o and an ionic strength of approximately 0.25M. If the rate of reaction (1.8) is similar to that of reaction (1.2), then ring-opening will be rate-determining, as was assumed by Harris and Sastri. This assumption will be tested in this present work.

It should be noted that the species *cis*-$(en)_2Co(OH)(CO_3H)^+$ in reaction (1.6) could be written in the tautomeric form, *cis*-$(en)_2Co(OH_2)(CO_3)^+$. There has been some vacillation in the literature on this point[15], and perhaps the best representation would show the proton shared between the hydroxo and carbonato oxygen atoms via intra-molecular hydrogen bonding.

The alkaline hydrolysis of $(en)_2CoCO_3^+$ has also been studied,[16] and the experimental rate law was found to be consistent with the reaction sequence (1.11)to (1.16).

$$(en)_2CoCO_3^+ + H_2O \underset{k_3}{\overset{k_{-3}}{\rightleftharpoons}} cis\text{-}(en)_2Co(OH)(CO_3H)^+ \qquad (1.11)$$

$$(en)_2CoCO_3^+ + OH^- \underset{k_4}{\overset{k_{-4}}{\rightleftharpoons}} cis\text{-}(en)_2Co(OH)(CO_3) \qquad (1.12)$$

$$cis\text{-}(en)_2Co(OH)(CO_3H)^+ \underset{}{\overset{K_{a2}}{\rightleftharpoons}} cis\text{-}(en)_2Co(OH)(CO_3) + H^+ \quad (1.13)$$

$$cis\text{-}(en)_2Co(OH)(CO_3) \underset{k_{-5}}{\overset{k_5}{\rightleftharpoons}} cis\text{-}(en)_2Co(OH)_2^+ + HCO_3^- \quad (1.14)$$

$$cis\text{-}(en)_2Co(OH)_2^+ \rightleftharpoons trans\text{-}(en)_2Co(OH)_2^+ \quad (1.15)$$

$$cis\text{-}(en)_2Co(OH)(CO_3) \rightleftharpoons trans\text{-}(en)_2Co(OH)(CO_3) \quad (1.16)$$

At 26° and an ionic strength of 1.0M($NaClO_4$), the values of $k_{-3}[H_2O]$, k_3 and k_{-4} were found to be 5.4×10^{-5} s^{-1}, 6.52×10^{-5} M^{-1} s^{-1}, and 3.17×10^{-3} M^{-1} s^{-1}, respectively.[16,17] Under the same conditions, k_5 has a value of approximately 4.6×10^{-5} M^{-1} s^{-1}.[16] The small amount of *trans* product observed was accounted for by reactions (1.15) and (1.16). An oxygen(18) study[17] showed that reaction (1.12) proceeds via Co-O bond breaking.

These results indicate that partial base hydrolysis of $(en)_2CoCO_3^+$ should be a convenient method for preparing solutions of the monodentate species, *cis*-$(en)_2Co(OH)(CO_3)$. It is the intention of this present work to study the kinetics of acid hydrolysis and possible ring-closure of the three monodentate carbonato species, *cis*-$(en)_2Co(OH_2)(CO_3H)^{+2}$, *cis*-$(en)_2Co(OH_2)(CO_3)^+$, and *cis*-$(en)_2Co(OH)(CO_3)$.

EXPERIMENTAL

Materials

Carbonato-*bis*-(ethylenediamine)cobalt(III) chloride, $(en)_2CoCO_3Cl$, was prepared as described previously by Schlessinger.[18] The product was recrystallized from hot water, and dried under vacuum over $CaSO_4$ for several days before use. *Analysis*. Calculated for $(en)_2Co(CO_3)Cl$: C, 22.0; H, 5.87; N,20.4. Found: C, 21.1; H, 5.72; N, 20.4.

The perchlorate salt of the complex was precipitated directly by mixing a warm saturated solution of $(en)_2Co(CO_3)Cl$ with a solution of sodium perchlorate. After cooling the solution, the precipitate was collected by filtration, washed with cold water, and dried under vacuum over $CaSO_4$. *Analysis*. Calculated for $(en)_2Co(CO_3)ClO_4$: C, 17.8; H, 4.76; N, 16.5. Found: C, 17.4; H, 4.84; N, 16.3.

The values of the molar absorptivity obtained from the electronic spectrum of a freshly prepared aqueous solution of $(en)_2Co(CO_3)ClO_4$ in 1 M $LiClO_4$ are in good agreement with those previously published, as shown in Table 1.

All solutions were prepared from water which was distilled twice in a glass apparatus. The second distillation was from alkaline permanganate.

Standard sodium hydroxide solutions were prepared by dilution of ampoules of concentrated reagent (J.T. Baker). Perchloric acid stock solutions were

Table 1

Molar Absorptivity of $(en)_2CoCO_3^+$

λ_{max} ,nm	ε_{max} $dm^3mol^{-1}cm^{-1}$	λ'_{max} ,nm	ε'_{max} $dm^3mol^{-1}cm^{-1}$	Reference
512	131.5	358	120.8	19[a]
516	136.0	363	123.7	16[a]
513	132.2	361	119.9	this work[b]

(a) Measured at 25° in 1 M $NaClO_4$.

(b) Measured at 23° in 1 M $LiClO_4$,<15 minutes after preparation of the solution.

prepared from concentrated reagent(70%, McArthur) by dilution, and were standardized against sodium hydroxide using bromothymol blue indicator. Stock solutions of lithium perchlorate were prepared from reagent grade material(G.F. Smith Co.). These solutions were filtered with a Millipore filter to remove insoluble material(<0.01%), and standardized by determining the amount of hydrogen ion released from a Dowex 50W-X8(100-200 mesh) cation exchange column, originally in the H^+ form. Analytical grade sodium carbonate and sodium bicarbonate were used as supplied(Matheson, Coleman, and Bell).

Stock solutions of the buffers sodium acetate (British Drug Houses), tri-sodium citrate(Fisher),

2-methoxypyridine(Aldrich), MES (2-(N-morpholino)ethanesulfonic acid)(Polysciences) and PIPES, (1,4-piperazino*bis*-(ethanesulfonic acid))(Polysciences) were prepared from the commercial materials as supplied. Aniline (Shawinigan, Reagent Grade) was purified by distillation in the presence of zinc dust. Stock solutions of aniline were prepared by dilution and used within several hours. The pK_a values used in ionic strength calculations are listed in Table 2.

Table 2

Acid Dissociation Constants of Buffers[a]

Buffer	pK_a	Reference
Acetate	4.8	(20)
Citrate	3.1,4.7,5.4	(20)
2-methoxy-pyridine	3.3	(20)
Aniline	4.6	(20)
MES	6.1	(21)
PIPES	6.8	(21)

(a) Values at 25°.

Kinetic Instrumentation

The kinetic data for the *cis-trans* isomerization of $(en)_2Co(OH_2)(OH)^{+2}$ were collected using a Cary Model 14 recording spectrophotometer. The temperature was

controlled at 25±0.5° by passing water from a thermostatted water bath through the metal cell holder.

All of the other kinetic data was obtained using a standard Aminco-Morrow stopped-flow apparatus. The curves of transmittance *versus* time were recorded on a Tektronix storage oscilloscope, and were permanently recorded on Polaroid film. The drive syringes on the stopped-flow apparatus were thermostatted at 26±0.5°, (except in the temperature study) with water circulated from a Colora constant temperature bath, the temperature of which was controlled by a Thermistemp Model 71 control device, with the thermistor probe mounted on the thermostatted housing of the drive syringes of the stopped-flow apparatus. The temperature was monitored with a Doric Model DS-100-T3 digital readout thermometer coupled with a copper-constantan thermocouple, which also was attached to the thermostatted housing of the stopped-flow apparatus. Both the thermistor probe and the thermocouple were shielded from air currents with insulation material.

In order to measure the pH of the product solutions, samples from 3-4 runs on the stopped-flow instrument were collected. The reported pH is the average of 2-3 such determinations. The pH was measured with a Metrohm Herisau pH meter and a Fisher combination micro-electrode. The electrode reference solution (KCl) was

replaced with 1.0M NaCl to prevent formation of insoluble $KClO_4$ in the solutions containing perchlorate ion. The pH meter was calibrated using standard buffer solutions (Fisher Certified).

Kinetic Measurement of the Rate of Decarboxylation

Solutions of *cis*-$(en)_2Co(OH)(CO_3)$ were prepared *in situ* by mixing a 20.0 ml aliquot of a 1.2×10^{-3}M stock solution of $(en)_2Co(CO_3)Cl$ with 5.00 ml of 1.00M NaOH, in a stoppered flask. After 30 minutes, this solution was mixed in the stopped-flow apparatus with a solution approximately 0.2M in $HClO_4$, and 0.16M in buffer. The concentration of the acid was adjusted so as to give the desired final pH after mixing. Lithium perchlorate was included in each solution, so that the ionic strength of the solutions before mixing was the same, and so that the product solutions would have an ionic strength of 1.0M. The concentration and type of buffer used in each kinetic run is given in Table 3.

Kinetic Measurement of the Rate of Isomerization

A stock solution of $(en)_2Co(OH_2)_2^{+3}$ was prepared by dissolving a weighed amount of $(en)_2CoCO_3Cl$ in dilute $HClO_4$, and flushing the solution with argon for several hours to remove the CO_2. After addition of MES buffer (0.04M) and $LiClO_4$, to give a final ionic strength of 1.0M, dilution to volume gave a solution of

8.79×10^{-3}M cobalt complex, at pH ≈ 3.

To begin a typical kinetic run, 6.0 ml of the diaquo stock solution were placed in a 2.00 cm cuvette, which was closed with a rubber serum cap. Then 20 to 50 µl of 3.95M NaOH was injected into the solution, so that the pH increased rapidly into the region of 6-7. After the reaction was complete, the pH of each run was measured. The decrease in absorbance at 510 nm was followed for at least five half-lives.

Kinetic Measurement of Carboxylation and Ring-Closing

Method 1

A solution of 3×10^{-4}M $(en)_2Co(CO_3)Cl$ in 0.2M $HClO_4$ was mixed in the stopped-flow apparatus with a solution of $NaHCO_3$ in 0.2M NaOH. The concentration of the $NaHCO_3$ was adjusted so as to give the desired pH after mixing, and the concentration of free CO_2 was determined from the known equilibrium constants of the carbonate system.

Method 2

An aliquot of 20 to 100 µl of 3.95M Na_2CO_3 solution was added to 25.0 ml of a stock solution of 2×10^{-4}M $(en)_2Co(OH_2)_2^{+3}$, prepared by dissolving a known amount of $(en)_2CoCO_3Cl$ in 10^{-3}M $HClO_4$. This solution was mixed in the stopped-flow apparatus with a solution of 0.16M buffer (MES or PIPES), and enough sodium hydroxide to give the desired final pH in the region of 5.4 to 7.2.

Since the acidic solutions of carbonate tended to give off CO_2 on standing, they were used as rapidly as possible after preparation. The concentrations of several of these reactant solutions of CO_2 were checked by adding an excess of standard carbonate-free sodium hydroxide to an aliquot of the reactant solution, and back titrating with standard $HClO_4$ solution to the bromocresol green end-point. The CO_2 concentration determined in this way was found to agree within 5% of the concentration determined from the amount of Na_2CO_3 added.

All reactant solutions contained enough $LiClO_4$ to give a final ionic strength after mixing of 1.0M.

Treatment of Kinetic Data

Throughout the course of this research, several different techniques were used to analyse the kinetic data more efficiently. The rate constants for *cis-trans* isomerization were determined from the slopes of plots of the logarithm of the absorbance change *versus* time. The plots of these data were linear for at least 90 % of reaction.

The data from the stopped-flow apparatus are in the form of oscilloscope traces of % transmittance *versus* time. The absorbance, A, is related to % transmittance, T, by

$$A = \log\left(\frac{100}{T}\right) = 2 - \log T \qquad (1.17)$$

For a reaction in which the absorbance is proportional to the concentration of the reactants and/or products, a first-order rate coefficient (k_{exp}) can be obtained from

$$\ln|A_\infty - A_t| - \ln|A_\infty - A_0| = -k_{exp}\, t \qquad (1.18)$$

where A_∞, A_t, and A_0 represent the absorbances after 10 half-lives of reaction, at time t, and before the reaction has begun, respectively. Substitution of (1.17) into (1.18) leads to

$$\ln\left\{\log \frac{(T_t)}{(T_\infty)}\right\} = \ln\left\{\log \frac{(T_0)}{(T_\infty)}\right\} - k_{exp}\, t \qquad (1.19)$$

where the subscripts have the same meaning as above. It was found most convenient to measure the difference, ΔT_t, defined as shown in Figure 1. When the transmittance increases during the reaction as in Figure 1(a), then

$$\Delta T_t \equiv (T_{offset} - T_t) \qquad (1.20)$$

where T_{offset} is obtained directly from the stopped-flow apparatus, and

$$\Delta T_\infty \equiv (T_{offset} - T_\infty) \qquad (1.21)$$

Substitution for T_t and T_∞ into (1.19), gives

$$\ln\left\{\log\left\{\frac{T_{offset} - \Delta T_t}{T_{offset} - \Delta T_\infty}\right\}\right\} = \ln\left\{\log\left\{\frac{T_0}{T_\infty}\right\}\right\} - k_{exp}\, t \qquad (1.22)$$

The value of k_{exp} is obtained from the slope of a plot of

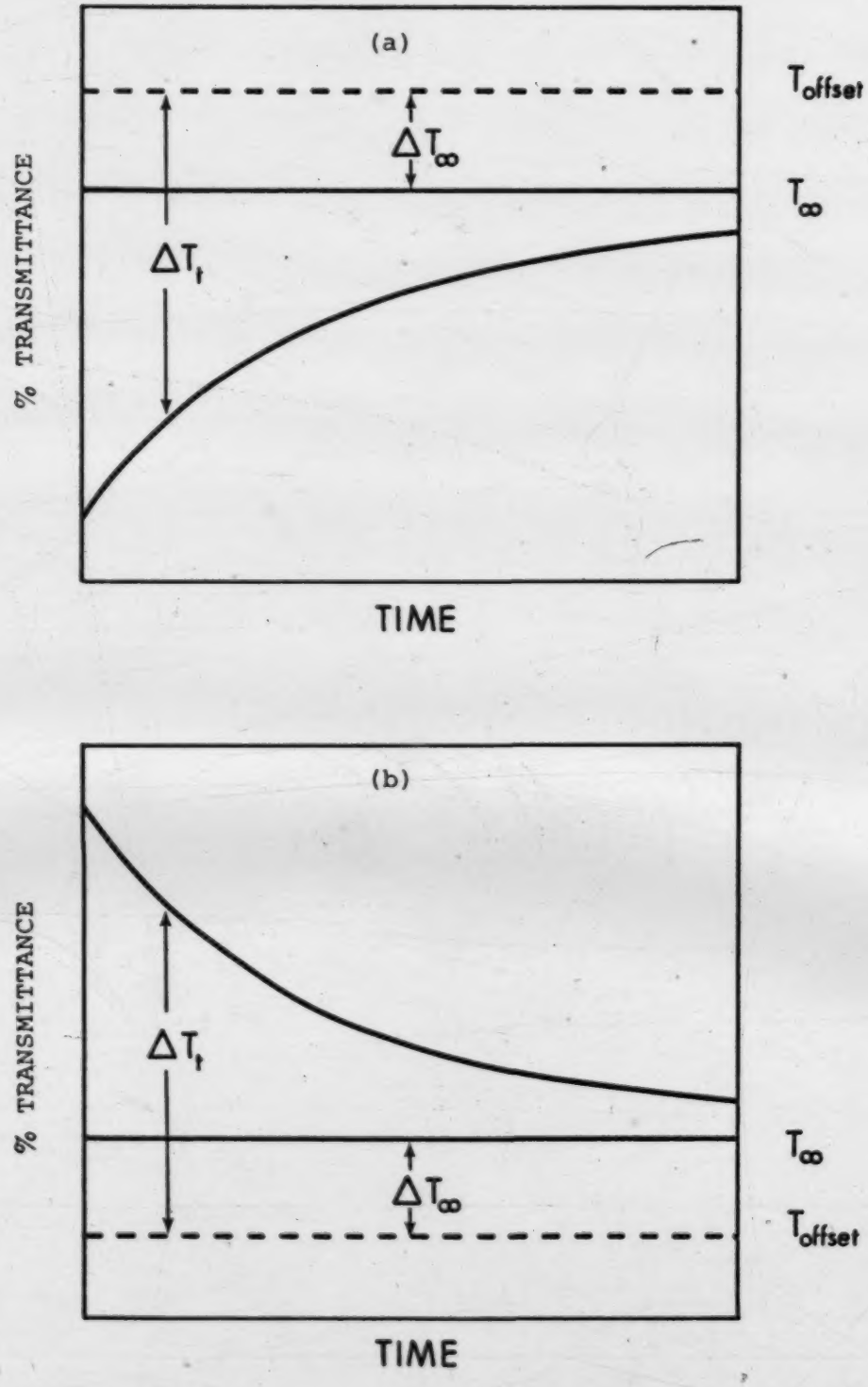

Figure 1. Analysis of transmittance-time data.

the left hand side of (1.22) *versus* time.

When the transmittance decreases during the reaction as in Figure 1(b),

$$\Delta T_t \equiv (T_t - T_{offset}) \tag{1.23}$$

$$\Delta T_\infty \equiv (T_\infty - T_{offset}) \tag{1.24}$$

and then k_{exp} can be obtained from the slope of a plot of $\ln\{\log((T_{offset} + \Delta T_t)/(T_{offset} + \Delta T_\infty))\}$ *verus* time. It is convenient to redefine ΔT_t and ΔT_∞ (as above) so that their values are always positive.

The values of k_{exp} for the decarboxylation study were obtained from the slopes of linear plots of equation (1.22). Such plots were linear for at least 75% reaction, except in cases where the value of ΔT_∞ was uncertain. In all cases, the best-fit line was approximated visually.

For the carboxylation and ring-closing data, least-squares "best-fit" values of k_{exp} were calculated using a computer program written for the Wang 500 programmable desk calculator. The program was written to accept ten data points equally spaced on the time-axis, and was found to be very efficient for the analysis of large amounts of stopped-flow data. The equations and the program used are described in Appendix A. Comparisons of values of k_{exp} obtained from some of the decarboxylation data using both graphical and least-squares methods

showed close agreement. The reported values of k_{exp} from the stopped-flow data in this work are usually the average of ten kinetic runs under identical conditions.

Values of k_{exp} were quoted with three figures, although the standard deviation indicates that the third figure is usually not significant. Likewise, the results quoted in the text usually contain one more figure than is significant as indicated by the confidence limits. However, only significant figures are retained in the tables of final results.

RESULTS AND DISCUSSION

Decarboxylation

It has been shown by Francis[16] that $(en)_2CoCO_3^+$ reacts moderately rapidly in dilute alkaline solution to produce *cis*-$(en)_2Co(OH)(CO_3)$, and that further reaction to give $(en)_2Co(OH)_2^+$ is much slower. This reaction gives a convenient *in situ* preparation of the monodentate carbonato species *cis*-$(en)_2Co(OH)(CO_3)$. The spectral changes accompanying the reaction in 0.2 M NaOH are shown in Figure 2.

When samples from this reaction solution were taken after 30 minutes and mixed in the stopped-flow system with acid and buffer, to give a final pH in the range of 1 to 6, a number of spectral changes were observed. If the sample is monitored at 520 nm, there is an increase in transmittance, but the magnitude of this change decreases markedly as the final pH of the solution increases above 4.5. In addition, above pH 5, the transmittance continues to increase slowly even after about eight half-lives of the initial transmittance change. This suggests that a second, slower reaction is occurring. If sodium bicarbonate is added to the solution of *cis*-$(en)_2Co(OH)(CO_3)$ before acidification to pH > 5, the magnitude of the initial transmittance increase at 520 nm is very small, and it is followed by a slow decrease in transmittance. A typical trace recorded under these

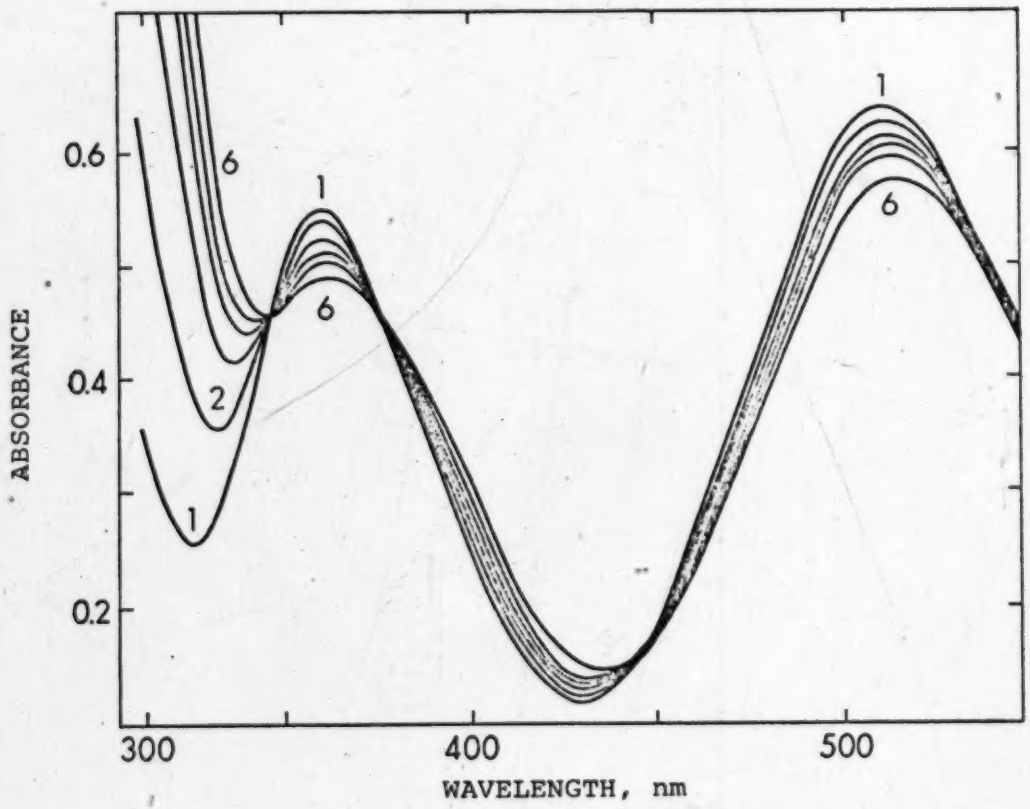

Figure 2. Consecutive scans of the electronic spectrum of a solution of 5×10^{-3} M $(en)_2CoCO_3^+$ in 0.20 M NaOH. Cell path length 1.00 cm. The spectra were initiated at (1) 1 min; (2) 6 min; (3) 12 min; (4) 24 min; (5) 80 min; (6) 3 hr after mixing with base.

conditions is shown in Figure 3. This slow decrease is also observed at pH> 5.8 even in the absence of added $NaHCO_3$.

If a wavelength of 320 nm is used to observe the acidified solutions, then an initial increase in transmittance is again seen. However the magnitude of this change is greater than that at 520 nm, as shown in Figure 4. The magnitude of the change at 320 nm is relatively independent of the pH. The slower change found at 520 nm is also much less significant at 320 nm relative to the initial change, and therefore causes much less difficulty in the analysis of the data for the first reaction. However, for pH > 5.8, the transmittance increase was not a simple first-order function as evidenced by the non-linearity of the plots of the logarithm of the absorbance change *versus* time. When sodium bicarbonate was added, there was a considerable reduction in the magnitude of the transmittance increase at pH > 5, but the slower change, noted for pH > 5.8 without added $NaHCO_3$, still could be observed.

A consideration of the known spectra of $(en)_2CoCO_3^+$ and *cis*-$(en)_2Co(OH_2)_2^{+3}$, [22] and of equilibrium mixtures of *cis* and *trans*-$(en)_2Co(OH)(OH_2)^{+2}$, indicates that the observations on acidification of $(en)_2Co(OH)(CO_3)$ can be understood in terms of the reaction sequence given in Scheme 1.

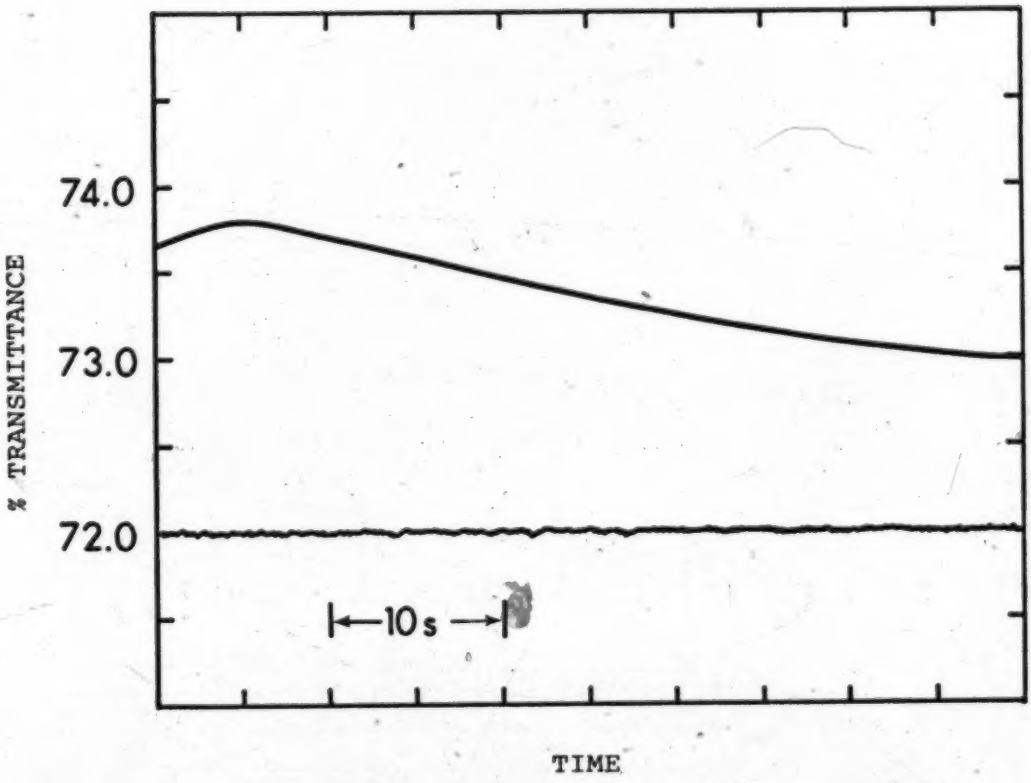

Figure 3. Transmittance changes observed at 520 nm upon rapid neutralization of a solution of 10^{-3} M *cis*-$(en)_2Co(OH)(CO_3)$ and 10^{-3} M $NaHCO_3$ to pH 6.5 . I= 1.0 M($LiClO_4$). T= 26°.

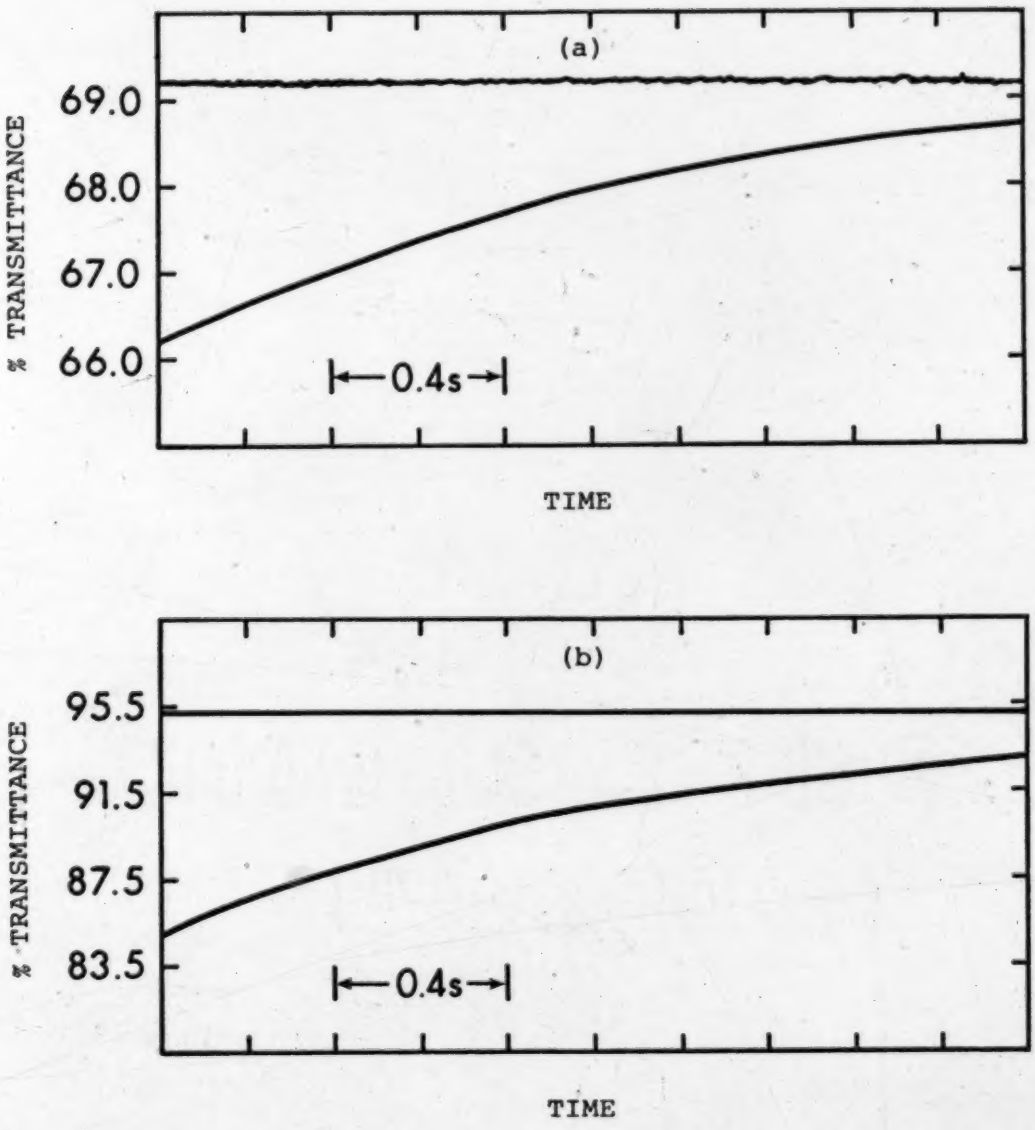

Figure 4. A comparison of the transmittance changes observed at 520 and 320 nm upon decarboxylation of *cis*-$(en)_2Co(OH_2)(CO_3H)^{+2}$. (a) λ = 520 nm, pH= 5.2, [Total Co(III)]= 9.7×10^{-4} M, [Buffer]= 0.080 M Acetate. I= 1.0 M($LiClO_4$). T= 26°. (b) λ = 320 nm, pH= 5.3, [Total Co(III)]= 4.0×10^{-4} M, [Buffer]= 0.080 M Citrate. I= 1.0 M($LiClO_4$) T = 26°.

Scheme 1

$$cis\text{-}(en)_2Co(OH)(CO_3) + H^+ \underset{}{\overset{1/K_{a2}}{\rightleftharpoons}} cis\text{-}(en)_2Co(OH_2)(CO_3)^+$$

$$cis\text{-}(en)_2Co(OH_2)(CO_3)^+ + H^+ \overset{1/K_{a1}}{\rightleftharpoons} cis\text{-}(en)_2Co(OH_2)(CO_3H)^{+2}$$

$$cis\text{-}(en)_2Co(OH_2)(CO_3H)^{+2} \xrightarrow{k_2} cis\text{-}(en)_2Co(OH_2)(OH)^{+2} + CO_2$$

$$cis\text{-}(en)_2Co(OH_2)(CO_3)^+ \xrightarrow{k_2'} cis\text{-}(en)_2Co(OH)_2^+ + CO_2$$

$$cis\text{-}(en)_2Co(OH_2)(CO_3)^+ \xrightarrow{k_3} cis\text{-}(en)_2CoCO_3^+ + H_2O$$

$$cis\text{-}(en)_2Co(OH_2)(OH)^{+2} \overset{K_{ct}}{\rightleftharpoons} trans\text{-}(en)_2Co(OH_2)(OH)^{+2}$$

The major initial transmittance change in the acidic solution is due to the decarboxylation reactions (k_2 and k_2'). The magnitude of the transmittance change observed at 520 nm may decrease as the pH is increased, because of a change either in the nature of the reactants (as $(en)_2Co(OH_2)(CO_3H)^{+2}$ is converted to $(en)_2Co(OH_2)(CO_3)^+$), or in the products, $(en)_2Co(OH_2)_2^{+3}$ and $(en)_2Co(OH_2)(OH)^{+2}$. This explanation is also consistent with the observation that the magnitude of the transmittance change at 320 nm is independent of pH, implying that the two reactants are nearly isosbestic with each other at this wavelength, and that the two products are also isosbestic with each other. Spectra of the products are consistent with this explanation.

The slower decrease in transmittance at 520 nm in the presence of $NaHCO_3$ at pH > 5, and the increase in transmittance observed at 320 nm for pH > 5.8, or in the presence of $NaHCO_3$ at pH > 5, can be attributed to the chelation reaction (i.e. formation of $(en)_2CoCO_3^+$). This is observed because the added carbonate suppresses the decarboxylation reactions. The directions of these transmittance changes are consistent with what is expected for chelation, and their identity is further confirmed by the observations made during the carboxylation studies to be discussed later.

The slowest change observed at 520 nm and pH > 5 is consistent with the isomerization reaction (K_{ct}). This was confirmed by an independent study desribed in the next section.

The experimental pseudo-first-order rate coefficients (k_{exp}) for the decarboxylation reaction are given in Table 3. The results at 320 nm and 520 nm are found to agree when experimental conditions have permitted observation at the two wavelengths. The pH dependence of k_{exp} is found to follow the empirical rate law

$$k_{exp} = \frac{a}{b + (H^+)} \qquad (1.25)$$

This result can be reconciled with the reactions shown

Table 3

Observed Rate Coefficients for the Decarboxylation Reaction[a]

pH	k_{exp}, s^{-1}[b]	No. of Runs	Buffer[c,d]
0.95[e]	1.10 ± .03	10	None
1.15[e]	1.10 ± .08	10	None
2.02[e]	1.10 ± .04	10	None
3.00[e]	1.11 ± .06	12	MP
3.00	1.12 ± .04	9	MP
3.12	1.21 ± .06	10	MP
3.14[e]	1.10 ± .05	7	
3.32	1.20 ± .04	10	MP
3.52	1.18 ± .04	10	MP
4.30	0.96 ± .06	10	AN
4.30	1.05 ± .06	10	AC
4.40	1.01 ± .05	12	AN
4.40	1.04 ± .04	11	
4.54	1.08 ± .03	10	AC
4.56	0.900 ± .04	10	AN
4.63	0.880 ± .03	10	AN
4.75	0.980 ± .04	10	AN
4.96	0.890 ± .05	12	
5.05	0.920 ± .05	6	AC
5.10	0.840 ± .06	11	

Table 3 (Cont'd)

pH	k_{exp} s^{-1}[b]	No. of Runs	Buffer[c,d]
5.12	0.890 ± .06	12	
5.12	0.850 ± .06	10	
5.20[e]	0.911 ± .02	8	AC
5.32	0.810 ± .03	14	
5.42	0.780 ± .02	10	
5.43	0.726 ± .03	8	
5.48	0.678 ± .06	8	
5.56	0.603 ± .03	9	
5.62	0.670 ± .05	14	
5.64	0.478 ± .04	6	MES, .04M
5.70	0.483 ± .03	10	
5.75	0.530 ± .03	10	
5.76	0.539 ± .01	11	
5.80	0.340 ± .02	6	
5.86	0.445 ± .02	10	
5.86	0.490 ± .03	12	
6.04	0.211 ± .02	10	MES, .04M
3.0[e,f]	0.301 ± .01	8	MP
1.9[e,f]	0.275 ± .02	10	None
3.0[e,g]	0.548 ± .03	10	MP
1.1[e,g]	0.513 ± .04	8	None
1.8[e,g]	0.490 ± .03	10	None

Table 3 (Cont'd)

pH	k_{exp} s^{-1}[b]	No. of Runs	Buffer[c,d]
1.8[e,h]	1.91 ±.07	8	None
2.9[e,h]	1.90 ±.12	10	MP
1.7[e,i]	8.79 ±.29	10	None

(a) Temperature(T) is 26.0° unless otherwise stated. I= 1.0 M ($LiClO_4$), λ = 320 nm, and total complex concentration 2-5 x 10^{-4} M after mixing, unless otherwise indicated.

(b) The error limits are one standard deviation.

(c) Citrate buffer was used unless designated as follows: AC, acetate; AN, aniline; MP, 2-methoxy-pyridine; MES, see experimental.

(d) The final buffer concentration after mixing was 0.08 M unless otherwise indicated.

(e) λ = 520 nm.

(f) T = 14.0°

(g) T = 20.0°

(h) T = 30.0°

(i) T = 41.0°

in Scheme 2.

Scheme 2

$$cis\text{-}(en)_2Co(OH)(CO_3) + H^+ \underset{}{\overset{1/K_{a2}}{\rightleftharpoons}} cis\text{-}(en)_2Co(OH_2)(CO_3)^+$$

$$cis\text{-}(en)_2Co(OH_2)(CO_3)^+ + H^+ \overset{1/K_{a1}}{\rightleftharpoons} cis\text{-}(en)_2Co(OH_2)(CO_3H)^{+2}$$

$$cis\text{-}(en)_2Co(OH_2)(CO_3H)^{+2} \xrightarrow{k_2} cis\text{-}(en)_2Co(OH_2)(OH)^{+2} + CO_2$$

$$cis\text{-}(en)_2Co(OH_2)(CO_3)^+ \xrightarrow{k_2'} cis\text{-}(en)_2Co(OH)_2^+ + CO_2$$

If the total reactant concentration is represented by

$$T = [(en)_2Co(OH_2)(CO_3H)^{+2}] + [(en)_2Co(OH_2)(CO_3)^+] + [(en)_2Co(OH)(CO_3)] \qquad (1.26)$$

and since

$$\frac{-d\,T}{dt} = k_{exp}\,T \qquad (1.27)$$

then it can be shown that

$$k_{exp} = \frac{k_2(H^+)^2 + k_2'K_{a1}(H^+)}{(H^+)^2 + K_{a1}\left((H^+) + K_{a2}\right)} \qquad (1.28)$$

Previous workers[23] reported a value of $K_{a2} = 1.8 \times 10^{-9}$ M, so that $(H^+) >> K_{a2}$ under the present experimental conditions, and equation (1.28) can be reduced to

$$k_{exp} = \frac{k_2(H^+) + k_2'K_{a1}}{(H^+) + K_{a1}} \qquad (1.29)$$

Consistency with the experimental rate law (equation (1.25)) requires that $k_2(H^+) >> k_2'K_{a1}$. Comparison of (1.29) with (1.25) then gives a= k_2 and b= K_{a1}. A computer fit of the results to an expression of the form of equation (1.29) confirmed that $k_2'K_{a1}$ is not distinguishable from zero. The least-squares "best-fit" values[24] of k_2 and K_{a1} are $1.11 \pm 0.04\ s^{-1}$ and $(2.2\pm0.4) \times 10^{-6}$ M respectively, where the errors quoted are estimates of the 95% confidence limits.[25] The results calculated from these values using an equation of the form of (1.25), are compared to the experimental results in Figure 5.

If it is assumed that $k_2'K_{a1}$ is less than 10% of the minimum value of $k_2(H^+)$, then an upper limit of $k_2' \leq 0.05\ s^{-1}$ is calculated.

The results of the decarboxylation study, together with those from the carboxylation study discussed later in this section, allow an independent calculation of an upper limit for k_2'. The reactions are shown in Scheme 3.

Scheme 3

$$\begin{array}{ccc} (en)_2Co(OH_2)(OH)^{+2} + CO_2 & \underset{k_2}{\overset{k_{-2}}{\rightleftharpoons}} & (en)_2Co(OH_2)(CO_3H)^{+2} \\ H^+ \uparrow\downarrow K_{a4} & & H^+ \uparrow\downarrow K_{a1} \\ (en)_2Co(OH)_2^+ + CO_2 & \underset{k_2'}{\overset{k_{-2}'}{\rightleftharpoons}} & (en)_2Co(OH_2)(CO_3)^+ \end{array}$$

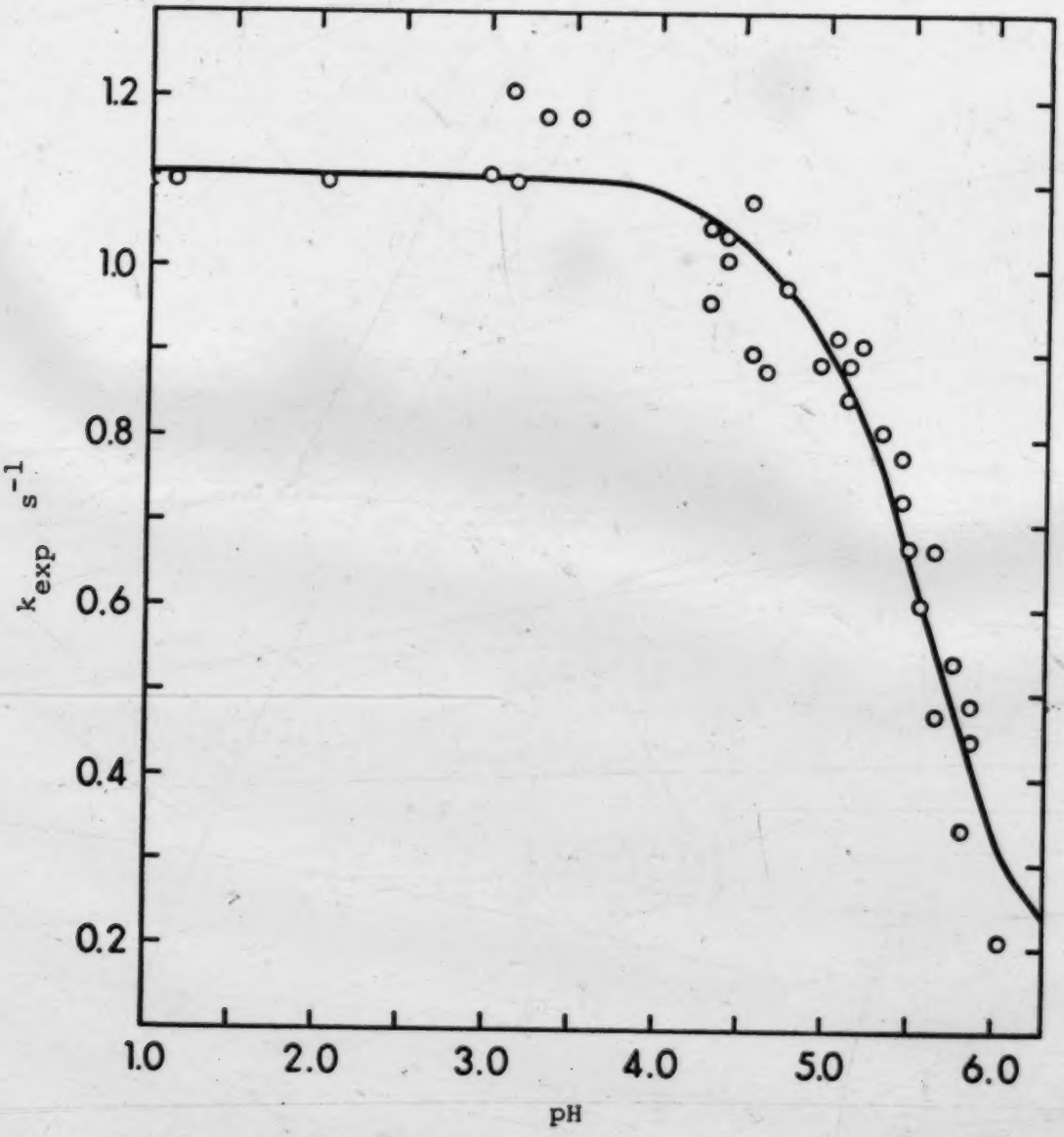

Figure 5. The pH dependence of k_{exp} for the decarboxylation of *cis*-$(en)_2Co(OH_2)(CO_3H)^{+2}$. I= 1.0 M($LiClO_4$). T= 26°. The solid line was calculated from (1.25) using values of a= 1.11 s^{-1} and b= 2.2 x 10^{-6} M.

All of the cobalt species in Scheme 3 have the *cis* configuration. From detailed balancing,

$$k_2' = \frac{K_{a4} k_2 k_{-2}'}{K_{a1}\, k_{-2}} \qquad (1.30)$$

Using values of $k_2 = 1.10\ s^{-1}$, $K_{a1} = 2.2 \times 10^{-6}$ M, $K_{a4} = 6.46 \times 10^{-9}$ M, $k_{-2} = 5.2 \times 10^{2}\ M^{-1}s^{-1}$, and $k_{-2}' \leq 50\ M^{-1}s^{-1}$, the latter two of which are evaluated later in this section, k_2' is estimated to have a value less than $3 \times 10^{-4}\ s^{-1}$.

The results of the temperature study of the decarboxylation reaction (Table 3) give $\Delta H^* = 95 \pm 9$ kJ mol^{-1} and $\Delta S^* = (8 \pm 3) \times 10^{1}$ J $K^{-1}mol^{-1}$. These values were determined by least-squares analysis of the transition-state equation,

$$\ln\left\{\frac{k_{exp}}{T}\right\} = -\frac{\Delta H^*}{RT} + \ln\left\{\frac{\kappa_b}{h}\right\} + \frac{\Delta S^*}{R} \qquad (1.31)$$

where the symbols have their usual meanings.

Isomerization

As noted in the previous section, a much slower reaction was observed at 520 nm following the decarboxylation reaction. A consideration of results in the literature[26,27] indicated that this might be *cis-trans* isomerization of the products of the decarboxylation reaction. However, the published results were not complete enough to allow an unambiguous assignment of this reaction. Therefore a study was undertaken to determine if the rate and direction of transmittance changes due to isomerization were consistent with those observed for the slow reaction following decarboxylation. Since this work was completed, results of a similar study have been published.[28]

Bjerrum and Rasmussen have shown[22] that at pH < 3, *cis*-$(en)_2Co(OH_2)_2^{+3}$ is the predominant species. However, when the pH is increased, isomerization involving the conjugate bases will occur. This is essentially the procedure which was used to follow the isomerization, as described in the experimental section.

It should be noted initially that the direction and magnitude of the transmittance change observed for this reaction are the same as those observed at 520 nm for the slow reaction following decarboxylation. The experimental pseudo-first-order rate coefficients are given in Table 4, and are found to fit the general equation

Table 4

Observed Rate Coefficients for *cis-trans* Isomerization[a]

pH	$10^3 k_{exp}$, s^{-1}
5.76	4.0
5.82	4.0
5.90	3.9
6.14	4.3
6.46	4.4
6.50	4.6
6.58	4.7

(a) The total concentration of cobalt(III) species was 8.79×10^{-3} M. Temperature was 25.0° , I = 1.0 M ($LiClO_4$) and 0.040 M MES buffer was included.

$$k_{exp} = \frac{a + b(H^+)}{c + (H^+)} \qquad (1.32)$$

The results of Bjerrum and Rasmussen[22] clearly show that under the present experimental conditions, (pH 5.8 to 6.6) the dominant species in solution will be the *cis* and *trans* isomers of $(en)_2Co(OH_2)_2^{+3}$ and $(en)_2Co(OH_2)(OH)^{+2}$. Therefore only the reactions in Scheme 4 will be considered in developing the rate law.

Scheme 4

$$cis\text{-}(en)_2Co(OH_2)_2^{+3} \underset{}{\overset{K_{a3}}{\rightleftharpoons}} cis\text{-}(en)_2Co(OH_2)(OH)^{+2} + H^+$$

$$trans\text{-}(en)_2Co(OH_2)_2^{+3} \underset{}{\overset{K_{a5}}{\rightleftharpoons}} trans\text{-}(en)_2Co(OH_2)(OH)^{+2} + H^+$$

$$cis\text{-}(en)_2Co(OH_2)_2^{+3} \underset{k_{t1}}{\overset{k_{c1}}{\rightleftharpoons}} trans\text{-}(en)_2Co(OH_2)_2^{+3}$$

$$cis\text{-}(en)_2Co(OH_2)(OH)^{+2} \underset{k_{t2}}{\overset{k_{c2}}{\rightleftharpoons}} trans\text{-}(en)_2Co(OH_2)(OH)^{+2}$$

Kinetic analysis of this system (given in Appendix B) gives the pseudo-first-order rate coefficient for the approach to equilibrium as

$$k_{exp} = \frac{k_{c1}(H^+) + k_{c2}K_{a3}}{K_{a3} + (H^+)} + \frac{k_{t1}(H^+) + k_{t2}K_{a5}}{K_{a5} + (H^+)} \qquad (1.33)$$

The previously determined values[22,26] for the rate and equilibrium constants in this system are summarized in Table 5. It is clear from these values that

Table 5

Rate and Equilibrium Constants for aquo Cobalt(III) Species

k_{c1} [a]	1.3×10^{-7} s^{-1}
k_{t1} [b]	6.8×10^{-6} s^{-1}
K_{a3} [c]	8.7×10^{-7} M
K_{a5} [c]	3.6×10^{-5} M
k_{c2}, k_{t2} [d]	$\simeq 2 \times 10^{-3}$ s^{-1}

(a) Obtained from a value[26] of $(k_{t1} + k_{c1}) = 6.8 \times 10^{-6}$ s^{-1} and a value of $k_{t1}/k_{c1} = 50$ appropriate to perchlorate media, as deduced from data of Henney.[30]

(b) Value at 25° and low ionic strength in $NaClO_4$ media.[26]

(c) Values reported at 25° and I = 1.0 M ($NaNO_3$).[22]

(d) Estimated from $k_{exp} = 8.0 \times 10^{-4} s^{-1}$ at pH ≃ 3.8[26] and $k_{c2}/k_{t2} = 1.25$.[29]

under the conditions of pH 5.8 to 6.6, it will be true that $K_{a5} >> (H^+)$, $k_{t2}K_{a5} >> k_{t1}(H^+)$, and $k_{c2}K_{a3} >> k_{c1}(H^+)$. Therefore equation (1.33) simplifies to give

$$k_{exp} = \frac{k_{c2}K_{a3}}{K_{a3} + (H^+)} + k_{t2} = \frac{(k_{c2} + k_{t2})K_{a3} + k_{t2}(H^+)}{K_{a3} + (H^+)} \qquad (1.34)$$

This equation has the same form as the experimental rate law, equation (1.32). With $K_{a3} = 8.7 \times 10^{-7}$M, values of $k_{c2} = 1.6 \times 10^{-3}s^{-1}$ and $k_{t2} = 3.4 \times 10^{-3}s^{-1}$ are determined from the slope and the intercept of the plot of k_{exp} *versus* $K_{a3}/(K_{a3} + (H^+))$ shown in Figure 6. These values are in good agreement with recent literature values of $k_{c2} = 1 \times 10^{-3}s^{-1}$ and $k_{t2} = 4 \times 10^{-3}s^{-1}$ (25°, I = 1.0 M, $NaClO_4$).[28]

The slow reaction following decarboxylation has an observed rate coefficient of $\lesssim 10^{-2}s^{-1}$ at pH 5.8. Comparison with the data in Table 4 supports the suggestion that the slow reaction is *cis-trans* isomerization of the decarboxylation products.

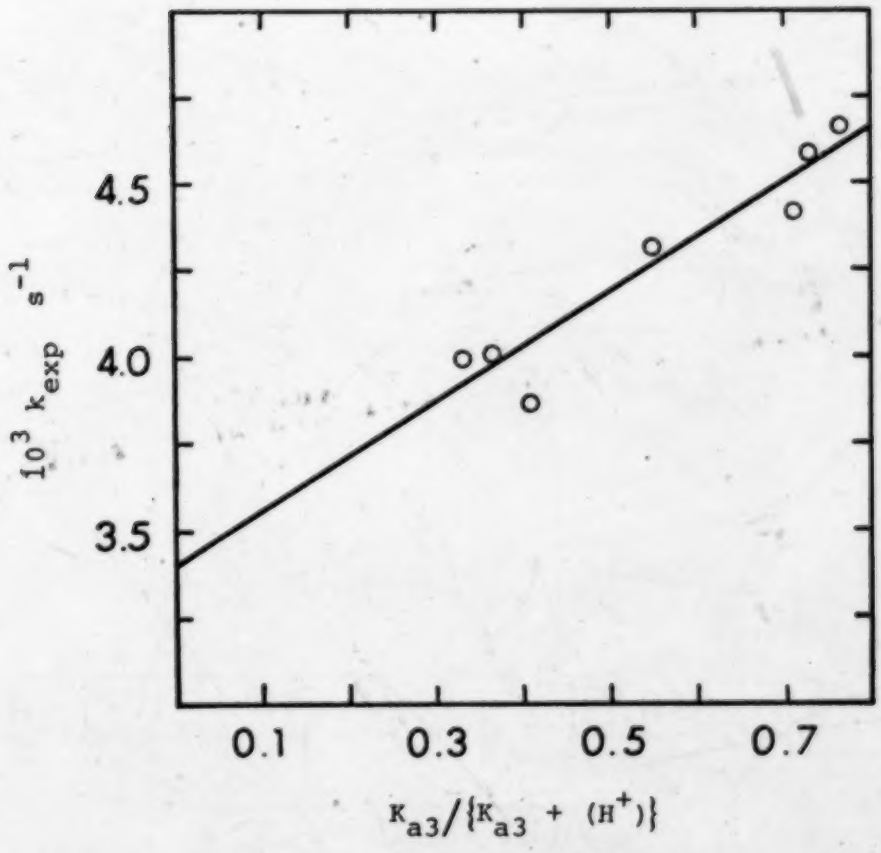

Figure 6. A plot of k_{exp} *versus* $K_{a3}/(K_{a3} + (H^+))$ for the isomerization of *cis*-$(en)_2Co(OH_2)(OH)^{+2}$. I = 1.0 M($LiClO_4$). T= 25°. Slope = 1.6×10^{-3} s^{-1}, Intercept = 3.4×10^{-3} s^{-1}.

Carboxylation and Chelate Ring-Closure

The reaction of intermediate rate between decarboxylation and isomerization was assigned earlier as chelate ring-closure to form $(en)_2CoCO_3^+$. Since this reaction was itself of considerable interest, an independent study of its rate was undertaken. Although in principle this reaction could be studied by starting with $(en)_2Co(OH)(CO_3)$, the results will always be obscured by the decarboxylation. Therefore a stopped-flow kinetic study of the carboxylation and subsequent ring-closure was made by observing the transmittance changes in a solution initially containing *cis*-$(en)_2Co(OH_2)_2^{+3}$ and CO_2. Both carboxylation and chelate ring-closure can be studied conveniently at 320 nm, since there is an initial decrease in transmittance followed by a slower increase to a final value, as shown in Figure 7. The relatively large transmittance changes and large rate difference make it possible to study both reactions under the same experimental conditions.

The reactions were studied by the two methods described in the experimental section. In the first method, solutions of sodium bicarbonate of known concentration were mixed with acidic solutions of *cis*-$(en)_2Co(OH_2)_2^{+3}$, to give a final pH in the region 7.5 to 8.5. The free CO_2 concentrations in these solutions were determined from the

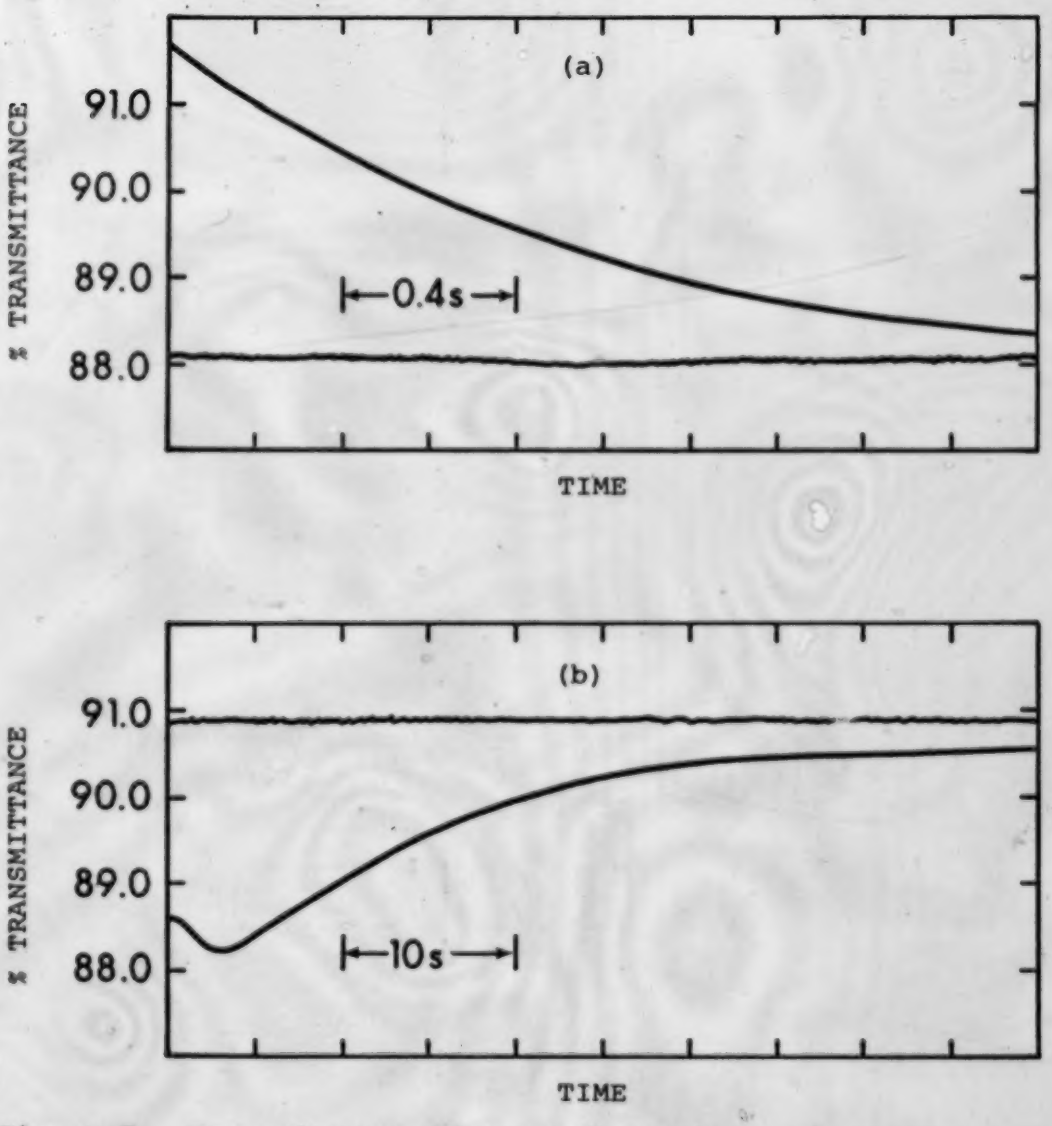

Figure 7. Transmittance changes observed at 320 nm upon rapid neutralization of a solution of CO_2 and *cis*-$(en)_2Co(OH_2)_2^{+3}$ to pH 6.52. [Total Co(III)] = 2.00×10^{-3}M, [CO_2] = 2.1×10^{-3}M. I= 1.0 M($LiClO_4$). T= 26°. [Buffer]= 0.20 M PIPES. (a) carboxylation, (b) ring-closure.

known values[16] for the equilibrium constants under these conditions of temperature and ionic strength. In all cases, $[CO_2] >> [cis\text{-}(en)_2Co(OH_2)_2^{+3}]$. The method has the disadvantage that the calculated CO_2 concentration depends on several equilibrium constants.

In the second method, an acidic solution (pH≈3) of $cis\text{-}(en)_2Co(OH_2)_2^{+3}$ and Na_2CO_3 was mixed with buffer in the stopped-flow system. This method relies on the fact that, before mixing, all the carbonate in solution is present as CO_2, and, as long as the pH after mixing is not too high, the CO_2 undergoes hydration quite slowly relative to the carboxylation of the cobalt(III) species. The rate constants k_{CO_2} and k_{OH} for the hydration reactions (1.35) and (1.36) have been reported by a number of workers[1,16,32], with values of 0.024 s^{-1} and 1.06 x 10^4 M^{-1} s^{-1} respectively at 26° and an ionic strength of 1.0 M ($NaClO_4$).

$$CO_2 + H_2O \xrightarrow{k_{CO_2}} H_2CO_3 \qquad (1.35)$$

$$CO_2 + OH^- \xrightarrow{k_{OH}} HCO_3^- \qquad (1.36)$$

The pseudo-first-order rate coefficients for the carboxylation reaction are given in Table 6. Because of the large number of species present in these reaction solutions, it does not seem meaningful to quote an empirical rate law based on the results in Table 6. However, it

Table 6

Observed Rate Coefficients for Carboxylation

pH	$10^3[CO_2]$,M	k_{exp} s^{-1}	No. of Runs	Conditions[a]
5.42	3.00	0.908±.09	12	b
5.65	3.00	0.990±.07	10	b
5.72	3.00	0.848±.06	10	b
5.85	3.00	1.05 ±.06	10	b
6.13	3.00	1.24 ±.09	10	b
6.36	3.00	1.22 ±.04	10	b
6.52	2.10	0.946±.05	10	c
6.55	4.20	1.80 ±.11	10	c
6.70	5.50	2.29 ±.13	8	c
6.72	6.60	2.72 ±.16	10	c
6.91	6.00	2.65 ±.18	4	c
7.09	6.00	3.18 ±.24	10	c
7.22	6.60	2.69 ±.10	10	c
7.25	3.00	1.36 ±.06	10	c
7.87	2.88	0.900±.04	10	d (0.193)
8.14	3.00	0.757±.05	10	d (0.381)
8.17	3.87	0.873±.04	10	d (0.529)
8.19	1.85	0.552±.02	10	d (0.264)
8.55	1.51	0.328±.01	10	d (0.518)

Table 6 (Cont'd)

(a) Total [Co(III)] = (1-3) x 10^{-4} M. Temperature 26°, I = 1.0 M ($LiClO_4$).

(b) Method 2. 0.10 M MES buffer.

(c) Method 2. 0.20 M PIPES buffer.

(d) Method 1. Self-buffered by $NaHCO_3$, the total molar concentration of which is given in the brackets.

should be noted that the results show a first-order dependence on $[CO_2]$. Also, a comparison of the observed rate coefficients for decarboxylation (see Table 3) with those listed in Table 6 for carboxylation indicates that the system under consideration can be best described at low pH as one which is approaching equilibrium, and thus the observed pseudo-first-order rate coefficient will contain a contribution from both carboxylation and decarboxylation. Therefore, a reaction scheme which will account for the pH and CO_2 dependence of k_{exp} must include the reverse reactions. The potential complexity of the system can be reduced if it is assumed that the reaction pathways for carboxylation will be similar to that found[31] for the pentaammine species. In the latter system, the pH dependence of the rate required that the major species reacting with CO_2 be $(NH_3)_5CoOH^{+2}$. Because of the slow rate of hydration of CO_2 already mentioned, very little bicarbonate or carbonate is present during the carboxylation reaction when the acidification method (Method 2) is used. Therefore the carboxylation results should be explained by the reactions shown in Scheme 5.

Scheme 5

$$cis\text{-}(en)_2Co(OH_2)_2^{+3} \underset{}{\overset{K_{a3}}{\rightleftharpoons}} cis\text{-}(en)_2Co(OH_2)(OH)^{+2} + H^+$$

$$cis\text{-}(en)_2Co(OH_2)(OH)^{+2} \overset{K_{a4}}{\rightleftharpoons} cis\text{-}(en)_2Co(OH)_2^{+} + H^+$$

$$cis\text{-}(en)_2Co(OH_2)(OH)^{+2} + CO_2 \overset{k_{-2}}{\underset{k_2}{\rightleftharpoons}} cis\text{-}(en)_2Co(OH_2)(CO_3H)^{+2}$$

$$cis\text{-}(en)_2Co(OH)_2^{+} + CO_2 \overset{k_{-2}'}{\underset{k_2'}{\rightleftharpoons}} cis\text{-}(en)_2Co(OH_2)(CO_3)^{+}$$

$$cis\text{-}(en)_2Co(OH_2)(CO_3H)^{+2} \overset{K_{a1}}{\rightleftharpoons} cis\text{-}(en)_2Co(OH_2)(CO_3)^{+} + H^+$$

$$cis\text{-}(en)_2Co(OH_2)(CO_3)^{+} \overset{K_{a2}}{\rightleftharpoons} cis\text{-}(en)_2Co(OH)(CO_3) + H^+$$

From the kinetic analysis of this mechanism, given in Appendix B, the pseudo-first-order rate coefficient is given by

$$k_{exp} = \left\{ \frac{k_{-2}K_{a3}(H^+) + k_{-2}'K_{a3}K_{a4}}{(H^+)^2 + K_{a3}(H^+) + K_{a3}K_{a4}} \right\} [CO_2] + \left\{ \frac{k_2(H^+)^2 + k_2'K_{a1}(H^+)}{(H^+)^2 + K_{a1}(H^+) + K_{a1}K_{a2}} \right\} \qquad (1.37)$$

The results in Table 6 were fitted to an equation of the form of (1.37), using a non-linear least-squares computer program.[24] Since there are eight independent parameters in equation (1.37), a meaningful fit results only when some of the parameters are fixed. The constants k_2 and K_{a1} can be fixed at the values previously

determined in the decarboxylation study. In addition, K_{a3} and K_{a4} have been measured previously,[22] and K_{a2} has been determined by the ring-closure study, discussed later in this section. Several different fits were obtained by allowing different parameters to vary, and a summary of the results of these fits is given in Table 7. Although K_{a2} and K_{a4} are not well-defined by the data-fitting, the value of k_{-2} is not very sensitive to either of these parameters, and thus k_{-2} is assigned a value of (5.2±0.5) x 10^2 M^{-1} s^{-1}. The rate coefficients calculated from the "best-fit" parameters (Fit A in Table 7), using equation (1.38), are compared to the observed values in Table 8.

The values of k_{-2}' and k_2' were not distinguished from zero in any of the computer fits. Therefore, the results being discussed here require that

$$k_{-2}K_{a3}(H^+) >> k_{-2}'K_{a3}K_{a4} \qquad (1.38)$$

from which the upper limit of $k_{-2}' < 50\ M^{-1}s^{-1}$ is determined.

Table 7

A Summary of the Results of Computer Fits of the Carboxylation Data

Parameter	Fit[a] A	B	C	D	E
$10^{-2}k_{-2}$, $M^{-1}s^{-1}$	5.20±.55	5.20±.54	5.17±.38	5.41±.61	5.10±.68
$10^{4}k_{-2}'$, $M^{-1}s^{-1}$	0	0	0.2 ± 10^{5}	0	0
$10^{4}k_{2}'$, s^{-1}	10^{-4}±20	0	0	0	10±30
10^{6} K_{a1}, M	2.20	2.48±2	2.20	2.20	2.20
10^{8} K_{a2}, M	0.092	3.44±80	0.092	0.092	2.50
10^{7} K_{a3}, M	8.57±4	8.71	7.85±4	7.56±4	8.71
10^{9} K_{a4}, M	6.46	6.46	6.46	8.45±4	7.08±4
S.E.[b]	0.161	0.162	0.163	0.156	0.168

(a) The value of k_2 was fixed at 1.11 s^{-1} throughout. In each fit, 2 or 3 of the parameters were allowed to vary, and its "best-fit" value is listed along with an estimate of its 95% confidence limits. The parameters without error limits were fixed at the values given.

(b) Minimization of the absolute residuals was used, from which this estimate of the standard error of the fit is derived.

Table 8

A Comparison of Observed and Calculated Rate Coefficients for Carboxylation

pH	k_{exp} s^{-1}	k_{cald} s^{-1}
5.42	0.908	0.990
5.65	0.990	0.991
5.72	0.848	0.998
5.85	1.05	1.02
6.13	1.24	1.11
6.36	1.22	1.21
6.52	0.946	0.929
6.55	1.80	1.74
6.70	2.29	2.35
6.72	2.72	2.82
6.91	2.65	2.67
7.09	3.18	2.70
7.22	2.69	2.94
7.25	1.36	1.35
7.87	0.900	1.01
8.14	0.757	0.823
8.17	0.873	1.03
8.19	0.552	0.481
8.55	0.328	0.237

Chelate Ring-Closure

The slower reaction observed when solutions of $(en)_2Co(OH_2)_2^{+3}$ and CO_2 are mixed has been attributed to chelate ring-closure for two reasons. First of all, the direction of the spectral change is consistent with ring-closure, and secondly, the reaction rate is independent of the CO_2 concentration. The latter observation rules out formation of possible dicarbonato species. The values of the pseudo-first-order rate coefficients (k_{exp}) are given in Table 9, and are shown plotted *versus* pH in Figure 8. The results can be accounted for by the reactions in the following scheme.

Scheme 6

$$cis\text{-}(en)_2Co(OH_2)(CO_3H)^{+2} \underset{}{\overset{K_{a1}}{\rightleftharpoons}} cis\text{-}(en)_2Co(OH_2)(CO_3)^{+} + H^{+}$$

$$cis\text{-}(en)_2Co(OH_2)(CO_3)^{+} \overset{K_{a2}}{\rightleftharpoons} cis\text{-}(en)_2Co(OH)(CO_3) + H^{+}$$

$$cis\text{-}(en)_2Co(OH_2)(CO_3)^{+} \xrightarrow{k_3} cis\text{-}(en)_2CoCO_3^{+} + H_2O$$

$$cis\text{-}(en)_2Co(OH)(CO_3) \xrightarrow{k_3'} cis\text{-}(en)_2CoCO_3^{+} + OH^{-}$$

If the total reactant concentration is given as

$$T = [cis\text{-}(en)_2Co(OH_2)(CO_3H)^{+2}] + [cis\text{-}(en)_2Co(OH_2)(CO_3)^{+}] + [cis\text{-}(en)_2Co(OH)(CO_3)] \qquad (1.39)$$

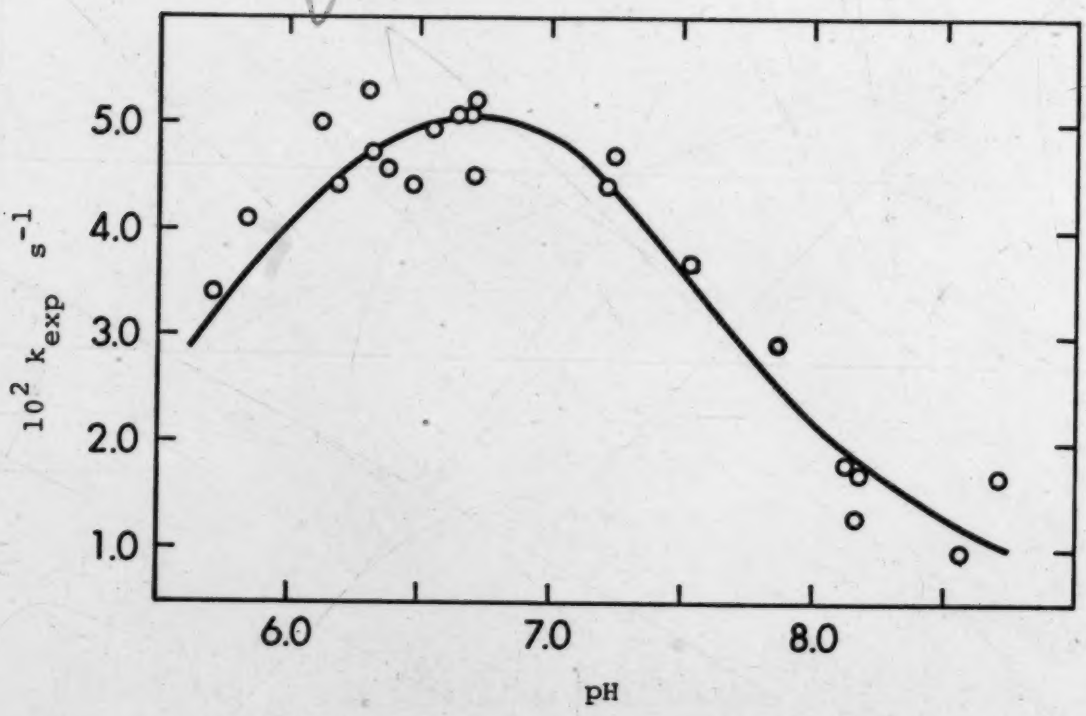

Figure 8. The pH dependence of k_{exp} for carboxylate chelate ring-closure. I= 1.0 M($LiClO_4$). T= 26°. The solid line was determined using equation (1.37) with the parameter values given in column C of Table 10.

Table 9

Observed Rate Coefficients for Chelate Ring-Closure

pH	$10^3[CO_2]$,M	$10^2 k_{exp}$ s^{-1}	No. of Runs	Conditions[a]
5.72	3.00	3.4±.4	8	b (MES)
5.85	3.00	4.1±.4	8	b (MES)
6.13	3.00	5.0±.4	6	b (MES)
6.20	7.0	4.4±.4	10	c
6.33	4.00	4.7±.3	10	c
6.36	3.00	5.3±.5	4	b (MES)
6.38	6.00	4.7±.2	10	c
6.48	9.0	4.4±.3	10	c
6.55	4.20	4.8±.4	10	b (PIPES)
6.65	3.00	5.1±.4	10	b (PIPES)
6.70	5.50	5.1±.4	8	b (PIPES)
6.70	18.5	4.5±.2	10	d (0.100)
6.72	6.60	5.2±.3	8	b (PIPES)
6.72	11	4.5±.5	2	b (PIPES)
7.22	6.60	4.4±.4	8	b (PIPES)
7.25	3.00	4.7±.3	8	b (PIPES)
7.54	3.05	3.7±.3	6	d (0.097)
7.87	2.88	2.9±.3	6	d (0.193)
8.14	3.00	1.8	1	d (0.381)

Table 9 (Cont'd)

pH	$10^3[CO_2]$,M	10^2k_{exp} s^{-1}	No. of Runs	Conditions[a]
8.17	3.87	1.3	1	d (0.529)
8.19	1.85	1.7	1	d (0.264)
8.56	1.51	1.1±.1	4	d (0.518)
8.71	1.94	1.7±.1	6	d (0.100)

(a) Total [Co(III)] = (1-3) x 10^{-4} M. Temperature 26.0° , I = 1.0M ($LiClO_4$).

(b) Method 2. 0.20 M buffer of type indicated in the brackets.

(c) Method 1. 0.05 M MES buffer included. [Na_2CO_3] = 0.02 M. λ = 520 nm.

(d) Method 1. Self-buffered by $NaHCO_3$, the total molar concentration of which is given in the brackets.

and since

$$\frac{-d\,T}{dt} = k_{exp}\,T \qquad (1.40)$$

then

$$k_{exp} = \frac{k_3K_{a1}(H^+) + k_3'K_{a1}K_{a2}}{(H^+)^2 + K_{a1}(H^+) + K_{a1}K_{a2}} \qquad (1.41)$$

A summary of the results of several least-squares fits of the data in Table 9 to an equation of the form of (1.41) is given in Table 10. The values of K_{a2} and k_3 are fairly independent of the other parameters, with values of $(2.5\pm1)\times 10^{-8}$ M and $(6.0\pm0.4)\times 10^{-2}$ s^{-1} respectively.

When the value of K_{a2} was fixed at the previously reported value[23] of 1.78×10^{-9} M, a very poor fit was obtained. Also, when the ratio K_{a2}/k_3 was fixed at 1.53×10^{-8} M s, as given by Francis,[16] the data could not be fitted to give reasonable values of k_3, K_{a1}, or K_{a2}.

The value of k_3' was not defined by the computer fits, suggesting that $k_3(H^+) > k_3'K_{a2}$ in the pH range of this study. An upper limit of $k_3' \simeq 5 \times 10^{-4}$ s^{-1} can be calculated from $K_{a2} = 2.5 \times 10^{-8}$ M and $(H^+) > 2 \times 10^{-9}$ M.

Table 10

A Summary of the Results of Computer Fits of the Ring-Closure Data

Parameter	Fit[a] A	B	C
10^6 K_{a1}, M	3.4±2	2.20	2.20
10^8 K_{a2}, M	1.9±1	0.178[b]	2.5±1
10^2 k_3 s^{-1}	5.61±.4	5.02±.7	6.01±.4
10^3 k_3' s^{-1}	6.1 ±.7	≈0	7.6 ±7
10^3 S.E.[c]	3.6	12	3.7

(a) The "best-fit" value is listed along with an estimate of its 95% confidence limits. The parameters without error limits were fixed at the value given.

(b) Previous literature value at 20°.[23]

(c) Minimization of the absolute residuals was used, from which this estimate of the standard error of the fit is derived.

CONCLUSION

Decarboxylation

The kinetic parameters measured in this present work for the decarboxylation of *cis*-$(en)_2Co(OH_2)(CO_3H)^{+2}$ are compared in Table 11 with the analogous parameters for the species $(NH_3)_5M\ CO_3H^{+2}$. The similarity in these rate constants supports the choice of a similar mechanism, which for $(NH_3)CoCO_3H^{+2}$ is known to proceed without Co-O bond-breaking.[12]

On the other hand, the significant difference in the activation parameters could be interpreted as resulting from a change in the mechanism of CO_2 loss for the species *cis*-$(en)_2Co(OH_2)(CO_3H)^{+2}$. However, if Co-O bond-breaking is occurring, and if the activation is dissociative in nature, then one must explain the unusual lability of the Co-O bond in this species as compared to others in which Co-O bond-breaking has been shown to occur. For example, one of the most rapid reactions in which Co-O bond-breaking must occur is the exchange of oxygen between $(en)_2Co(OH_2)(OH)^{+2}$ and water. This reaction has a rate coefficient of about 10^{-3} s^{-1} at 25°,[26] compared to values of ~1 s^{-1} for the decarboxylation reaction. It thus seems most probable that the decarboxylation of *cis*-$(en)_2Co(OH_2)(CO_3H)^{+2}$ proceeds via

Table 11

A Comparison of the Kinetic Parameters for Decarboxylation of Monodentate Carbonato Complexes

Complex	k, s^{-1}	ΔH^*, kJ/mol	ΔS^*, J/K mol	$10^6 K_a$, M	Reference
cis-$(en)_2Co(OH_2)(CO_3H)^{+2}$	1.11	95	+75	2.3	this work
$(NH_3)_5Co(CO_3H)^{+2}$	1.25	71.1	-2	0.4	8[a]
	(1.10)	(70.3)	(-8)	(0.2)	32[b]
$(NH_3)_5Rh(CO_3H)^{+2}$	1.13	71.1	-4	0.11	32[c]
$(NH_3)_5Ir(CO_3H)^{+2}$	1.45	79.5	+25	0.16	32[c]

(a) T = 25°, I = 0.5 M($NaClO_4$).

(b) Revised values from data at 25° in both $NaClO_4$ and $NaNO_3$. I = 0.5 M.

(c) T = 25°, I = 0.5 M($NaNO_3$).

C-O bond-breaking.

It is also noted from Table 11 that K_{a1} (Scheme 2) is considerably larger than the analogous values for the $(NH_3)_5M\ CO_3H^{+2}$ species. This could result from the increased stability of the conjugate base, *cis*-$(en)_2Co(OH_2)(CO_3)^+$, due to internal H-bonding.

In an earlier calculation, an upper limit of $k_2' < 3 \times 10^{-4}\ s^{-1}$ was determined (Scheme 3). From the results of Dasgupta and Harris,[33] an analogous value can be determined for the complex carbonatoaquo(β,β',β''-triaminotriethylamine)cobalt(III), ((tren)$Co(OH_2)(CO_3)^+$) from detailed balancing of a system of reactions analogous to those of Scheme 3, in which (tren) is substituted for $(en)_2$. If one assumes a value of 1.1 s^{-1} for the rate constant analogous to k_2, and uses values [33] of ~5 x 10^{-6}M, 44 $M^{-1}s^{-1}$, 170 $M^{-1}s^{-1}$ and 1.25 x 10^{-8}M for the constants corresponding to K_{a1}, k_{-2}, k_{-2}' and K_{a4}, then a value of $10^{-2}\ s^{-1}$ is calculated for the rate constant for decarboxylation of (tren)$Co(OH_2)(CO_3)^+$.

As mentioned earlier, two tautomeric forms of the carbonatoaquo complex are possible, as shown below.

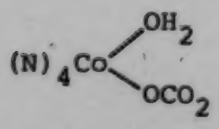

I

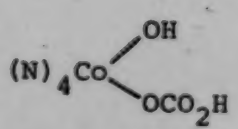

II

The small values of k_2' estimated for decarboxylation of the $(en)_2$ and (tren) complexes, as compared to the value of 1.25 s^{-1} for decarboxylation of $(NH_3)_5CoCO_3H^{+2}$,[8] suggests that Structure I predominates over Structure II.

Isomerization

As previously mentioned, the kinetic results reported here for the *cis-trans* isomerization (k_{c2}=1.6 x 10^{-3} s^{-1}, k_{t2}= 3.4 x 10^{-3} s^{-1}) are in good agreement with values from another recent study,[28] which gave 1 x 10^{-3} s^{-1} and 4 x 10^{-3} s^{-1} respectively. These two studies yield values for the equilibrium ratio [*cis*-$(en)_2Co(OH_2)(OH)^{+2}$]/ [*trans*-$(en)_2Co(OH_2)(OH)^{+2}$] of 2.1 and 4 compared to earlier equilibrium studies which gave 1.42[22] (25°, 1M $NaNO_3$) and 1.25[29] (30°, 1M $NaClO_4$). The experimental uncertainties in both k_{c2} and k_{t2} probably make the equilibrium ratios from the kinetic method least accurate.

Carboxylation

The present kinetic results for the carboxylation reactions are compared in Table 12 with the previous results for several similar species.

The rate constant reported here for the reaction of *cis*-$(en)_2Co(OH_2)(OH)^{+2}$ with CO_2 is quite similar to the values reported for the pentaammine species, for which a mechanism involving nucleophilic attack by coordinated hydroxide at the carbon centre of the CO_2 molecule has been proposed.[31] This is therefore the most likely path for *cis*-$(en)_2Co(OH_2)(OH)^{+2}$, and supports the earlier suggestion that the reverse process occurs without Co-O bond-breaking, since both the forward and the reverse reactions must involve the same activated complex.

A comparison of the rate constants for the reactions of $(tren)Co(OH_2)(OH)^{+2}$ and $(tren)Co(OH)_2^{+}$ with CO_2 (Table 12) shows that the latter is somewhat more reactive than the former. This is in contrast with the results for *cis*-$(en)_2Co(OH_2)(OH)^{+2}$ and *cis*-$(en)_2Co(OH)_2^{+}$, where the former is at least 10 times more reactive than the latter at 25°. However, such a comparison may be misleading, since the reactions being compared could have different mechanisms, as suggested by the large differences in the activation parameters. Re-evaluation of the

activation parameters of the (tren) complexes gave values (Table 12) which were more consistent with the reported data,[33] but which still differ considerably from each other. Thus any comparison of the relative reactivities is temperature dependent. For example, the rate constants for the reactions of the (tren) complexes are found by extrapolation to be equal at 10°.

A less ambiguous rate comparison can be made between *cis*-$(en)_2Co(OH_2)(OH)^{+2}$ and $(tren)Co(OH_2)(OH)^{+2}$, which shows the former to be considerably more reactive than the latter. A comparison of the basicities of these two complexes, as determined from the base dissociation constants, (K_b) shows that the coordinated hydroxide in the former complex is more basic than that in the latter. (Table 12) Thus the order of reactivity of these two complexes parallels the basicity of the coordinated hydroxide. This is consistent with a mechanism involving nucleophilic attack by coordinated OH^- on CO_2.

A comparison of the dihydroxo species shows that *cis*-$(en)_2Co(OH)_2^+$ is at least 3 times less reactive than $(tren)Co(OH)_2^+$, but this does not correlate with the corresponding values of K_b shown in Table 12.

A comparison can also be made between reactions (1.35) and (1.42).

$$H\text{–}OH + CO_2 \xrightarrow{k_{CO_2}} H\text{–}OCO_2H \qquad (1.35)$$

$$(en)_2(H_2O)Co\text{–}OH^{+2} + CO_2 \xrightarrow{k_{-2}} (en)_2(H_2O)Co\text{–}OCO_2H^{+2} \qquad (1.42)$$

If the first-order rate constant k_{CO_2} is converted into a second-order one by dividing by the solvent concentration (55 M), to obtain $8 \times 10^{-4} M^{-1}s^{-1}$, then a comparison with k_{-2} ($5.2 \times 10^{2} M^{-1}s^{-1}$) is possible. Coordination to the metal ion instead of to the proton increases the rate constant for hydration of CO_2 by a factor of 10^6. It has been suggested by several workers[28,31] that this effect is analogous to the catalysis of CO_2 hydration by the enzyme carbonic anhydrase, in which a hydroxide ligand is thought to be coordinated to the zinc ion at the active site at biological pH.[2]

In a recent study of the reaction of 2,4-pentanedione(acac) with *cis*-$(en)_2Co(OH_2)_2^{+3}$ and its conjugate bases, Buckingham *et al.*[28] report values of $5 \times 10^{-2} M^{-1}s^{-1}$ and $3 \times 10^{-2} M^{-1}s^{-1}$ (25°, 1M $NaClO_4$) for k_{12} and k_{32} as given in reactions (1.43) and (1.44) below.

$$cis\text{-}(en)_2Co(OH_2)(OH)^{+2} + acac \xrightarrow{k_{12}} cis\text{-}(en)_2Co(acac)^{+2} + 2\,H_2O \qquad (1.43)$$

$$cis\text{-}(en)_2Co(OH)_2^{+} + acac \xrightarrow{k_{32}} cis\text{-}(en)_2Co(acac)^{+2} + H_2O + OH^- \qquad (1.44)$$

These authors also showed that these reactions proceed without Co-O bond-breaking. They prefer a mechanism in which the overall rate of acac addition is controlled by initial bond formation, and thus k_{12} and k_{32} refer to initial nucleophilic attack by coordinated hydroxide at the carbonyl carbon centre of acac. A comparison of k_{12} and k_{32} with the rate constants k_{-2} and k_{-2}' (Scheme 5) shows that acac is much less reactive than CO_2. It is of interest to note, however, that the ratio of the rate constants for the reactions of CO_2 and acac with *cis*-$(en)_2Co(OH_2)(OH)^{+2}$ of ~10^4 is similar to the analogous ratio for the reactions of these ligands with OH^-, with rate constants of ~1.6×10^4 $M^{-1}s^{-1}$ and 0.5 $M^{-1}s^{-1}$ at 35°.[34,35]

Chelate Ring-Closure

A previous literature value[23] of the observed rate coefficient for chelate ring-closure of ~0.011 s^{-1} (pH 8.7, 20°) agrees with the data in Table 9. A value of $k_3K_w/K_{a2} = 1.11 \times 10^{-6}$ $M^{-1}s^{-1}$ (26°, 1M $NaClO_4$) was previously reported by Francis and Jordan,[17] from which K_{a2} can be calculated to be 9.7×10^{-10} M, using the value of k_3 reported here (0.060 s^{-1}) and $K_w = 1.79 \times 10^{-14}$ M^2.[36] This value of K_{a2} agrees fairly well with the previously reported value[23] of 1.78×10^{-9} M(20°). Both these values disagree considerably from the value of 2.5×10^{-8} M determined in the kinetic study. As mentioned earlier, the kinetic data are not consistent with either of the smaller values of K_{a2}. However, it should be pointed out that the value of K_{a2} so determined is almost solely dependent on the last 6 data points, which were obtained under conditions in which a large excess of both HCO_3^- and $CO_3^=$ were present. Under these conditions, the formation of significant amounts of ion-pair complexes of *cis*-$(en)_2Co(OH_2)(CO_3)^+$ with HCO_3^- and $CO_3^=$ is likely. Such ion-pair complexes might be considerably less reactive than "free" *cis*-$(en)_2Co(OH_2)(CO_3)^+$, and this could explain the decrease in k_{exp} previously accounted for by the larger value of K_{a2}. Because of this uncertainty in the k_{exp} values at

pH > 7.2, the upper limit previously calculated for k_3' is probably not meaningful.

The rate constant for ring-closure of *cis*-$(en)_2Co(OH_2)(CO_3)^+$ (k_3) is compared with the analogous constants for several other similar complexes in Table 12.

Table 12

Rate Constants for Ring-Closure of Cobalt(III) Complexes

Complex	10^2k, s^{-1}	Reference
cis-$(en)_2Co(OH_2)(CO_3)^+$	6.0	this work[a]
cis-$(tren)Co(OH_2)(CO_3)^+$	5.0	(33)[b]
cis-$(en)_2Co(OH)(PO_4H)$	0.083	(37)[c]
$(en)_2Co(OH_2)(C_2O_4)^+$	~0.01	(15b)[d]

(a) T = 26°, I = 1.0 M($LiClO_4$).

(b) T = 25°, I = 0.5 M(NaCl).

(c) T = 22.5°, I = 1.0 M($NaClO_4$).

(d) Extrapolated to 25°, I = 0.37 M($NaNO_3$).

The values for the two carbonato complexes in Table 12 are very similar to each other, suggesting that these species undergo ring-closure by a similar mechanism.

If the mechanism of chelate ring-closure involves dissociative water loss, then the rate constant

for the process should be similar to that for water exchange on the reactant species. Unfortunately, such values are not available, but a value of 9.2×10^{-4} s^{-1} (25°) has been reported[26] for the exchange of oxygen between H_2O and *cis*-$(en)_2Co(OH_2)(OH)^{+2}$. This value is about 50 times smaller than the ring-closure rate constants of the $(en)_2$ and (tren) complexes, suggesting that chelate ring-closure in these species proceeds by a different mechanism, or that the release of water from *cis*-$(N)_4Co(OH_2)(CO_3)^{+}$ species is considerably more facile than from *cis*-$(en)_2Co(OH_2)(OH)^{+2}$. If the latter were the case, it implies that the carbonate ligand has an unusually large *cis* labilizing effect.

In contrast to the carbonato complexes, the rate constant for ring-closure of *cis*-$(en)_2Co(OH)(PO_4H)$ to give $(en)_2CoPO_4$ is quite similar to that for oxygen exchange on *cis*-$(en)_2Co(OH_2)(OH)^{+2}$. Therefore for this species a dissociative ring-closure mechanism seems most probable. The monodentate phosphato complex in this study was formed from the reaction of $(en)_2Co(OH_2)(OH)^{+2}$ with phosphate, and it has been suggested[33] that the rate of isomerization of *trans*-$(en)_2Co(OH)(PO_4H)$ rather than ring-closure of *cis*-$(en)_2Co(OH)(PO_4H)$ may control the observed reaction rate. However, this possibility is clearly eliminated by the results of Lincoln and Stranks.[29,37]

The observed rate constant for the formation of $(en)_2CoC_2O_4$ from $(en)_2Co(OH_2)(C_2O_4)^+$ has a magnitude which is consistent with rate-limiting dissociative water loss. However, the possibility that the observed rate is controlled by the isomerization of an intermediate *trans* oxalato species is not excluded by the results in this case.

These comparisons suggest that the carbonato complexes may undergo ring-closure without Co-O bond-breaking. Oxygen(18) labelling experiments have shown that Co-O bond-breaking occurs in the acid and base-catalysed ring-opening of $(en)_2CoCO_3^+$, but the uncatalyzed path, reaction (1.45), has not been studied.

$$(en)_2CoCO_3^+ + H_2O \underset{k_3}{\rightleftharpoons} (en)_2Co(OH_2)(CO_3)^+ \qquad (1.45)$$

CHAPTER II

INTRODUCTION

Numerous kinetic and equilibrium studies of the reactions of first row transition metal ions with ligands have been reported in recent years. The results of these studies have been reviewed,[38,39,40,41,42] and further detailed discussion will not be given here. Much of the kinetic data has been interpreted using the S_N1IP mechanism, as formulated by Eigen and Wilkins.[43] This mechanism can be described by reactions (2.1) and (2.2),

$$M(S)_n^m + L^q \underset{}{\overset{K_o}{\rightleftharpoons}} \underbrace{\left\{M(S)_n \cdot L\right\}^{m+q}}_{\text{ion pair}} \qquad (2.1)$$

$$\left\{M(S)_n \cdot L\right\}^{m+q} \xrightarrow{k_{ex}} M(S)_{n-1}(L)^{m+q} + S \qquad (2.2)$$

where $M(S)_n^m$ refers to the solvated metal ion of charge m, L^q refers to the ligand of charge q, and S refers to the solvent molecule. Complex formation in solution is considered to proceed in two steps, the first of which is the rapid formation of an ion pair or outer sphere complex. The second step involves the replacement of a solvent molecule in the first or inner coordination sphere with the ligand molecule. This second step is dissociative in character, and thus the rate constant k_{ex} should be similar to that for solvent exchange on that metal ion.

The ion pair formation constant, K_o, is a

function of several variables, of which the charges on the metal and ligand species are two of the most important. The rates of formation and dissociation of the ion pair complex are determined by the rates at which the species can diffuse together or apart, and, since these processes are very rapid, equilibrium is always maintained. For low ligand concentrations, i.e. when $1 >> K_o[L]$, the rate law derived from (2.1) and (2.2) is $-d[L]/dt = K_o k_{ex}[M][L]$, which is the same as that observed experimentally for the reactions of a wide range of metal ions and ligands.[39]

The evidence in support of the S_N1IP mechanism is of two kinds, the first of which comes from kinetic studies. For a particular ligand reacting with a series of metal ions, the observed rate constant is usually similar to the rate constant for solvent exchange on that metal ion. This is predicted by the S_N1IP mechanism for systems in which the value of K_o is close to unity. The rates of reaction of a metal ion with a series of unidentate ligands are insensitive to the size or nature of the ligand, but are very dependent on the charge on the ligand. This is consistent with dissociative activation along with a prior step to account for the effect of the charge.

The second kind of evidence concerns the existence of the outer sphere complex. Before a reaction

can occur, the reactants must be brought together. The outer sphere complex satisfies this requirement. In inert systems, such as those of cobalt(III) complexes, rapid spectral changes often occur upon addition of ligand,[44] which suggest some association of the reactants prior to the substitution process. Other measurements on more labile systems by ultrasonic absorption[45] lead to the same conclusion. While these results give fairly conclusive evidence of the existence of outer sphere complexes, they do not prove that inner sphere substitution proceeds through such outer sphere complexes. An equation has been derived[46,47] from theory which allows calculation of the value of K_o, and the calculated and measured values are in fair agreement for systems where a measurement of K_o has been made.

Much of the kinetic evidence in support of the Eigen mechanism has come from studies with nickel(II) ion.[39] This is mainly because the reactions with nickel(II) are generally slower than those with other +2 metal ions, and are therefore easier to study. A wider range of reaction conditions is usually available, and the choice of ligands is thus less restricted. The nickel(II) ion is also convenient for study because it is not subject to oxidation, and hydrolysis in aqueous solution is not a problem, at least below pH 7.

In this study, the validity of the Eigen mechanism will be accepted. The purpose here will be to exploit the previous knowledge and conclusions to investigate the order of events which occurs when a multidentate ligand reacts with a metal ion to form a chelated complex. For the simplest case of a bidentate ligand, there already have been a number of studies.[48-51] Unfortunately, it has been shown recently[52] that much of the previous work was interpreted incorrectly. For example, in the case of glycine, the mechanism for complexation with a metal ion, M, has been interpreted by Cassatt and Wilkins[50] using the reactions in Scheme 7.

Scheme 7

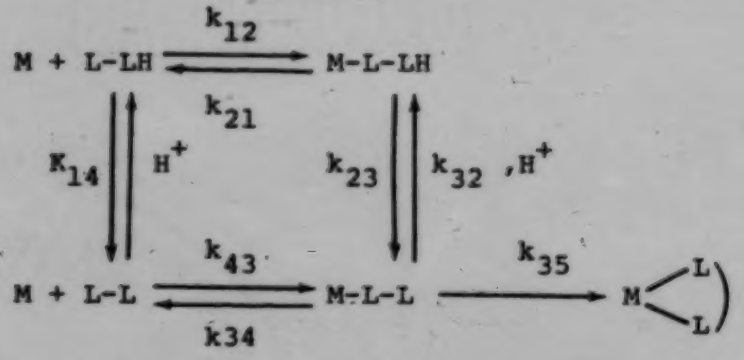

L-LH represents the glycine zwitterion, $^{-}O_2CCH_2NH_3^{+}$ and L-L represents the anion, $^{-}O_2CCH_2NH_2$. Throughout this discussion, it is assumed that the rate constants k_{12} and k_{43} are really appropriate products of K_o and k_{ex} . If the steady-state approximation is made for the

monodentate species M-L-LH and M-L-L, and if the equilibrium governed by K_{14} is considered rapid, then the rate law is

$$\text{Rate} = k_{obs}[M]\ L_t$$

$$= \frac{\left\{k_{12}k_{35}k_{23}(H^+) + (k_{21} + k_{23})k_{35}k_{43}K_{14}\right\}[M]\ L_t}{(K_{14}+(H^+))\left\{(k_{21}k_{32}(H^+) + (k_{35}+k_{34})(k_{23}+k_{21})\right\}} \qquad (2.3)$$

where

$$L_t = ([L\text{-}L] + [L\text{-}LH]) \qquad (2.4)$$

If $k_{23} > k_{21}$, and for $[M] > L_t$, equation (2.3) can be reduced and rearranged to give

$$\frac{k_{obs}(K_{14}+(H^+))}{(H^+)} = \frac{k_{12}k_{23}k_{35} + k_{43}k_{23}k_{35}K_{14}(H^+)^{-1}}{k_{21}k_{32}(H^+) + k_{23}(k_{35}+k_{34})} \qquad (2.5)$$

In order to obtain the same form of equation as that observed experimentally, a further approximation is necessary. Cassatt and Wilkins[50] assumed that

$$k_{21}k_{32}(H^+) < k_{23}(k_{35}+k_{34}) \qquad (2.6)$$

and if $k_{35} > k_{34}$, then equation (2.5) reduces to

$$\frac{k_{obs}(K_{14}+(H^+))}{(H^+)} = k_{12} + \frac{k_{43}K_{14}}{(H^+)} \qquad (2.7)$$

For a large number of amino acids and other bidentate

ligands, a plot of the experimental function on the left-hand side of equation (2.7) *versus* $(H^+)^{-1}$ yields a straight line. The intercepts of such plots are generally close to zero, and this implies that $k_{12} \approx 0$. This result has been interpreted[50] as proof that the zwitterion form of the amino acid is unreactive.

However, a recent reappraisal[52] of the approximation in equation (2.6) suggested that the inequality should be reversed. For an amino acid, the acid dissociation constant K_{14} is usually less than 10^{-9}M. The acid dissociation constant for the monodentate complex, M-L-LH, defined as $K_{23} = k_{23}/k_{32}$, is expected to be less than 3×10^{-9} M, which is the value reported[53] for the proton dissociation constant of coordinated glycine in $(NH_3)_5CoO_2CCH_2NH_3^{+3}$. Common experimental conditions require that $(H^+) \geq 10^{-7}$ M. If k_{21} is given a value[54] of $10^4 s^{-1}$, and $(k_{35}+k_{34}) < 5 \times 10^4 s^{-1}$, as expected if k_{34} is similar to k_{21} and if k_{35} is similar to the rate constant for water exchange[55] on $Ni(OH_2)_6^{+2}$, then it is seen that $k_{21}(H^+) > K_{23}(k_{35}+k_{34})$. With this approximation equation (2.5) reduces to

$$\frac{k_{obs}(K_{14}+(H^+))}{(H^+)} = \frac{k_{12}k_{35}}{k_{21}(H^+)} \qquad (2.8)$$

This equation also predicts a linear plot of $k_{obs}(K_{14}+(H^+))/(H^+)$ *versus* $(H^+)^{-1}$, with an intercept of zero. As mentioned earlier, this is the result found experimentally. This equation does not require that the zwitterion be unreactive, but instead suggests that the process of chelate ring-closure is rate determining for this type of reaction under the conditions specified.

The present work will be concerned with the complexing of the amino acid histidine, and several of its derivatives. Histidine is an interesting ligand from several points of view. Like many amino acids, it has an asymmetric carbon centre, and thus exists in both *D*- and *L*-isomers. It has been located near the active site in a number of proteins,[56] and its coordination to the metal ion at the active site is proposed in some of these enzymatic species.[57] As a chelating ligand, histidine is potentially tridentate, and its three basic groups should be quite unique in their coordinating abilities.

Two previous kinetic studies of the reaction of *L*-histidine with $Ni(OH_2)_6^{+2}$ have been reported.[49,50] These results were interpreted using the simplest approach, which begins by assuming that initial bond formation is rate determining, and that all further chelation steps proceed rapidly. Using this approach, one obtains an expression of identical form to equation

(2.7), except that K_{14} now refers to the acid dissociation constant for the imidazole proton rather than the amine proton, and k_{12} and k_{43} are the rate constants for reaction of the metal ion with the cationic and zwitterionic forms of histidine respectively. The experimental results gave linear plots of $k_{obs}(K_{14}+(H^+))/(H^+)$ *versus* $(H^+)^{-1}$, with intercepts close to zero. A discussion of these results using a more complex model will be included later.

A second slower reaction was also observed in previous studies with *L*-histidine.[49,50] It was proposed by Letter and Jordan[49] that this slow reaction involved formation of a binuclear nickel(II) species, formed by attack by a second nickel ion at the remote pyrrole nitrogen of the histidine ligand. In a similar study[51] with the modified species, *L*-3-methylhistidine, in which the pyrrole nitrogen is blocked, the slower reaction was not observed. This complication seems to arise because of the reaction conditions, in which the nickel(II) concentration is kept in large excess over that of the ligand.

In the present work, a stable Schiff base complex of nickel(II), triaquotribenzo[*b*,*f*,*j*]-[1,5,9]-triazacycloduodecinenickel(II),(Figure 9) known as $NiTRI(OH_2)_3^{+2}$, was chosen for study for a number of reasons. Formation of *bis* complexes of $NiTRI(OH_2)_3^{+2}$

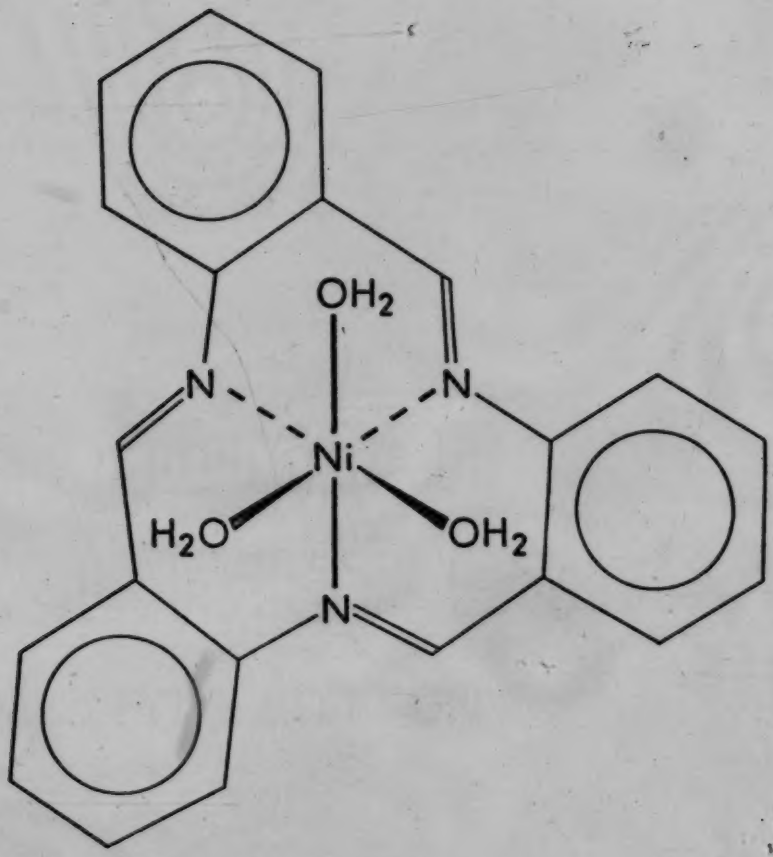

Figure 9. The structure of the Schiff base complex $NiTRI(OH_2)_3^{+2}$.

with a multidentate ligand is unlikely to occur, since only three positions are available for substitution. This allows for a greater range of possible concentration conditions, which could be quite advantageous. In particular, if a study of the histidine reaction could be made under conditions of high ligand to metal ratio, complications arising from attack by a second metal species would be unlikely to occur.

The rate constant for water exchange on $NiTRI(OH_2)_3^{+2}$ ($3.8 \times 10^4 s^{-1}$, 25°)[59] is similar to that reported for $Ni(OH_2)_6^{+2}$ ($3.3 \times 10^4 s^{-1}$)[55]. Thus it is expected that conclusions regarding the pathways for formation of a chelate complex of $NiTRI(OH_2)_3^{+2}$ should be generally applicable to $Ni(OH_2)_6^{+2}$, assuming that both undergo substitution by an S_N1IP mechanism.

The structure of $NiTRI(OH_2)_3^{+2}$ contains no axis of improper rotation, S_n, and thus can exist as either of two isomers, which are mirror images of each other. In fact, a resolution of these isomers has been reported.[60] The reaction of one optical isomer of $NiTRI(OH_2)_3^{+2}$ with an optically active ligand such as histidine, might show a kinetic stereoselectivity, which would be interesting to investigate, and might also help to determine the order in which the chelation steps occur.

In summary, the intention of this study is to

investigate the binding of several multidentate ligands such as histidine and its derivatives with the nickel(II) complex $NiTRI(OH_2)_3^{+2}$.

EXPERIMENTAL

Materials

The nickel complex, triaquotribenzo[*b*,*f*,*j*]-[1,5,9]triazacycloduodecinenickel(II)nitrate, $NiTRI(OH_2)_3^{+2}$, was prepared as suggested by Taylor and Busch.[61] The compound o-amino-benzaldehyde was prepared by reduction of o-nitro-benzaldehyde with $FeSO_4$ as described by Smith and Opie.[62] A sample (4.5 gm) of this was allowed to trimerize by self-condensation in dilute HCl under a nitrogen atmosphere, (as described by McGeachin,[63]) to form the tridentate ligand 13-hydroxy-6,12-benzo-6H-quinazolino[3,4,a]quinazoline. A suspension of this ligand (1.0 gm) was heated with an equimolar amount of nickel(II) nitrate hexahydrate in 40 ml of absolute ethanol for one hour. The initially green solution gradually became yellow-orange, and the nickel complex precipitated. The $NiTRI(OH_2)_3(NO_3)_2$ (1.5 gm) was isolated by filtration, and re-dissolved in 100 ml of warm water. After addition of ~10 ml of 3M $NaClO_4$, the solution was cooled for several hours. The precipitate, $NiTRI(OH_2)_3(ClO_4)_2$, was collected by filtration, and recrystallized twice from water and $NaClO_4$ as described above. The product was washed with cold water, and dried for several days under vacuum over $CaSO_4$. *Analysis*. Calculated for

$NiTRI(OH_2)_3(ClO_4)_2$: C, 40.62; H, 3.41; N, 6.78. Found: C, 40.75; H, 2.79; N, 6.85.

The electronic spectrum of a sample of $NiTRI(OH_2)_3(ClO_4)_2$ dissolved in 10^{-2} M $HClO_4$ has absorption maxima at 315 nm (ε 1.18 x 10^4 $dm^3mol^{-1}cm^{-1}$) and at 275 nm (ε 4.10 x 10^4 $dm^3mol^{-1}cm^{-1}$), which are in good agreement with the previously reported[60] maxima at 325 nm (ε 1.15 x 10^4 $dm^3mol^{-1}cm^{-1}$) and at 275 nm (ε 4.17 x 10^4 $dm^3mol^{-1}cm^{-1}$). A comparison of the complete electronic spectrum (250-1100 nm) of an aqueous solution of $NiTRI(OH_2)_3(ClO_4)_2$ with that shown in reference 60 further supports the characterization of the product. The IR spectrum of a sample of the complex was in agreement with that previously reported.

Aqueous solutions of $NiTRI(OH_2)_3(ClO_4)$ at pH< 7 are reasonably stable, as confirmed by the reproducibility of the electronic spectrum over a period of three days. However, for the kinetic experiments fresh solutions were prepared directly by weighing just prior to use.

A stock solution of nickel(II) perchlorate was prepared by mixing reagent grade nickel(II) carbonate (J.T. Baker) with an equivalent amount of perchloric acid. This solution was standardized by titration with

EDTA, using murexide indicator (Fisher).

The ligands *D*-histidine, *DL*-histidine, *L*-3-methylhistidine, and *L*-1-methylhistidine (the latter two of which are named using biochemical nomenclature) were used as supplied by Sigma Chemical Co. The ligand *L*-histidine, (free base, Nutritional Biochemicals Corp.) was recrystallized from 50% aqueous ethanol, and dried under vacuum over $CaSO_4$ before use. *Analysis.* Calculated for $C_6H_9N_3O_2$: C, 46.5; H, 5.81; N, 27.1. Found: C, 46.9; H, 5.83; N, 27.5. Glycine (free base) was prepared by dissolving 8 gm of the hydrochloride salt (Eastman) in 100 ml of hot 50 % aqueous ethanol solution containing 3 gm of NaOH. Upon refrigeration, the free base crystallized, and was collected by filtration. The crystals were washed with cold distilled water and with ethanol, and dried under vacuum over $CaSO_4$. A sample dissolved in water was found to contain very little chloride ion, as indicated by testing with $AgNO_3$. Histamine (free base) was used as supplied (Matheson, Coleman, and Bell), after drying under vacuum over $CaSO_4$ for several days. *Analysis.* Calculated for $C_5H_9N_3$: C, 54.0; H, 8.11; N, 37.8. Found: C, 53.4; H, 8.07; N, 38.2. Solutions of these ligands were prepared by weighing the

appropriate amount of the solid directly into a 25 ml volumetric flask, adding aliquots of the $LiClO_4$ and indicator stock solutions as needed, and diluting to volume. All ligand solutions were prepared just prior to use.

The concentrations of *L*-3-methylhistidine and *L*-1-methylhistidine were checked in a few cases by pH titration of a small aliquot of the solution prepared for the stopped-flow experiments. Corrections of 16.4% and 9.2% were applied respectively, to account for the difference between the weighed amount and the actual concentration. This discrepancy is assumed to be due to absorbed water.

Solutions of *L*-histidine methyl ester were prepared from the dihydrochloride salt of *L*-histidine methyl ester (Aldrich). *Analysis*. Calculated for $C_7H_{13}N_3O_2Cl$: C, 34.7; H, 5.41; N, 17.4. Found: C, 34.4; H, 5.32; N, 17.4. Each sample of the salt was weighed directly into a 15 ml centrifuge tube, and then dissolved in 5.00 ml of distilled water. Then 1.00 ml of a solution containing enough $AgClO_4$ (British Drug Houses) to precipitate 98% of the chloride ion present was added. After shaking well, the mixture was centrifuged for fifteen minutes. Exactly 5.00 ml of the clear

supernatant were removed for preparation of the solution to be used in the kinetic experiments.

The ligand α-N,N,N-trimethyl-*L*-histidine (hercynine) was prepared by the method of Reinhold *et al.*[64] The recrystallized product was dried under vacuum, and melted with decomposition at 239-241°. The proton NMR spectrum also confirmed the structural characterization. *Analysis*. Calculated for $C_9H_{15}N_3O_2$: C, 54.8; H, 7.67; N, 21.3. Found: C, 53.8; H, 7.60; N, 20.8.

The ligand N-methyliminodiacetic acid (MIDA) was used without further purification as supplied by K and K Laboratories.

Stock solutions of the buffers MES (2-(N-morpholino)ethanesulfonic acid) and PIPES (1,4-piperazinebis-(ethanesulfonic acid)) were prepared from the commercial products as supplied (Polysciences). Stock solutions (5×10^{-4} M) of the indicators bromothymol blue and bromocresol purple (Matheson, Coleman, and Bell) were prepared by dissolving the commercial products in water containing an equivalent amount of NaOH.

Stock solutions of $LiClO_4$ (Alfa Inorganic), perchloric acid, and sodium hydroxide were prepared as described in the experimental section of Chapter I. All solutions were prepared from water which had been

distilled twice in glass apparatus, and the last distillation was from alkaline potassium permanganate. $k_{12} = (1 \pm 0.6) \times 10^{-7}$ M^{-1} s^{-1} and $k_{35}K_{a4}/k_{21} = (4 \pm 3) \times 10^{-7}$ M. This analysis suggests that a thorough kinetic study of the $Ni(OH_2)_6^{+2}$-histamine system is warranted. The k_{12} value above is consistent with the other rate constants in Table 30.

Resolution of $NiTRI(OH_2)_3^{+2}$

Ion Exchange Method

Approximately 10 gm of the weak acid cation exchange resin, CCC-271 (Baker), were washed thoroughly with ethanol and diethyl ether. The resin was then treated several times with 100 ml of 1.0M NaOH, to convert it into the Na^+ form. The resin was then slurried in water, and transferred to a glass column 20 cm long and 2 cm in diameter. The resin was eluted with distilled water until no pH change could be detected on passage through the column. The pH of the column was then adjusted to ~6 by elution with acetate buffer (50 ml of 0.04M sodium acetate adjusted to pH 6 with acetic acid). A solution containing 0.077 gm of *L*-histidine, 0.062 gm of racemic $NiTRI(OH_2)_3(ClO_4)_2$ and sodium acetate buffer (0.04M) at pH 6 was placed on the column. The column was then eluted with acetate buffer containing *L*-histidine (10^{-2}M). The concentration of the buffer was increased step-wise to 0.80M, at which point the complex was seen

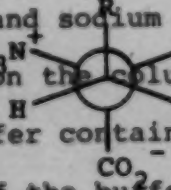

XI

178

The study of the reaction of hercynine with $Ni(OH_2)_6^{+2}$ resulted in a value of $k_{46} + k_{43}k_{35}/(k_{35} + k_{34})$ (Scheme 8). This parameter relates to the reactivity of the hercynine zwitterion, and thus should be comparable to the k_{12} values for histidine or 3-methylhistidine. The results in Table 30 show that hercynine is about four times less reactive than the histidine zwitterion, but is similar in reactivity to the cationic ligands, histamine(k_{12}) and histidine methyl ester(k_{12}). A possible explanation for the slower than expected reaction rate of hercynine is suggested by a recent carbon(13) nmr study[78] which indicated that 95% of the hercynine molecules in an aqueous solution at pH 5-7 exists as the *trans* rotamer XI, where R≡$C_3H_3N_2$.

to move down the column. Six 20 ml fractions of eluent were collected sequentially, and the optical rotation of each was measured using a Perkin-Elmer Model 241 polarimeter. The optical rotation of a blank containing 10^{-2}M *L*-histidine in 0.8M sodium acetate buffer was also measured. The electronic and ORD spectra of acidified (pH 2, $HClO_4$) samples of the second and sixth fractions were recorded. Upon addition of minimal volumes of 6M $HClO_4$ and 4M $NaClO_4$, crystalline $NiTRI(OH_2)_3(ClO_4)_2$ could be recovered after cooling.

Precipitation Method

An aqueous solution of 0.060 gm of racemic $NiTRI(OH_2)_3(ClO_4)_2$ (10 ml) was added with stirring to 10 ml of water containing 0.240 gm of *L*-histidine and sufficient acetic acid to adjust the initial pH to 6.2. Precipitation of a yellow-orange product begins after about 30 s of rapid stirring. After 15 minutes, this precipitate was collected by filtration in a sintered glass filter funnel, washed with cold distilled water, and air-dried. A sample of this precipitate was dissolved in 10^{-2}M $HClO_4$, and its optical rotation was measured. The remainder of the precipitate was dissolved in 10^{-2}M acetic acid. A solution containing a 20 fold excess of *L*-histidine was added, together with enough NaOH to neutralize the acetic acid, to a

The size and possibly the charge of the trimethylamine substituent, which is fixed in the vicinity of the imidazole ring, may inhibit close approach of the metal ion to the imidazole nitrogen thus causing k_{46} to be smaller than expected. Metal ion attack at the carboxylate oxygen is still favorable in XI but there may be steric inhibition to ring-closure (k_{35}) resulting in a smaller than expected value of $k_{43}k_{35}/(k_{35}+k_{34})$. Therefore the known conformation and steric effects may explain the observed reactivity of hercynine.

It is interesting to note that histidine is only about 50% in the conformation analogous to XI[79], and of course it lacks the bulky methyl substituents. Therefore the type of steric inhibition suggested for hercynine should not be important for histidine. A comparison of the formation rate constants for the reactions of histidine and its derivatives (Tables 29 and 30) suggests that $NiTRI(OH_2)_3$ is slightly more reactive than $Ni(OH_2)_6$. Within the experimental error limits, this difference can be explained by taking account of the greater water exchange rate (~14%) on $NiTRI(OH_2)_3$[42] and the small differences in reaction conditions. Thus on the basis of the available results, it is concluded that steric

final pH of 6. Again a precipitate was formed, and it was separated by filtration. A sample was taken for measurement of the optical rotation. This process was repeated once again to ensure complete resolution of the isomers. A sample of the washed, dry crystalline material was sent for microanalysis, and another was dissolved in 10^{-2}M $HClO_4$ for measurement of the ORD spectrum. The remaining precipitate was dissolved in 10^{-2}M $HClO_4$, and 4M $NaClO_4$ was added. After cooling, $NiTRI(OH_2)_3(ClO_4)_2$ was recovered by filtration.

The other isomer could be obtained by either of two methods. When a few ml of 4M $NaClO_4$ was added to the filtrate obtained earlier, a precipitate was formed upon cooling. This precipitate was re-dissolved in 10^{-2}M $HClO_4$ and re-precipitated by addition of excess 4M $NaClO_4$ and cooling. The electronic and ORD spectra of a sample of this precipitate dissolved in 10^{-2} M $HClO_4$ were recorded.

This second isomer could also be recovered by addition of an aqueous solution of *D*-histidine to the original filtrate obtained earlier. The $NiTRI(OH_2)_3(ClO_4)_2$ was recovered from solution by addition of $NaClO_4$ as described above.

A collection of kinetic results for the reactions of α-amino acids with nickel(II) is shown in Table 31. The rate parameter (a/K_{a2}) shows an apparent decrease in value as the size of the α-substituent increases. This variation has been attributed by Voss and Jordan[80] to an increase in k_{34} with increased ligand size. This explanation is consistent with the rate expression derived for Scheme 12 (equation (2.68)).

However the present analysis predicts that a/K_{a2} will also depend on k_{32} for amino acids with $pK_{a2} < 9$. As pK_{a2} decreases k_{32} should decrease and a/K_{a2} should decrease. Unfortunately, the available results (Table 31) neither confirm nor deny the effect of k_{32} on a/K_{a2}.

Comparison shows that the rate parameters (a/K_{a2}) for the reactions of glycine with $NiTRI(OH_2)_3^{+2}$ and $Ni(OH_2)_6^{+2}$ are very similar with a value of ~1.6 x $10^4 M^{-1}s^{-1}$. As shown previously, the expression for a/K_{a2} for glycine reduces to $a/K_{a2} = k_{43}k_{35}/k_{34} + k_{46}$. The apparent lack of difference in the a/K_{a2} values, in contrast to the larger rate constants for $NiTRI(OH_2)_3^{+2}$ with histidine derivatives, could indicate the importance of the $k_{43}k_{35}/k_{34}$ term. If the values of k_{43} and k_{35} are larger in the

Determination of the Acid Dissociation Constant of Hercynine

The value of the pK_a for hercynine in 0.30 M $LiClO_4$ at 25±0.2° was determined by pH titration. Samples of the ligand were titrated with 0.202 M $HClO_4$, using a Metrohm Dosimat titration apparatus. The pH was measured using a Metrohm E300B pH meter and combination microelectrode previously described (Chapter). Three titrations were made, from which the average pK_a was determined from the half-neutralization point to be 6.05±0.03.

Kinetic Measurements

The rates of the reactions of $NiTRI(OH_2)_3^{+2}$ with histidine, *L*-3-methylhistidine, *L*-1-methylhistidine, histamine, glycine, and *L*-histidine methyl ester have been measured in the pH range 5-7. In initial runs with histidine, the reaction was followed directly by observation of the decrease in transmittance at 275 nm. All of the remaining studies were made by following the rate of release of H^+, using the transmittance change due to an acid-base indicator in the solution. The Aminco-Morrow stopped-flow apparatus described in Chapter was used to obtain the kinetic data. The temperature was controlled and monitored at 25.0±0.5° using the equipment

Table 31. Results for the Reactions of Several α-Amino Acids with Nickel(II)

Amino acid	α-substituent	pK_{a2}	$10^{-4}(a/K_{a2})$, M^{-1} s^{-1}	Reference
Glycine	-H	9.71	1.5 ±.2	this work[b]
			1.1 ±.1	81
			1.1 ±.1	c
			2.1	82
			4.2	80
Serine	$-CH_2OH$	9.34	2.2	80
Aspartic Acid Amide	$-CH_2CONH_2$	8.8	0.87	80
Diaminobutyric Acid	$-(CH_2)_2NH_3^+$	~8.4[d]	0.56	80
Ornithine	$-(CH_2)_3NH_3^+$	8.83[d]	0.43	80
Lysine	$-(CH_2)_4NH_3^+$	9.22[d]	0.58	80
1-methylhistidine	$-CH_2C_4H_5N_2$	8.60	0.5 ±.1	this work[b,e]
Tyrosine	$-CH_2C_6H_4OH$	9.28[d]	0.54	80

described earlier in Chapter I. The ligand was always kept in at least a ten-fold molar excess over the $NiTRI(OH_2)_3^{+2}$. The pH of each of the reactants was adjusted prior to mixing with a small volume of $HClO_4$ (less than 100 µl), and the pH of the products was measured within 10 minutes of mixing in the stopped-flow system, using the pH meter and probe described in Chapter I.

Blank experiments, made by mixing in the stopped-flow apparatus solutions of $NiTRI(OH_2)_3^{+2}$ and bromothymol blue indicator, each containing PIPES buffer, showed a small (~3%), slow increase in transmittance at 620 nm at pH 6.2. In most of the histidine results, the indicator was not included in the $NiTRI(OH_2)_3^{+2}$ solutions, but identical runs in which the bromothymol blue was included in both solutions showed no significant difference in the observed rate coefficient. Similar blank experiments with bromocresol purple indicator at pH 6.2 (λ=590 nm) showed no transmittance change. In all of the studies with the other ligands, the indicator was included in both reactant solutions. Blank experiments in which a histidine solution was mixed in the stopped-flow system with bromothymol blue or bromocresol purple and MES buffer showed no transmittance changes at 620 or 590 nm respectively (pH 6.2).

The pseudo-first-order rate coefficients were

Table 31 (cont'd)

(a) The parameter a is defined by the experimental rate law equation (2.65).

(b) Value at 25°, I = 0.30 M($HClO_4$). The error estimates are approximate 95% confidence limits.

(c) Least-squares "best-fit" value and 95% confidence limits calculated from data in reference 48.

(d) Microacidic dissociation constants as given and discussed in reference 80.

(e) Value of a/$K_{a1}K_{a2}$ as defined in equation (2.70).

determined from the photographic traces using the least-squares program described in Appendix A.

Several different combinations of optical isomers of $NiTRI(OH_2)_3^{+2}$ and histidine were studied. Racemic $NiTRI(OH_2)_3^{+2}$ was used for all of the studies with the other ligands.

The reaction of $Ni(OH_2)_6^{+2}$ with *L*-histidine was studied under conditions of excess ligand. The ligand solutions were prepared similarly to those already described, while the $Ni(OH_2)_6^{+2}$ solution was prepared by dilution of the stock solution described earlier. Both reactants contained indicator and 0.30 M $LiClO_4$, and the $Ni(OH_2)_6^{+2}$ solution contained a small amount (0.002M) of buffer to stabilize its initial pH.

In the study of the reaction of $Ni(OH_2)_6^{+2}$ with *L*-hercynine, the metal ion was kept in excess over the ligand, since under these conditions complex formation was most favorable, and easier to study.

NMR Measurements

Measurements of the solvent proton longitudinal relaxation time, T_1, in an aqueous solution of $NiTRI(OH_2)_3^{+2}$ containing various known amounts of ligand, were made using a Brüker SXP 4-100 pulsed nmr instrument operating at 60 MHz. A triplet pulse sequence (180-τ-{90-180-90}-τ-

system because of the greater water exchange rate, but k_{34} is also increased as a result of the steric effects of TRI ligand, then a/K_{a2} could remain constant for the two metal complexes. This cancelling would not result if only the k_{46} term were present. Although this argument is potentially useful, it does not confirm the importance of the $k_{43}k_{35}/k_{34}$ term because the experimental uncertainties in the a/K_{a2} values in Table 31 are larger than the expected difference of ~14% in the forward rate constants.

The results for the reaction of 1-methylhistidine with $NiTRI(OH_2)_3^{+2}$ yield a value of $a/K_{a1}K_{a2}$ from the experimental rate law. When interpreted by Scheme 9, $a/K_{a1}K_{a2}$ is given by equation (2.74). Since the k_{46} path was not included in Scheme 9, the expression for $a/K_{a1}K_{a2}$ in equation (2.74) is equivalent to that given in equation (2.68) for a/K_{a2}. Therefore $a/K_{a1}K_{a2}$ for 1-methylhistidine is compared to the values of a/K_{a2} for other systems in Table 31. The comparison shows that the 1-methylhistidine value fits into the same pattern as the other values in Table 31.

In order to better understand the implications of the kinetic results, it is useful to consider the mechanisms in some detail. The expression derived for Scheme 10 (equation (2.38)) shows that, in general,

{90-180-90} ...) was used, and the magnetization constant each 180° pulse was displayed as a function of time on the oscilloscope screen, after storage in a Tracor Northern N S 570 data accumulator. This first-order decay was compared visually to an exponential curve simulated by the output from a series R-C network. Variation of the resistance (R) and the amplitude of the signal allowed the simulated curve to be superimposed upon the experimental trace, the former of which was displayed on the oscilloscope screen via a second channel. The time constant was then determined directly from the simulator values of R and C. Comparisons of the T_1 values obtained by this method were found to agree within ±5% of those determined by least-squares analysis of the digitized experimental data.

The experiments were made using a titration technique, in which incremental volumes (100–500 µl) of the ligand solution were added to 2.00 ml of 4.0×10^{-3} M $NiTRI(OH_2)_2(ClO_4)_2$ solution in 0.10 M MES buffer initially adjusted to pH 6.20 (or 6.98). The T_1 was measured after each addition of ligand solution, as well as on pure solutions of $NiTRI(OH_2)_4^{+2}$ and ligand. The temperature was 25±1° in all cases.

Solutions of the ligands *L*-histidine, *L*-hercynine, histamine, *L*-histidine methyl ester, and MIDA were prepared by dissolving weighed amounts of the compounds

four terms can contribute to the forward rate constant k_f. Comparison of equation (2.38) with the experimental rate laws for the reactions of ligands having k_{a2}^+ led to the conclusion that the pH independent terms in the numerator of (2.38) do not contribute significantly to the observed rate under the experimental conditions. Of the two terms remaining in equation (2.38), the $k_{46}K_{a2}$ is eliminated relative to $k_{12}k_{35}K_{a4}/k_{21}$ because of the upper limit placed on k_{46} by the stopped-flow mechanism. These simplifications led to Scheme II.

The mechanism shown in Scheme II is proposed as the most favorable reaction sequence for the reactions of histidine, 3-methylhistidine, and histamine. This reaction sequence consists of three steps, as illustrated by the reaction coordinate diagrams shown in Figure 18. The reactants at A are the nickel(II) species and the monoprotonated ligand species. Initial bond formation at the imidazole nitrogen (k_{12}) gives the protonated monodentate intermediate B in Figure 18. Since $k_{12} \gg k_{21}$, formation of B is favorable. Loss of the proton leads to the fully deprotonated monodentate intermediate, C, which undergoes ring-closure by k_{35} to give the bidentate product, D. It has been assumed in constructing these diagrams that initial bond-formation (k_{12}) and ring-closure (k_{35}) are controlled by dissociative water loss, and

in water, to give final concentrations of 0.020 or 0.040M. MES buffer (0.10M) was included in these solutions, and the pH of each was adjusted as required with 2.0M $HClO_4$.

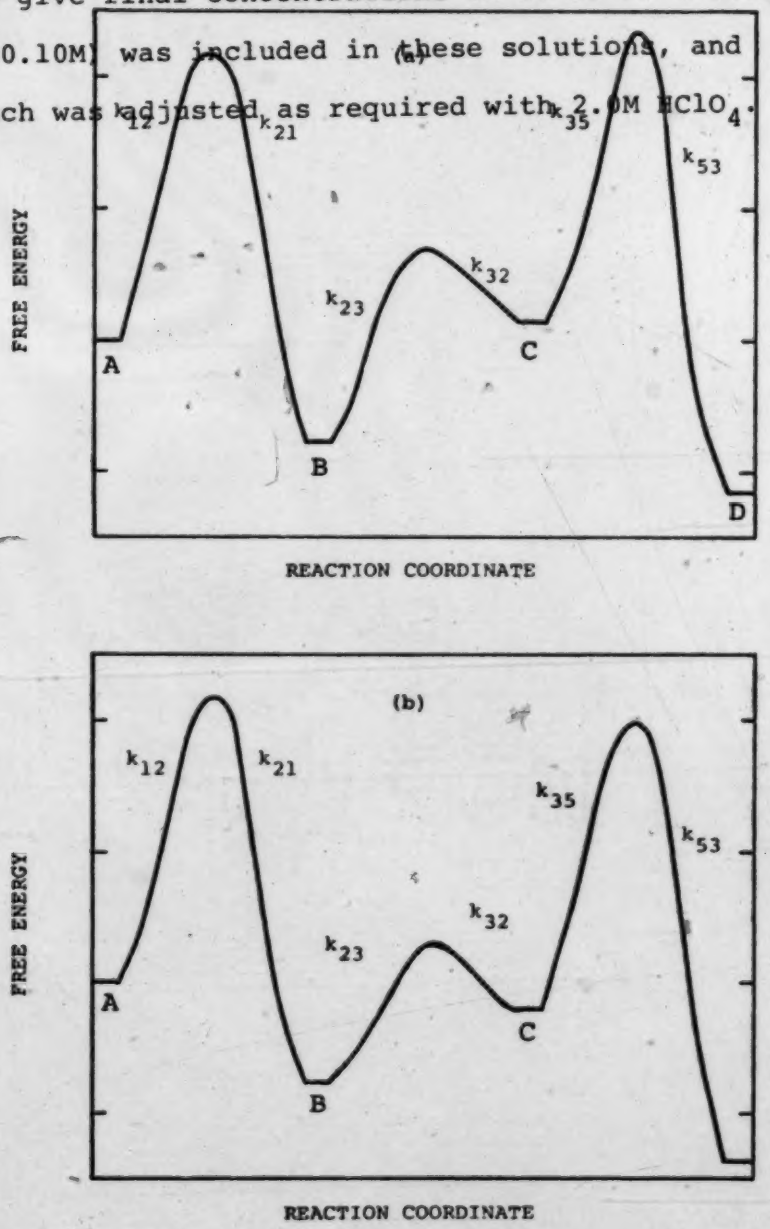

Figure 18. Reaction coordinate diagrams illustrating the mechanism of chelation of a bidentate ligand.
(a) Ring-closure is rate-determining .
(b) Initial bond formation is rate-determining.

thus have similar activation barriers. Also $k_{21} << k_{23} < k_{32}$, as estimated in the analysis of Scheme 11.

In Figure 18(a), the k_{35} path leads to the point of highest energy on the reaction coordinate, and thus, by definition, k_{35} is the rate-determining step. By relating the free energy changes to the rate constants, it can be shown that Figure 18(a) is applicable when $k_{35}k_{23} < k_{32}k_{21}$, or when $k_{35}/k_{21} < (H^+)/K_{a4}$ (since $k_{23}/k_{32} = K_{a4}/(H^+)$). This condition is approached in the lower part of the experimental pH range, when the deprotonated intermediate C is least stable.

In some systems at low pH, the bidentate product may become less stable than the monodentate intermediate B (Figure 18). This was suggested in the histamine-$NiTRI(OH_2)_3^{+2}$ system. However, it is noted that the fraction of the total ligand in the fully protonated form increases as the pH is lowered, with the result that the formation of B becomes less favorable. In order for the concentration of B to be significant relative to A and D, the equilibria require that $k_{53}(H^+) \gtrsim k_{35}K_{a4}$, and also $k'_{12} \equiv k_{12}K_{a1}L_t/(K_{a1}+(H^+)) \gtrsim k_{21}$.

These requirements limit considerably the optical isomers of $NiTRI(OH_2)_3^{+2}$ by selective precipitation from systems in which B is likely to be present at detectable concentrations.

Preliminary attempts to separate the number of cation exchange column indicated that resolution could

As the pH is increased, the stability of C

increases, as illustrated in Figure 18(b). This results from the increase in k_{23}, since all of the other rate constants in Figure 18 are pH independent. The diagrams show a change in the rate-determining step from ring-closure (k_{35}) to initial bond formation (k_{12}) as the pH is increased. This interpretation is implied by the rate law derived for Scheme 11 (equation (2.49)), which in turn is consistent with the experimental results for the reactions of histidine, 3-methylhistidine, and histamine.

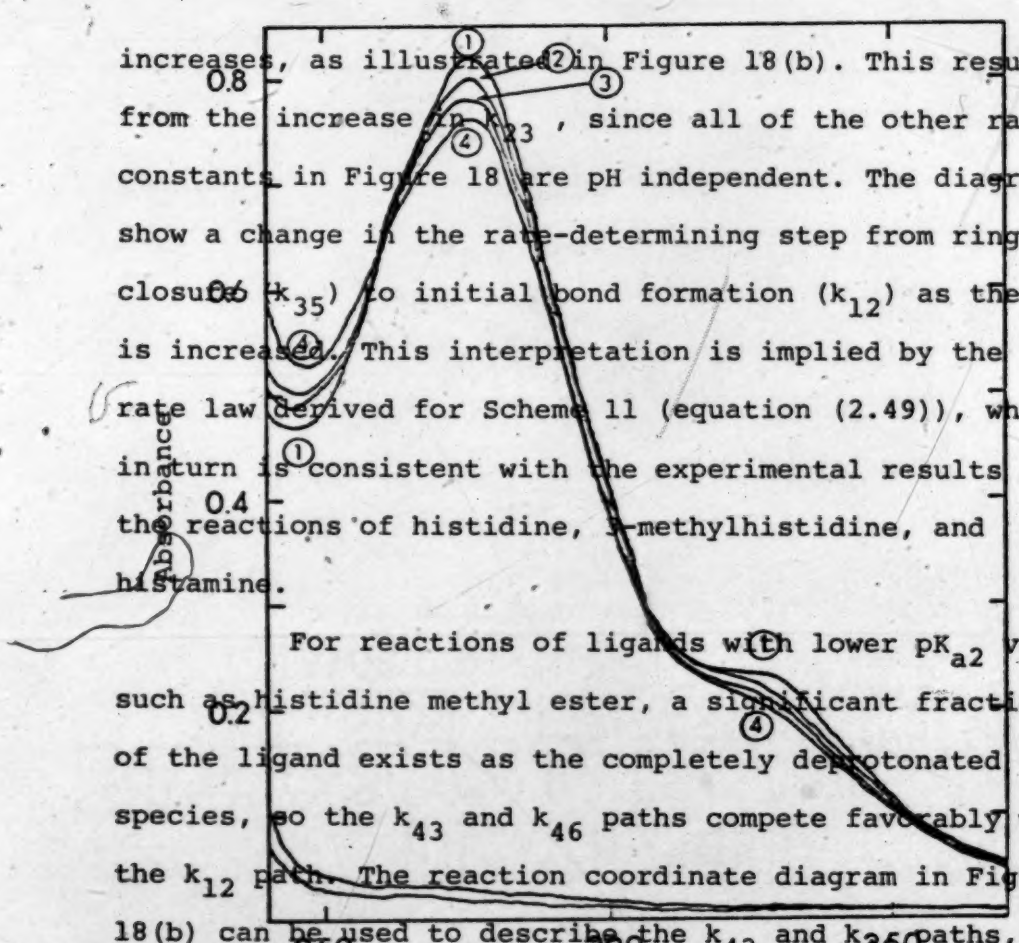

Figure 10. Electronic absorption spectra of solutions of $NiTRI(OH_2)_3^+$ and L-histidine. The spectra were measured at 23° in a cell of 1.00 cm path length. Total [NiTRI] = 2.003×10^{-6} M. Solutions contained L-histidine as follows: (1) none (2) 2.00×10^{-4} M (3) 8.00×10^{-4} M (4) 8.00×10^{-3} M. NaO_2CCH_3 buffer(0.10M) at pH 6.23 was included in all solutions.

For reactions of ligands with lower pK_{a2} values, such as histidine methyl ester, a significant fraction of the ligand exists as the completely deprotonated species, so the k_{43} and k_{46} paths compete favorably with the k_{12} path. The reaction coordinate diagram in Figure 18(b) can be used to describe the k_{43} and k_{46} paths, if species C and the proton transfer steps k_{23} and k_{32} are omitted. Since ring-closure (k_{35} or k_{65}) is expected to be more favorable than breaking of the nickel(II)-nitrogen bond (k_{34} or k_{64}), initial bond formation will always be rate-determining for the k_{43} and k_{46} pathways in Scheme 10. This is another consequence of the requirement of consistency with the S$_{\text{N}}$1IP mechanism. The other mechanisms discussed in this work are in many respects similar to Scheme 10. However, since

be obtained if the eluent contained 10^{-2} M *L*-histidine and was buffered at pH 5-7. Under these conditions, the details of which are given in the experimental section, the eluent fractions gave optical rotations as listed in Table 13.

Table 13

Apparent Optical Rotations of Eluent Fractions[a]

Fraction	Wavelength, nm 365	436	546	578
1	-0.031	+0.021	+0.012	+0.008
2	-0.035	+0.031	+0.016	+0.011
3	-0.017	+0.013	+0.007	+0.005
4	-0.001	0.000	0.000	0.000
5	+0.007	-0.012	-0.007	-0.005
6	+0.008	-0.016	-0.010	-0.008
Blank[b]	-0.009	-0.006	-0.003	-0.002

(a) The tabulated values are in degrees, and were measured in a 1.00 dm path length cell at 23°.

(b) A solution of 10^{-2} M *L*-histidine in 0.80 M NaO_2CCH_3 at pH 6.

the nickel(II)-oxygen bond is much more labile than the nickel(II)-nitrogen bond, the stability of B will be decreased significantly. In the k_{12} path of Schemes 9 and 12, loss of the amine proton will remain unfavorable as in Scheme 10, so it is likely that k_{35} will normally be rate-determining, and Figure 18(a) will apply. However, it is apparent from Figure 18 that proton loss will become rate-determining. Since $k_{32} \simeq (2 \times 10^{-4}/K_{a4})M^{-1}s^{-1}$, rate-determining proton transfer is expected for less basic amino acids.

From similar considerations to those discussed for Scheme 10, initial bond formation should be rate-determining in the k_{46} paths in Schemes 9 and 12. On the other hand, for $k_{35} \simeq k_{34}$, either of the two steps in the k_{43} paths of Schemes 9 and 12 could be rate-determining.

It is interesting to note that in several cases it has been possible to obtain more kinetic information from the $NiTRI(OH_2)_3^{+2}$ reactions than from comparable reactions with $Ni(OH_2)_6^{+2}$. Inspection of the rate laws for these two metal ions shows that, with $NiTRI(OH_2)_3^{+2}$, $(H^+) \simeq k_{35}K_{a4}/k_{21}$ within the experimental pH range, and thus $k_{35}K_{a4}/k_{21}$ can be evaluated from the kinetic data. However with $Ni(OH_2)_6^{+2}$, $(H^+) < k_{35}K_{a4}/k_{21}$ over the usual experimental pH range(6-7), and so

$k_{35}K_{a4}/k_{21}$ cannot be determined. Previous arguments indicate that k_{35} and k_{a4} should be similar for these two metal ion systems. Therefore k_{21} must be larger than $k_{53}K_{a2}$ as might be expected if the TRI ligand causes steric enhancement of ligand dissociation. Unfortunately there are no simple model systems which can be used to provide a precedent for the larger k_{21} values with $NiTRI(OH_2)_3^{+2}$.

The kinetic results for the $Ni(OH_2)_6^{+2}$-glycine system can be combined with the known formation constant ($\beta_1 = 6.0 \times 10$ M) to obtain $k_{53} = 2.7 \times 10$ s^{-1}. Similarly, the reanalysed kinetic results for the $Ni(OH_2)_6^{+2}$-histamine reaction, and the β_1 value of 6.0×10 M, yield $k_{53} = 0.66$ s^{-1}. These values are 4.3 times smaller than the corresponding k_{53} values of $NiTRI(OH_2)_3^{+2}$ complexes (see Results section). The observation that k_{53} is larger in the $NiTRI(OH_2)_3^{+2}$ systems is consistent with the argument that k_{21} is also larger in these systems.

The kinetic results can be used to calculate formation constants for the $NiTRI(OH_2)_3^{+2}$ complexes from the relationship $\beta_1 = k_{12}k_{35}K_{a4}/k_{21}k_{53}K_{a2}$. From the kinetic results for histidine, this calculation gives $\beta_1 = 1.1 \times 10$ M, as compared to 1.7×10 M from the nmr results. These two values agree within their

Recovery of the perchlorate salts yielded 0.0124 gm (40%) of the (+)$_{436}$ $NiTRI(OH_2)_3(ClO_4)_2$ isomer from Fractions 1 and 2 (Table 13), and 0.0087 gm (30%) of (-)$_{436}$ $NiTRI(OH_2)_3(ClO_4)_2$ from Fractions 5 and 6. Yields are based on the maximum amount of the isomer that could be obtained.

In the precipitation method, a solution of L-histidine was added to a buffered solution of $NiTRI(OH_2)_3(ClO_4)_2$. At pH > 5.4, a yellow-orange precipitate was formed, which gave a positive rotation at 436 nm. This isomer thus corresponds to the one eluted first from the ion exchange column in the previous method. Fractional recrystallization of this yellow-orange $Ni(OH_2)_6^{+2}$-histamine reaction, and the β_1 value of precipitate gave an improvement in the resolution of the (+)$_{436}$ isomer, as shown in column A of Table 14.

After removal of the (+)$_{436}$ isomer from the original solution, the (-)$_{436}$ isomer was precipitated by addition of sodium perchlorate solution. Recrystallization of the perchlorate salt of this isomer from dilute perchloric acid and sodium perchlorate resulted in an increase in its molecular rotation, as shown in column B of Table 14.

Because of the low yields, further recrystallizations of these samples were not undertaken. The ORD spectra of solutions of the (+)$_{436}$ and (-)$_{436}$ isomers

experimental uncertainties, but a larger nmr value could be explained by some carboxylate complexing which is not accounted for in the kinetic result.

The β_1 values for complexes of $Ni(OH_2)_6^{+2}$ and $NiTRI(OH_2)_3^{+2}$ are compared in Table 32.

Table 32

Formation Constants for Nickel(II) Complexes

	$Ni(OH_2)_6^{+2}$	$NiTRI(OH_2)_3^{+2}$
β_1	4.7×10^8	1.7×10^7 [b]
		1.1×10^7 [c]
β_2	6.0×10^6	1.5×10^6 [c]
β_3	6.0×10^5	$\leq 1.9 \times 10^5$ [c]

(a) The molecular rotation, $[\phi]_\lambda$, is defined as $10^{-3} \times$ Observed rotation (deg) / (Molarity x Cell pathlength (dm)). These measurements were made at 23° using a 1.00 dm pathlength cell. $[NiTRI(OH_2)_3^{+2}] = (2-4) \times 10^{-5}$ M as determined from the electronic spectra of the solutions, and the molar absorptivities reported in the experimental section.

Table 14

Molecular Rotations of $NiTRI(OH_2)_3^{+2}$ Isomers[a]

Initial Precipitate			Precipitate from Filtrate		
Number of Crystallizations	$10^{-3}[\phi]_{365}$	$10^{-3}[\phi]_{436}$	$10^{-3}[\phi]_{365}$	$10^{-3}[\phi]_{436}$	
1	-5.0	+2.0	+6.3	-5.1	
2	-7.7	+4.0	+7.6	-5.2	
3	-9.6	+4.6			

(a) Observed Rotations of $NiTRI(OH_2)_3^{+2}$ Isomers

	$10^{-3}[\phi]_{365}$	$10^{-3}[\phi]_{436}$
histidine	-5.0	+2.0
histamine	-7.7	+4.0
glycine	-9.6	+4.6

(a) Values at 25° and I = 0.10 M.

(b) Value at 25° and I = 0.10 M(MES) determined from the nmr measurements.

(c) Value at 25° and I = 0.30 M($LiClO_4$) determined from the kinetic results.

Since the formation rate constants are similar for these two metal ions, the smaller β_1 values observed for the $NiTRI(OH_2)_3^{+2}$ complexes are consistent with the suggestion that the dissociation rate constants (k_{21} and k_{53}) are larger for these complexes. It may be noted that the β_1 value for the histidine complex with $NiTRI(OH_2)_3^{+2}$ is ~28 times smaller than that for $Ni(OH_2)_6^{+2}$, while the values for the histamine complexes of $NiTRI(OH_2)_3^{+2}$ are only 3-4 times smaller than those for the analogous $NiTRI(OH_2)_3^{+2}$ complexes. The larger difference in the histidine complexes perhaps indicates more or stronger carboxylate binding in the complex with $Ni(OH_2)_6^{+2}$ because of less steric interaction.

Some suggestions for future investigations appropriate at this stage. It is apparent from the analysis and discussion in this work that chelation reactions are much more complex than had been previously assumed. As a result, many of the earlier $Ni(OH_2)_6^{+2}$ studies with multidentate ligands should be considered as merely exploratory. More thorough studies clearly are required of the $Ni(OH_2)_6^{+2}$-histamine reaction for example. The results reported here indicate that it would be of benefit to extend the pH range of kinetic studies as low as feasible in order to make $(H^+) \approx k_{35}K_{a4}/k_{21}$ and thus allow evaluation of this rate

Table 15

Ion Exchange Method	$10^{-5}[\phi]_{283}$	$10^{-5}[\phi]_{254}$	$10^{-5}[\phi]_{283}$	$10^{-5}[\phi]_{254}$
	$(\lambda)_{436}$		$(\lambda)_{436}$	
Precipitation Method	-1.9	+0.70	+2.1	-0.68
	+2.0	+0.65	+1.2	-0.38

(a) The molecular rotations were determined directly from the ORD spectra at 23° in 10^{-2} M $HClO_4$. $[\phi]_\lambda$ is defined under Table 14.

The results of an analysis of the precipitate of L-histidine and (+)-$NiTRI(OH_2)_3^{+2}$ are shown in Table 16.

parameter. Studies under conditions of excess ligand may also be advantageous.

The nmr titration technique discussed here should prove valuable in establishing the denticity of multidentate ligands. The *bis*(histidino)nickel(II) system is of particular interest. Quantitative measurements of the ratio of monodentate to bidentate species in systems similar to $NiTRI(OH_2)_3^{+2}$-histamine should be valuable in the interpretation of kinetic and equilibrium studies.

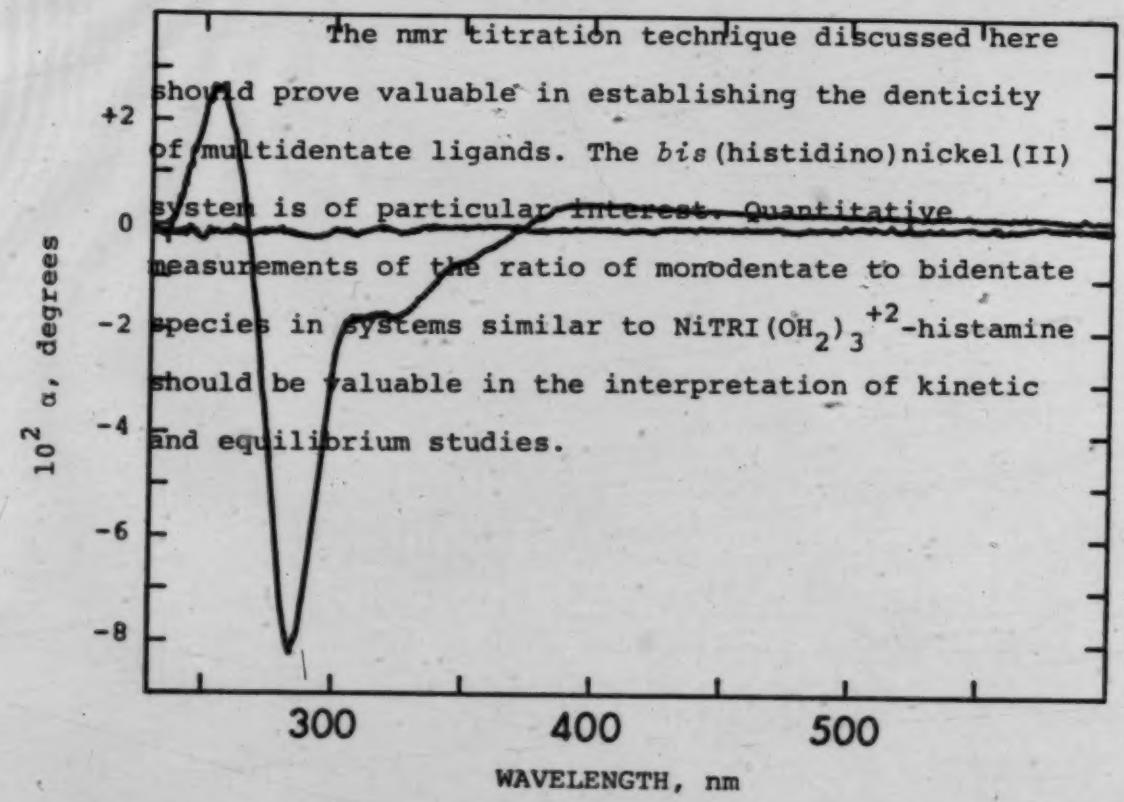

Figure 11. ORD spectrum of $(+)_{436}$ $NiTRI(OH_2)_3^{+2}$. $[NiTRI(OH_2)_3^{+2}] = 4.13 \times 10^{-5}$M, in 10^{-2}M $HClO_4$. The spectrum was measured in a 1.00 cm path length cell at 23°.

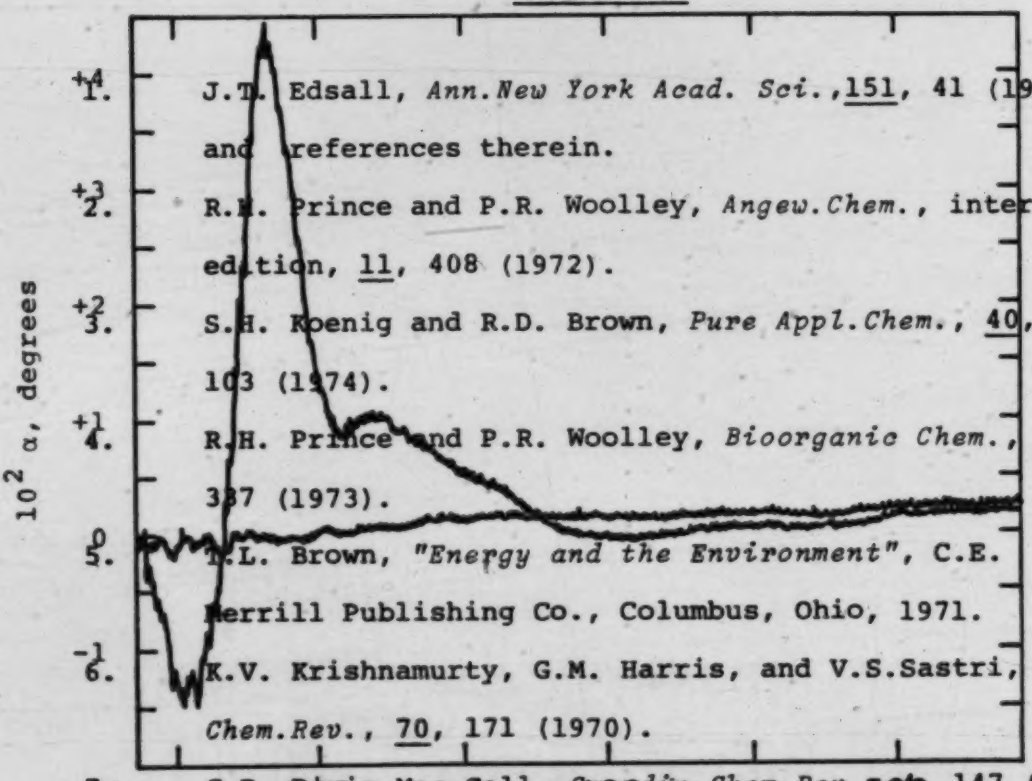

Figure 12. ORD spectrum of (-)$_{436}$-$NiTRI(OH_2)_3^{+2}$ in $HClO_4$. The spectrum was measured in a 1.00 cm path length cell at 23°.

REFERENCES

1. J.T. Edsall, *Ann.New York Acad. Sci.*, 151, 41 (1968). and references therein.
2. R.H. Prince and P.R. Woolley, *Angew.Chem.*, international edition, 11, 408 (1972).
3. S.H. Koenig and R.D. Brown, *Pure Appl.Chem.*, 40, 103 (1974).
4. R.H. Prince and P.R. Woolley, *Bioorganic Chem.*, 2, 337 (1973).
5. T.L. Brown, *"Energy and the Environment"*, C.E. Merrill Publishing Co., Columbus, Ohio, 1971.
6. K.V. Krishnamurty, G.M. Harris, and V.S.Sastri, *Chem.Rev.*, 70, 171 (1970).
7. C.R. Ruiz Mac-Coll, *Can.J.Chem.Rev.*, 147 (1969).
8. T.P. Dasgupta and G.M. Harris, *J.Am.Chem.Soc.*, 90, 6360 (1968).
9. The symbol K_a will be used throughout to indicate a "mixed" acid dissociation constant, defined as $K_a = [Base](H^+)/[Acid]$, where (H^+) refers to the hydrogen ion activity. $[NiTRI(OH_2)_3^{+2}] = 3.73 \times 10^{-5}$ M, in 10^{-2} M $HClO_4$.
10. G.M. Harris, *168th ACS National Meeting, Abstracts*, 1974, 145 (1974).
11. D.A. Palmer and G.M. Harris, *Inorg.Chem.*, 13, 965 (1974).
12. (a) J.B. Hunt *et al.*, *J.Am.Chem.Soc.*, 74, 268 (1952).
    (b) C.A. Bunton and D.R. Llewellyn, *J.Chem.Soc.*, 1692 (1953).

Table 16

Analytical Results for the Precipitate

	C	H	N	MW
Found :	50.7	3.98	12.5	
Calculated for :				
NiTRI(his)(ClO_4)[a]	52.2	3.73	13.5	621.68
NiTRI(his)$(ClO_4)(OH_2)$	50.7	3.94	13.1	639.70
NiTRI(his)$(ClO_4)(OH_2)_2$	49.3	4.14	12.8	657.71

(a) (his) ≡ histidine, $C_6H_8N_3O_2^-$. (TRI) ≡ $C_{21}H_{15}N_3$.

Of the possible molecular formulae listed in Table 16, the analytical results seem most consistent with NiTRI(his)$(ClO_4)(OH_2)$. Formulae with two histidines per nickel(II) or with the histidine zwitterion and two perchlorate ions per nickel(II) are clearly eliminated by the analysis.

The formula NiTRI(his)$(ClO_4)(OH_2)$ can be interpreted as a tridentate histidine complex, in which the water molecule occupies the sixth coordination site on the nickel(II) ion. On the other hand, the histidine could be tridentate and the water molecule might be held in the

13. G.M. Harris and V.S. Sastri, *Inorg.Chem.*, 4, 263, (1965).

14. V.S. Sastri and G.M. Harris, *J.Am.Chem.Soc.*, 92, 2943 (1970).

15. (a) For example, footnotes 268, 14, and 23 in references 6, 15(b), and 33 respectively.

(b) S.C. Chan and G.M. Harris, *Inorg.Chem.*, 10, 1317 (1971).

16. D.J. Francis, Ph.D. Thesis, University of Alberta, Edmonton, Alta. (1970).

17. D.J. Francis and R.B. Jordan, *J.Am.Chem.Soc.*, 91, 6626 (1969).

18. G.S. Schlessinger, *"Inorganic Laboratory Preparations"*, Chemical Publishing Co. Inc., New York, N.Y.,1962.

19. I. Hargis, Ph.D. Thesis, Ohio University (1966).

20. L.G. Sillen and A.E. Martell, Ed., *"Stability Constants"*, Special Publication No.17, The Chemical Society, London, 1964.

21. N.E. Good *et al.*, *Biochemistry*, 5, 467 (1966).

22. P. Bjerrum and S.E. Rasmussen, *Acta Chem.Scand.*, 6, 1265 (1952).

23. M. Scheidegger and G. Schwartzenbach, *Chimia*, 19, 156 (1965).

24. L. Rines, J.A. Plambeck and D.J. Francis, "CH:ENLLSQ Reprogrammed", Dept. of Chemistry Program Library, University of Alberta, Edmonton, Alta. (1970).

crystal lattice by hydrogen bonding. The nature of the histidine complex will be further discussed in connection with the kinetic and nuclear magnetic resonance results.

Acid Dissociation Constants

Literature values[65] of pK at 25° for the ligands used in this work are collected in Table 17. These are apparent, or "mixed",[9] constants, as obtained directly from pH titration, or by applying an activity correction[65] (for I= 0.30 M) to the concentration constants tabulated in reference 65.

25. P.D. Lark, B.R. Craven and R.C.L. Bosworth, *"The Handling of Chemical Data"*, 1st Ed., Pergammon Press, Oxford, 1968, p 148.

26. W. Kruse and H. Taube, *J.Am.Chem.Soc.*, 83, 1280 (1961).

27. (a) M.E. Baldwin, *et al.*, *J.Chem.Soc.*, 4637 (1961).
(b) R.D. Gillard, *J.Chem.Soc.A*, 1945(1968).

28. D.A. Buckingham *et al.*, *J.Am.Chem.Soc.*, 95, 7281 (1973).

29. S.F. Lincoln and D.R. Stranks, *Aust.J.Chem.*, 21, 1745 (1968).

30. R.C. Henney, *Inorg.Chem.*, 8, 389 (1969).

31. E. Chaffee *et al.*, *J.Am.Chem.Soc.*, 95, 4169 (1973).

32. D.A. Palmer and G.M. Harris, *Inorg.Chem.*, 13, 965 (1974).

33. T.P. Dasgupta and G.M. Harris, *J.Am.Chem.Soc.*, 97, 1733 (1975).

34. D.M. Kern, *J.Chem.Educ.*, 37, 14 (1960).

35. R.G. Pearson and E.A. Mayerle, *J.Am.Chem.Soc.*, 73, 926 (1951).

36. Estimated for 1 M $NaClO_4$[16] from data for 1 M NaCl.[20]

37. S.F. Lincoln and D.R. Stranks, *Aust.J.Chem.*, 21, 57 (1968).

38. D.J. Hewkin and R.H. Prince, *Coordin.Chem.Rev.*, 5, 45 (1970).

39. K. Kustin and J. Swinehart, *Prog.Inorg.Chem.*, 13, 107 (1970).

Table 17

Acid Dissociation Constants of the Ligands

Ligand	pK_{a1}	pK_{a2}	Reference
L-histidine	6.18	9.22	65
3-*L*-methylhistidine	5.79	9.30	66
histamine	6.21	9.97	65
L-histidine methyl ester	5.39	7.36	65
L-hercynine	6.05		this work
glycine		9.71	65
1-*L*-methylhistidine	6.58	8.60	66

(a) Measured with I = 0.10 M at an unspecified temperature.

40. R.G. Wilkins, *Acc.Chem.Res.*, 3, 408 (1970).

41. S.T. Chow and C.A. McAuliffe, *Prog.Inor.Chem.*, 19, 51 (1975).

42. H. Hoffman, *Pure Appl.Chem.*, 41, 327 (1975).

43. M. Eigen and R.G. Wilkins, *Advan.Chem.Soc.*, 49, 55 (1965).

44. F. Basolo and R.G. Pearson, *"Mechanisms of Inorganic Reactions"*, 2nd Ed., Wiley, 1967, p 37.

45. (a) M. Eigen, *Z.Elektrochem.*, 64, 115 (1960).
(b) M. Eigen and K. Tamm, *Z.Elektrochem.*, 66, 93 (1962).
(c) M. Eigen in *"Advances in the Chemistry of the Coordination Compounds"*, S. Kirchner, Ed., Macmillan, New York, N.Y., 1961, p 371.

46. R.M. Fuoss, *J.Am.Chem.Soc.*, 80, 5059 (1958).

47. M. Eigen, *Z.Physik.Chem.(Frankfurt)*,N.F.,1, 176 (1954).

48. J.C. Cassatt and R.G. Wilkins, *J.Am.Chem.Soc.*, 90, 6045 (1968).

49. J.E. Letter, Jr. and R.B. Jordan, *Inorg.Chem.*, 10, 2692 (1971).

50. J.C. Cassatt *et al.*, *J.Am.Chem.Soc.*, 94, 8399 (1972).

51. J.E. Letter, Jr. and R.B. Jordan, *Inorg.Chem.*, 13, 1152 (1974).

52. J.E. Letter, Jr. and R.B. Jordan, *J.Am.Chem.Soc.*, 97, 2381 (1975).

Kinetics and Mechanisms. R. Holyer, E. Deutsch and H. Taube, *Inorg.Chem*, 11, 1965 (1972).

The reaction of $NiTRI(OH_2)_3^{+2}$ with histidine

54. H. Hoffman, *Ber.Bunsenges Phys.Chem.*, 73, 432 (1969).

55. M. Grant *et al.*, *Inorg.Chem.*, 9, 2321 (1970).

56. M.O. Dayhoff, *Atlas of Protein Sequence and Structure*", Vol.5, Nat'l Biomedical Research Foundation, Georgetown University Center, 1972.

57. R.J. Sundberg and R.B. Martin, *Chem.Rev.*, 74, 471 (1974).

58. S.A. Nelson and D.W. Margerum, *J.Am.Chem.Soc.*, 87, 1708 (1965).

59. J.E. Letter, Jr. and R.B. Jordan, *J.Am.Chem.Soc.*, 93, 864 (1971).

60. L.T. Taylor and D.H. Busch, *ibid.*, 89, 5372 (1967).

61. L.T. Taylor *et al.*, *ibid.*, 88, 3170 (1966).

62. L.I. Smith and J.W. Opie, *Org.Synth.*, 28, 11 (1948).

63. S.G. McGeachin, *Can.J.Chem.*, 41, 2324 (1966).

64. V.N. Reinhold *et al.*, *Med.Chem.*, 11, 258 (1968).

65. A.E. Martell and R.M. Smith, *Critical Stability Constants*, Vol.1 and 2, Plenum Press, New York, N.Y. 1975.

66. R.W. Cowgill, *J.Am.Chem.Soc.*, 79, 2242 (1957).

67. E.F. Caldin, *Fast Reactions in Solution*, Wiley and Sons, New York, N.Y. 1964, p 268.

68. R.H. Voss and R.B. Jordan, *Biochemistry*, 98, 6926 (1976).

The rate of the reaction of $NiTRI(OH_2)_3^{+2}$ with histidine was followed both directly and indirectly through the glucose-hexokinase coupled reaction. The indirectly followed reaction was observed, in agreement with the spectral results discussed earlier, to be of interest by the appropriate choice of reactant concentrations and indicator wavelength. Most of the systems studied were self-buffering in the pH region studied due to the large molar excess of ligand present. While this was convenient in some respects it necessitated increasing the $NiTRI(OH_2)_3^{+2}$ concentration when the ligand concentration was increased in order to compensate for the increased buffering. In kinetic studies at a particular pH the ratio of [ligand] to $[NiTRI(OH_2)_3^{+2}]$ was kept constant. Under these conditions, the total observed transmittance change at pH 6.8 was fairly constant as the reactant concentrations were increased. In similar studies at pH 6.2, the total observed transmittance change increased as the reactant concentrations were increased, implying that complex formation is not complete under these latter

conditions. The previously mentioned spectral observations yielded the same result.

The experimental pseudo-first-order rate coefficients (k_{exp}) for the reaction of $NiTRI(OH_2)_3^{+2}$ with histidine are listed in Table 18. The variation of k_{exp} with total histidine concentration (L_t) at constant pH is consistent with equation (2.9), as indicated by the linearity of the plot shown in Figure 13.

$$k_{exp} = k_f (L_t) + k_r \qquad (2.9)$$

Similar plots at pH 5.5, 5.9 and 6.8 are also linear, and all have intercepts close to 0.1 s^{-1}.

A consideration of the results in Table 18 shows that variation of the optical forms of the reactants has no significant effect on the observed rate coefficients. It is therefore concluded that stereospecific rate behavior is absent in this reaction system.

The data in Table 18 are not suited to a comparison of the direct and indicator methods of following the reaction because of the necessary differences in the concentration conditions. However, the linearity of the plot shown in Figure 13 implies agreement of the two methods, since half of the points plotted were obtained by each method.

69. R.D. Gillard, *Inorg.Chim.Acta Rev.*, 1, 69 (1967).
70. J.H. Ritsma *et al.*, *Rec.Trav.Chem.Pays Bas*, 88, 411 (1969).
71. P.J. Morris and R.B. Martin, *J.Inorg.Nucl.Chem.*, 32, 2891 (1970).
72. D.S. Barnes and L.D. Pettit, *ibid.*, 33, 2177 (1970).
73. L.D. Pettit and J.L.M. Swash, *J.Chem.Soc., Dalton*, 1976, 589 (1976).
74. K.A. Fraser and M.M. Harding, *J.Chem.Soc.A*, 415 (1967).
75. M.M. Harding and H.A. Long, *ibid.*, 2554 (1968).
76. R. Candlin and M.M. Harding, *ibid.*, 384 (1970).
77. F.J. Rossotti, in *"Modern Coordination Chemistry"*, Interscience Inc., New York, N.Y., 1960, p 51-52.
78. R.B. Jordan, *Inorg.Chem.*, 15, 748 (1976).
79. W.G. Esperson and R.B. Martin, *J.Phys.Chem.*, 80, 741 (1976).
80. R.H. Voss and R.B. Jordan, *J.Am.Chem.Soc.*, 98, 2173 (1976).
81. G.G. Hammes and J.I. Steinfeld, *ibid.*, 84, 4639 (1962).
82. M.W. Grant, *Trans.Farad.Soc.*, 69, 560 (1973).

Table 18
APPENDIX A

Observed Rate Coefficients for the Reaction of $NiTRI(OH_2)_3^{+2}$ with Histidine[a]
The Method of Linear Least-Squares using Relative Residuals

The least-squares fits in this work have minimized the sum of the squares of the relative residuals, defined as

pH	$10^4 L_t$, M	k_{exp}, s^{-1}	k_{cald}[b], s^{-1}	Conditions[c]
5.55	33.3	0.691±.04	0.585	(+) D BCP
5.56	30.5	0.690±.02	0.568	(+) BCP
5.56	31.5	0.788±.02	0.578	BCP
5.57	28.3	0.460±.02	0.493	BCP
5.81	29.9	0.923±.04	0.879	BCP
5.87	33.3	1.21±.08	1.24	BCP
5.87	38.6	1.38±.06	1.39	BCP
5.89	17.2	1.65±.04	1.63	BCP
5.91	25.3	2.30±.2	2.49	BCP
6.00	20.3	0.613±.05	0.679	
6.15	3.03	0.362±.01	0.380	(-) 275
6.15	23.3	1.70±.12	1.78	BCP
6.16	30.3	2.27±.09	2.28	(-) 275
6.16	9.95	0.824±.05	0.809	275
6.17	14.97	0.490±.05	0.535	(-) 275
6.18	49.9	3.94±.1	3.65	(-) 275
6.18	33.3	2.35±.1	2.58	BCP
6.20	10.3	1.00±.04	0.983	

$$\Sigma \Delta_i^2 = \frac{\{(y_i - Y'_i)\}^2}{y_i} \qquad \text{(A-1)}$$

where y_i is the experimentally observed dependent variable, and Y'_i is the predicted value of y_i. The latter is calculated from the linear equation

$$Y_i = a + b\, x_i \qquad \text{(A-2)}$$

where x_i is the independent variable (in the present case, the time). For n data points ($1 \le i \le n$), the values of a and b obtained when $\Sigma \Delta_i^2$ is a minimum are given by

$$a = \frac{\Sigma(1/y_i) - b\Sigma(x_i/y_i^2)}{\Sigma(1/y_i^2)} \qquad \text{(A-3)}$$

$$b = \frac{\left\{\Sigma(x_i/y_i)\Sigma(1/y_i^2)\right\} - \left\{\Sigma(1/y_i)\Sigma(x_i/y_i^2)\right\}}{\left\{\Sigma(x_i/y_i)^2\Sigma(i/y_i^2)\right\} - \left\{\Sigma(x_i/y_i^2)\right\}^2} \qquad \text{(A-4)}$$

An estimate of the standard error of the least-squares fit can be calculated from

Table 18 (cont'd)

$$s_e^2 = \frac{\Sigma \Delta_i^2}{(n-2)} = \frac{n - a\Sigma(1/y_i) - b\,\Sigma(x_i/y_i)}{(n-2)} \qquad \text{(A-5)}$$

pH	$10^4 L$, M	k_{exp}, s^{-1}	k_{calc}, s^{-1}	Conditions[c]
6.20	9.59	0.954±.07	0.927	
6.21	30.5	2.71±.1	2.62	(+)
6.21	31.5	2.96±.1	2.55	(+)
6.28	9.47	1.19±.09	1.05	
6.32	5.15	0.610±.05	0.678	(-) 275
6.46	9.47	1.47 .09	1.40	
6.60	5.15	0.910±.03	0.962	(-) 275
6.60	5.48	0.920±.05	1.02	(-) 275
6.70	9.59	2.00±.1	1.90	
6.77	9.56	1.82±.03	1.99	(+)
6.79	18.7	3.53±.1	3.93	(+)
6.80	5.48	1.14±.05	1.23	(-) 275
6.91	9.40	2.48±.2	2.24	
6.94	9.59	2.59±.1	2.34	
7.01	9.59	2.60±.2	2.45	
7.10	9.40	2.58±.1	2.52	
7.11	9.71	2.85±.2	2.62	
7.21	9.71	2.90±.2	2.74	
7.21	9.71	2.97±.2	2.74	

Description of the computer Program

The program written for the Wang 500 Programmable Desk Calculator to calculate the values of a, b and s_e consists of three sequential parts, which are chained together by use of the cassette memory tape. Once the first part has been manually loaded into the "core" memory from the cassette tape, the second and third parts are loaded automatically by the program at the appropriate times.

Part 1 of the program initially accepts a value of T_{offset}, and of a conversion factor, CF, both of which are stored in memory. The conversion factor takes into account the amplification of the signal and the direction of the observed transmittance change. For example, if the amplification is 0.5% T per graticule unit (20%T full vertical scale), and the transmittance increases with time as in Figure 1a, then the conversion factor is -0.5. Ten data points (ΔT_t in Figure 1b), which are read directly from the photograph of the observed oscilloscope trace at equal time intervals, are then entered sequentially into the computer. These are measured

in the units of the oscilloscope graticule (full vertical

Table 18 (cont'd)

scale = 40 graticule units). Each point is multiplied by CF, converted to %T using T_{offset}, and stored in a memory register. Two data points are stored in each of five memories (01-05) in the form of two five digit numbers separated by a decimal. Lastly, ΔT_∞ is entered (in the same units as ΔT_t), T_∞ is calculated and stored, and Part 2 of the program is loaded.

(a) The value of k_{exp} reported is the average of 10 identical runs at 25°. I= 0.30M ($LiClO_4$). The error limits given are one standard deviation.

Total [NiTRI] = $(0.5\text{-}3.0) \times 10^{-4}$M after mixing.

(b) Calculated using equation (2.49) and the "best-fit" values given in the text.

(c) The reactants were racemic $NiTRI(OH_2)_3^{+2}$ and *L*-histidine, except where specified as follows: (+) ≡ (+)$_{436}$ $NiTRI(OH_2)_3^{+2}$; (-) ≡ (-)$_{436}$ $NiTRI(OH_2)_3^{+2}$; *D* ≡ *D*-histidine; *DL* ≡ *DL*-histidine. Bromothymol blue indicator (2.5×10^{-5}M) was used unless specified as follows: BCP ≡ Bromocresol purple (2.5×10^{-5}M); 275 ≡ No indicator present, reaction followed directly at 275 nm.

Part 2 of the program recovers the values of T_t sequentially. The odd-numbered points (1,3,5,7,9) precede the decimal, and are obtained as $10^3 T_t$. The even-numbered points follow the decimal, and are recovered from the difference between the total (10 digit) numbers and their integer parts, as $10^2 T_t$. Values of y_i ($\ln|\log(T_t/T_\infty)|$) and of the sums in equations (A-3) and (A-4) are then calculated, with x_i values 1-10 supplied by an internal counter.

Part 3 of the program calculates values of b, a, and 8 x (s_e^2), and the latter appears in the display at the end of the calculation. The time interval Δt, defined as 0.1 x (full horizontal sweep time), can then be entered, and the display gives $-k_{exp}$.

Before entering another data set, Part 1 must be re-loaded and initiated. It should be noted that the values of T_t and T_∞ used in the last calculation can be recovered if desired, before beginning a second

calculation. The memories are cleared upon initiation of Part 1.

The program is given in the following pages.

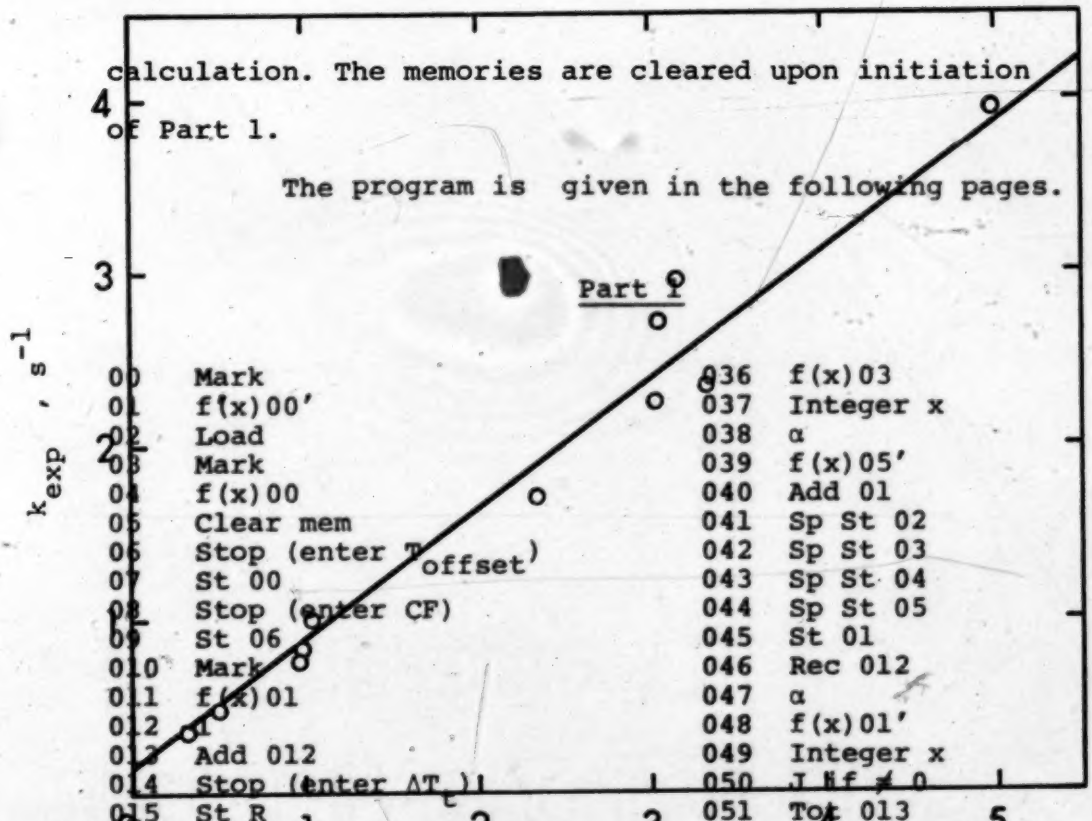

00	Mark	036	f(x)03
01	f(x)00'	037	Integer x
02	Load	038	α
03	Mark	039	f(x)05'
04	f(x)00	040	Add 01
05	Clear mem	041	Sp St 02
06	Stop (enter T_{offset})	042	Sp St 03
07	St 00	043	Sp St 04
08	Stop (enter CF)	044	Sp St 05
09	St 06	045	St 01
010	Mark	046	Rec 012
011	f(x)01	047	α
012	1	048	f(x)01'
013	Add 012	049	Integer x
014	Stop (enter ΔT_t)	050	J if ≠ 0
015	St R	051	Tot 013
016	Rec 06	052	f(x)01
017	Mult R	053	Stop
018	Rec 00	054	Mult 06
019	Add R	055	Tot 06
020	St L	056	Add 00
021	Rec 013	057	α
022	J if 0	058	f(x)03
023	Rec L	059	St 00
024	f(x)03	060	Tot 013
025	Rec L	061	f(x)00
026	α	062	END (verify 815)
027	f(x)03		
028	Integer x		
029	St 01		
030	1		
031	St 013		
032	f(x)01		
033	Mark		
034	f(x)03		
035	α		

Figure 13. Variation of k_{exp} with ligand concentration for the reaction of $NiTRI(OH_2)_3$ with histidine at pH ~6.15.

203

Part 2

It was previously suggested that the reaction of $(+)_{436}NiTRI(OH_2)_3^{+2}$ with *L*-histidine may produce a complex in which histidine is bidentate. This is supported by molecular models of the reactants, which show that histidine may prefer bidentate coordination in at least two of the four possible diastereoisomeric products. However, the lack of an observable rate difference between reactions leading to optically unique products indicates a similarity in the rate-determining process. These observations imply either that a bidentate complex forms in all cases, or that chelation of the third donor group has no effect on the observed rate. With these considerations in mind, it is reasonable to consider only those mechanisms which lead to a bidentate product.

There are three possible ways in which a bidentate product can be formed from $NiTRI_\alpha$ and histidine. The first of these mechanisms is shown in Scheme 8.

```
00  Mark
01  f(x)00
02  1
03  0
04  St 012
05  Rec 01
06  Mark
07  f(x)01
08  Integer x
09  St L
010 Rec 00
011 Div L
012 log y
013 |y|
014 ln y
015 1/y
016 St L
017 St R
018 Add 06 (Σ1/y)
019 Rec 012
020 Mult L
021 Add 08 (Σx/y)
022 Rec L
023 Square
024 Add 010 (Σx²/y²)
025 Rec R
026 Square
027 St L
028 Add 07 (Σ 1/y²)
029 Rec 012
030 Mult L
031 Add 09 (Σx/y²)
032 1
033 Subtr 012
034 Rec 013
035 J if ≠0
036 1
037 f(x)02
038 Tot 013
039 Rec 00
040 Sp St 02
041 Sp St 03
042 Sp St 04
043 Sp St 05
044 St 01
045 Rec 012
046 J if 0
047 Rec 01
048 f(x)01
049 Lbl 00'
050 Mark
051 f(x)03
052 St 013
053 Rec 01
054 St L
055 Integer x
056 Subtr L
057 f(x)04
058 f(x)05
059 f(x)01
060 END (verify 878)
```

Scheme 8

Part 3

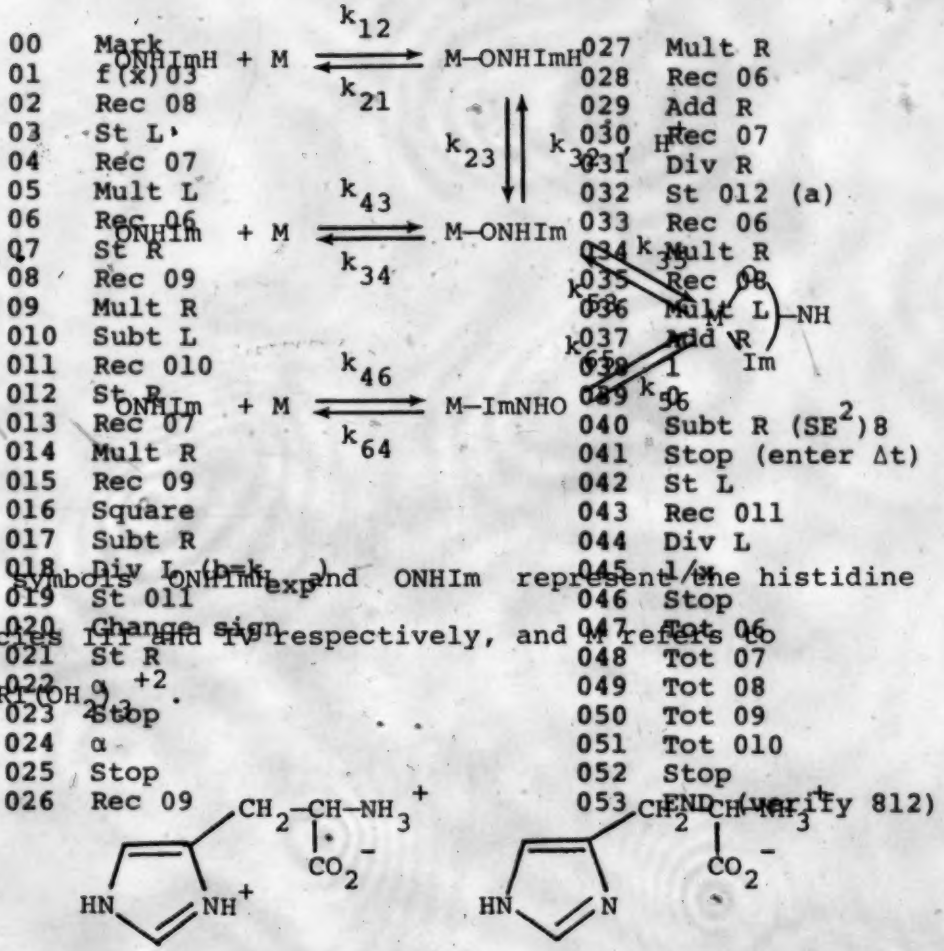

The symbols $ONHImH_{exp}$ and ONHIm represent the histidine species III and IV respectively, and M refers to $NiTRI(OH_2)_3^{+2}$.

III

IV

In this reaction sequence, bonding occurs with the carboxylato oxygen (O) and the imidazole nitrogen (Im). It is assumed that the contribution from the amine

deprotonated species (ONIm) is not significant because its concentration is small under the present experimental conditions of $(H^+) >> K_{a2}$.

APPENDIX B

Derivations of the Rate Laws for the Mechanisms in Chapter I

Isomerization

The fundamental requirement of any proposed mechanism is that it predict a rate law which is consistent in form and magnitude with the experimental rate law. In this work, the observed first-order dependence of the metal ion concentration implies that a single exponential decay governs the rate $-d[M]/dt$. With this restriction, a fairly complete rate expression corresponding to k_{exp} can be derived from a kinetic analysis of Scheme 8, as described in Appendix C. Simplification of this "complete" expression using estimates of the magnitudes of the rate constants in Scheme 8 are rapidly maintained, then the following equations can be derived:

$$k_{21} \approx k_{34} \approx k_{56} \approx k_{85} \approx k_{65} > k_{64} \approx k_{53} \; ; \; k_{43} \approx k_{46} \approx k_{12} \qquad (2.10)$$

$$H_2C = \frac{(H^+)}{K_{a3}+(H^+)}, \qquad HC = \frac{K_{a3}}{K_{a3}+(H^+)} \qquad (B-3)$$

Since the final form of the predicted rate law is quite dependent on the magnitudes of k_{23} and k_{32}, a detailed evaluation is warranted. Equations (2.11), (2.12) and (2.13) show the proton transfer processes which most likely contribute to k_{23}.

$$H_2B = \frac{(H^+)}{K_{a5}+(H^+)}, \qquad HB = \frac{K_{a5}}{K_{a5}+(H^+)} \qquad (B-4)$$

From Scheme 3,

$$\frac{-d(H_2C)}{dt} = k_{c1}(H_2C) - k_{t1}(H_2B) \qquad (B-5)$$

and $$M\text{—}ONHImH + H_2O \underset{k_{-1}}{\overset{k_1}{\rightleftharpoons}} M\text{—}ONHIm + H_3O^+ \qquad (2.11)$$

$$\frac{-d(HC)}{dt} = k_{c2}(HC) - k_{t2}(HB) \qquad (B\text{-}6)$$

Substitution of (B-3) and (B-4) into (B-5) and (B-6), $$M\text{—}ONHImH + B \underset{k_a}{\overset{k_b}{\rightleftharpoons}} M\text{—}ONHIm + BH \qquad (2.12)$$

and defining $$TCB \xrightarrow{k_3} CT + BT \qquad (B\text{-}7)$$

gives $$M\text{—}ONHImH + OH^- \underset{k_{-3}}{\overset{k_3}{\rightleftharpoons}} M\text{—}ONHIm + H_2O \qquad (2.13)$$

$$\frac{-d(CT)}{dt} = \left\{ \frac{k_{c1}(H^+) + k_{c2}K_{a3}}{K_{a3} + (H^+)} + \frac{k_{t1}(H^+) + k_{t2}K_{a5}}{K_{a5} + (H^+)} \right\} CT \qquad (B\text{-}8)$$

$$- \left\{ \frac{k_{t1}(H^+) + k_{t2}K_{a5}}{K_{a5} + (H^+)} \right\} TCB$$

$$= (k_{cb} + k_{bc})\,CT - k_{bc}\,TCB$$

The linear operator method, described in detail in reference 1, can be used to solve this simple first-order differential equation. This method is chosen for use here because of its simple introduction, prior to its use in Appendix C to solve the more complicated kinetic systems discussed in Part II.

In applying the operator method, one replaces differentiation by multiplication, in which the multiplier is the operator $S = d/dt$. Under the initial conditions of this case, $CT = TCB$ at $t = 0$, and equation (B-8) is transformed to

Thus the rate constant k_{23} is given by

$$k_{23} = k_1[H_2O] + k_2[ONHIm] + k_3[OH^-] \qquad (2.14)$$

It can be shown that the acid dissociation constant of the imidazole proton in the species M—ONHImH is given by

$$\frac{k_{23}}{k_{32}} = \frac{k_1[H_2O] + k_2[ONHIm] + k_3[OH^-]}{k_{-1}(H^+) + k_{-2}[ONHIm] + k_{-3}[H_2O]} = \frac{K_{a3}}{(H^+)} \qquad (2.15)$$

Since coordination of histidine to the metal ion at the carboxylate oxygen probably has only a small effect on the fairly distant imidazole nitrogen, it is

likely that K_{a3} is equal to or slightly greater than K_{a1}. (B-9)

For histidine, $K_{a1} = 6.61 \times 10^{-7}$ M, so K_{a3} is estimated to have a value of ~8 x 10^{-7} M. The term $k_1[H_2O]$ in equation (2.14) can now be evaluated from the equality $k_1[H_2O] = k_{-1}K_{a3}$, using an estimate of 10^{10} $M^{-1}s^{-1}$ for k_{-1}, to give $k_1[H_2O] = 8 \times 10^{3}$ s^{-1}.

The second term in equation (2.14) can be rewritten

$$CT = TCB \left\{ \frac{bc}{cb + bc} + \frac{cb}{cb + bc} e^{-(cb + bc)t} \right\} \quad (B\text{-}11)$$

Equation (B-11) has the same form as that derived for a simple first-order reversible reaction[4], which implies that Scheme 3 can be rewritten as

$$CT \underset{cb}{\overset{bc}{\rightleftharpoons}} BT \quad (B\text{-}12)$$

At equilibrium,

$$\frac{[BT]_e}{[CT]_e} = \left\{\frac{K_{a3}}{[H^+]}\right\} \left\{\frac{cb}{bc}\right\} = K_{cb} \quad (B\text{-}13)$$

Also,

$$TCB = [BT]_e + [CT]_e = [CT]_e \left\{\frac{cb}{bc} + 1\right\} \quad (B\text{-}14)$$

Substitution of (B-14) into (B-11), and rearrangement, gives

$$CT = [CT]_e \left\{\frac{cb}{bc}\right\} e^{-(cb + bc)t} \quad (B\text{-}15)$$

$$= [CT]_e K_{cb} \; e^{-(cb + bc)t}$$

The third term in equation (2.14) can be estimated directly, since $k_3 = 2 \times 10^{10}$ $M^{-1}s^{-1}$.[67] For most of the pH range of the histidine study, the approximation $k_3[OH^-] < k_1[H_2O]$ will be valid.

$$-S(CT) + S(TCB) = (cb + bc)\,CT - bc\,TCB \quad (B\text{-}9)$$

Equation (B-9) can be rearranged to

$$(S + bc)\,CT = \frac{(S + bc)\,TCB}{S + (cb + bc)} \quad (B\text{-}10)$$

From a table of Laplace transforms,[2,3] the "original" corresponding to the solution of equation (B-10) is

$$CT = TCB \left\{ \frac{bc}{cb + bc} + \frac{cb}{cb + bc} e^{-(cb + bc)t} \right\} \quad (2.16)$$

where

$$L_t = [ONHImH] + [ONHIm] \quad (2.17)$$

The value of k_2 can be estimated from the Brönsted relationship

$$\ln k_2 = 0.492 \ln \left\{\frac{K_{a3}}{K_{cb}}\right\} + \ln (1.7 \times 10^5) \quad (2.18)$$

which was determined experimentally for the ligand 2-aminomethylpyridine.[68] From the known values of K_{a1} and K_{a3}, calculation shows that $k_{-1}[ONHIm]\left\{\frac{cb}{bc}\right\} < k_1[H_2O]$ for the concentration conditions of the histidine study.

These calculations show that k_{23} in Scheme 8 is relatively pH independent, and has a value of ~8 x 10^3 s^{-1}

Differentiation of (B-15) with respect to time yields

$$-\frac{d(CT)}{dt} = \left\{(cb + bc)\,[CT]_e K_{cb}\right\} e^{-(cb + bc)t} \qquad \text{(B-16)}$$

Substitution for k_{32}, [HL], and [L] from equations (2.15) and (2.19), which, after substitution from (B-15), gives

$$[HL] \equiv [ONHImH] = \frac{-\frac{d(CT)}{dt}\,(H^+)\,L_t}{K_{a1} + (H^+)} = (cb + bc)\left\{CT - [CT]_e K_{a1}\right\} \frac{L_t}{K_{a1} + (H^+)} \qquad \text{(B-17)}$$

$$[L] \equiv [ONHIm] = \frac{K_{a1}\,L_t}{K_{a1} + (H^+)} \qquad (2.19)$$

Experimentally,

$$-\frac{d(CT)}{dt} = k_{exp}\left\{CT - [CT]_e\right\} \qquad \text{(B-18)}$$

into equations (C-25) and (C-26) in Appendix C permits simplification of these equations to give the ligand dependent term in k_{exp}

Therefore

$$k_{exp} = \left\{\frac{k_{c1}(H^+) + k_{c2}K_{a3}}{K_{a3} + (H^+)} + \frac{k_{t1}(H^+) + k_{t2}K_{a5}}{K_{a5} + (H^+)}\right\} \qquad \text{(B-19)}$$

$$\left\{\left(k_{46}K_{a1} + \frac{k_{12}K_{35}K_{a3}}{k_{21}}\right)(H^+) + \left(k_{46}(k_{35} + k_{34}) + k_{43}k_{35}\right)\left(\frac{k_{23} + k_{21}}{k_{23}k_{21}}\right)K_{a1}K_{a3}\right\}$$

$$k_f = \frac{}{CT + \left(K_{a1} + (H^+)\right)\left[\left(\frac{k_{23}k_{21}}{k_{23}k_{21}}\right)[(en)_2Co(OH_2)(OH)^{+2}] + k_{35}[(en)_2Co(OH_2)_2^{+3}] + k_{34}K_{a3}[(en)_2Co(OH)_2^{+}]\right]} \qquad (2.20)$$

Carboxylation

The reactant species in Scheme 4 can be represented by

$$= H_2C + HC + C \qquad \text{(B-20)}$$

Likewise, the ligand independent term reduces to

and

$$k_r AT = \frac{(k_{64}k_{56} + k_{65}k_{53})\left\{k_{34}(k_{23} + k_{21}) + k_{32}k_{21}\right\}}{(k_{65} + k_{56})\left\{(k_{35} + k_{34})(k_{23} + k_{21}) + k_{32}k_{21}\right\}} \qquad (2.21)$$

$$= k_{53}\,H_2A + HA + A \qquad \text{(B-21)}$$

where all the species are *cis*-isomers.

A consideration of the form of equations (2.20) and (2.21) shows that the k_{exp} values in Table 18 should be consistent with

$$k_{exp} = \left\{ \frac{B(1)\ (H^+) + B(2)}{\{K_{a1} + (H^+)\}\{B(4) + (H^+)\}} \right\} L_t + B(5) \qquad (2.22)$$

A least-squares fit[24] of the data in Table 18 to equation (2.22) gave the results summarized in columns A and B of Table 19. It is evident from these results that B(1) is poorly defined by the data, and similar results were obtained from a third fit in which B(1) was fixed at zero. Comparison of equations (2.20) and (2.22) shows that the parameters in the latter should be consistent with the equations (2.23) to (2.25).

$$B(1) = k_{46}K_{a1} \qquad (2.23)$$

$$B(2) = k_{46}K_{a1}\left(\frac{k_{35}ca + k_{34}ac}{ca + ac}\right)\left(\frac{k_{23} + k_{21}}{k_{23}k_{21}}\right)K_{a3} \qquad (2.24)$$

$$B(4) = (k_{35} + k_{34})\left(\frac{k_{23} + k_{21}}{k_{23}k_{21}}\right)K_{a3} \qquad (2.25)$$

Equation (B-24) can be solved using the operator method described earlier, to give

$$CT = TCA\left\{\frac{ac}{ca + ac} + \left(\frac{ca - ac}{ca + ac}\right)e^{-(ca + ac)t}\right\} \qquad (B-27)$$

By analogy with (B-10), it follows that

$$\frac{-d(CT)}{dt} = (ca + ac)\left\{CT - \frac{k_{43}K_{a1}k_{35}\left(\frac{k_{23} + k_{21}}{k_{23}k_{21}}\right)K_{a3}}{[CT]_e}\right\} \qquad (B-28)$$

Equation (B-24) can be solved using the operator method described earlier, to give

$$CT = TCA\left\{\frac{ac}{ca + ac} + \left(\frac{ca - ac}{ca + ac}\right)e^{-(ca + ac)t}\right\} \qquad (B-27)$$

By analogy with (B-10), it follows that

$$\frac{-d(CT)}{dt} = (ca + ac)\left\{CT - \frac{k_{43}K_{a1}k_{35}\left(\frac{k_{23} + k_{21}}{k_{23}k_{21}}\right)K_{a3}}{[CT]_e}\right\} \qquad (B-28)$$

Equation (B-23) can be rewritten in a form analogous to (B-8), to give

$$\frac{-d(CT)}{dt} = (ca + ac)\,CT - ac\,TCA \qquad (B-24)$$

where

$$ca = \frac{k_{-2}[CO_2]K_{a3}(H^+) + k_{-2}'[CO_2]K_{a3}K_{a4}}{(H^+)^2 + K_{a3}(H^+) + K_{a3}K_{a4}} \qquad (B-25)$$

$$ac = \frac{k_2(H^+)^2 + k_2K_{a1}(H^+)}{(H^+)^2 + K_{a1}(H^+) + K_{a1}K_{a2}} \qquad (B-26)$$

The experimental rate law is

$$\frac{-d(CT)}{dt} = k_{exp}[CT][Histidine]_e \quad (B\text{-}29)$$

From a comparison of equations (B-28) and (B-29), it follows that

$$k_{exp} = ca + ac \quad (B\text{-}30)$$

Table 19

A Summary of the Data Fits for the Reaction of $NiTRI(OH_2)_3^{+2}$

Parameter	A	B[b]
$10^4 B(1)$, s^{-1}	0.9±	0.75±1
$10^{10} B(2)$, $M\ s^{-1}$	6.8±.6	9.7±.6
$10^7 B(4)$, M	2.8±.4	4.4±.4
$B(5)$, s^{-1}	0.2±.6	0.2±1
S.E.[c]	0.174	0.163

Parameter	C	D[b]	E
$10^9 P(1)$, s^{-1}	1.55±.1	1.19±.07	1.09±.06
$10^{17} P(2)$, $M^{-2}\ s^{-1}$	5.9±3	1.6±1	1.1±.8
$10^7 P(4)$, $M^{-1}\ s^{-1}$	11.0±1	6.5±.5	5.2±.4
$P(5)$, s^{-1}	0.9±.6	0.23±.1	0.37±.2
S.E.[c]	0.176	0.156	0.154

(a) Results obtained by fitting to equation (2-22) (A and B), to equation (2-36) (C and D) and to equation (2-40) (E). The parameter error estimates are 95% confidence limits. K_{a1} and K_{a2} were fixed at the values given in Table 17. Relative residuals were minimized unless otherwise indicated.

References

1. C. Capellos and B. Bielski, *"Kinetic Systems, A Mathematical Approach"*, Wiley-Interscience, Toronto, 1972, p 134.
2. *ibid.*, p 137.
3. R.C. Weast (Editor), *"Handbook of Chemistry and Physics"*, 49th Ed., The Chemical Rubber Co., Cleveland, Ohio, 1968, p A234.
4. A.A. Frost and R.G. Pearson, *Kinetics and Mechanism"*, 2nd Ed., John Wiley and Sons, Inc., New York, N.Y., 1961, p 186.

Table 19 (cont'd)

(b) The absolute residuals, $(y_i - Y'_i)$, were minimized in this fit (see Appendix A).

(c) The standard error of the fit was determined from the absolute residuals.

APPENDIX C

Derivations of the Rate Laws for the Mechanisms in Chapter II

Scheme 8

The mechanism in Scheme 8 can be rewritten in the general form shown in Scheme C-I.

Scheme C-I

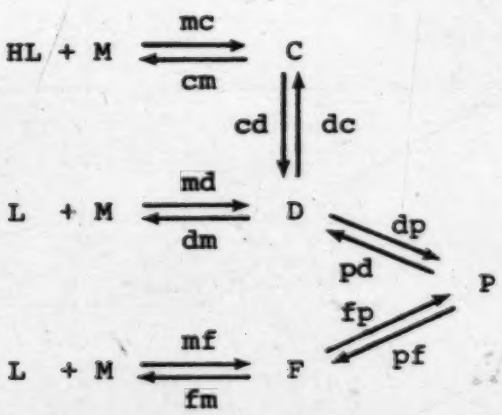

where HL and L refer to the protonated and unprotonated forms of the ligand, and the rate constants are designated by letters (e.g. for the path M → C, the pseudo-first-order rate constant is represented by mc).

The species in Scheme C-I are related by equations (C-1) to (C-5).

Detailed balancing of Scheme 8 gives

$$\frac{d[C]}{dt} = mc[M] - (cm + cd)[C] + dc[D] \quad (C\text{-}1)$$

$$\frac{d[D]}{dt} = md[M] - cd[C] + (dm+dc+dp)[D] + pd[P] \quad (C\text{-}2)$$

$$\frac{d[F]}{dt} = mf[M] - (fm + fp)[F] + pf[P] \quad (C\text{-}3)$$

leads to

$$\frac{d[P]}{dt} = \quad (C\text{-}4)$$

$$M_t = [M] + [C] + [D] + [F] + [P] \quad (C\text{-}5)$$

Since $k_{34} \simeq k_{35}$ (equation (2.10)), it follows from equation (2.25) that

$$k_{46}K_{a1}B(4) + \frac{k_{12}k_{34}K_{a3}}{k_{21}} + dp[D] - kt\ fp[F] - (pf + pd)[P] \quad (C\text{-}4)$$

$$B(2) = k_{46}K_{a1}B(4) + \frac{k_{12}k_{34}K_{a3}}{k_{21}} \quad k_{35}\left(\frac{k_{23} + k_{21}}{k_{23}k_{21}}\right)K_{a3} \quad (2.27)$$

$$k_{46}K_{a1}B(4) \leq B(4) \quad (2.28)$$

Combination of equations (2.23), (2.27) and (2.28) results in

$$B(2) \leq \left(k_{46}K_{a1} + \frac{k_{12}k_{34}K_{a3}}{k_{21}}\right)B(4) = B(1)\ B(4) \quad (2.29)$$

If the lower limit on B(2) and the upper limits on B(1) and B(4) are 6.2×10^{-10} M s^{-1}, 3.8×10^{-4} s^{-1} and 3.2×10^{-7} M respectively, then

$$6.2 \times 10^{-10} \leq B(2) > 1.5 \times 10^{-10} \geq B(1)\ B(4) \quad (2.30)$$

Clearly the results do not satisfy equation (2.29) and thus Scheme 8 is eliminated.

The validity of equation (C-6) therefore depends on the magnitudes of the individual rate constants in the specific chemical system under consideration. On the basis of the estimated rate constants given later in this appendix, the choice of C and D as the "steady-state" intermediates can be justified.

A number of approximations are necessary in order to obtain a useful solution from equations (C-1) to (C-5). The first and most familiar of these is the "steady-state" approximation, which when applied to the species C and D, gives

$$\frac{d[C]}{dt} = \frac{d[D]}{dt} = 0 \quad (C\text{-}6)$$

This approximation implies that the rates of formation of C and D equal their respective rates of decomposition.

A second possible mechanism leading to bidentate chelation of histidine is shown in Scheme 9.

In the method of linear transforms introduced in Appendix B, d/dt is replaced by the operator S. With this substitution and rearrangement of terms, equations (C-1) to (C-5) can be rewritten in matrix form as

$$\begin{bmatrix} 0 \\ 0 \\ 0 \\ 0 \\ M_t \end{bmatrix} = \begin{bmatrix} mc & cd & L3 & 0 & 0 \\ md & L2 & k_{72} & pd & C \\ mf & 0 & L6 & L4 & pf \\ 0 & 0 & k_{21} & fp & L5 \\ 1 & 1 & k_{23} & 1 & 1 \end{bmatrix} \begin{bmatrix} M \\ C \\ D \\ F \\ P \end{bmatrix} \qquad \text{(C-7)}$$

where

$$\text{OImN} + M \underset{k_{34}}{\overset{k_{43}}{\rightleftharpoons}} \text{M–OImN} \underset{k_{53}}{\overset{k_{35}}{\rightleftharpoons}} \text{M(O,N)–Im} \qquad \text{(C-8)}$$

The histidine species (OImHNH, OImNH and OImN) and V are represented in this scheme by OImHNH , OImNH and OImN respectively.

$$L2 = -(cm + cd) \qquad \text{(C-9)}$$

$$L4 = -(S + fm + fp) \qquad \text{(C-10)}$$

$$L5 = -(S + pf + pd) \qquad \text{(C-11)}$$

$$L1 = L6 = 0 \qquad \text{(C-12)}$$

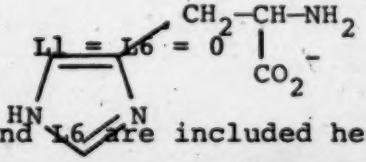

The terms L1 and L6 are included here for convenience in the later discussion of Scheme 9. From equation (C-7), the solution for [M] is given by Cramer's Rule as

$$[M] = \frac{M_t (cof)_{51}}{|A|} \qquad \text{(C-13)}$$

In contrast to Scheme 8, the species (OImN) is included in this case because it can lead directly to the

final product. It is assumed, however, that binding with (OImN) occurs preferentially at the carboxylate oxygen because of its negative charge.

Comparison shows that the rate constants k_{12} and k_{27} in Scheme 9 correspond to k_{23} and k_{32} in Scheme 8, and thus $k_{12}/k_{27} = K_{a2}/(H^+)$. Likewise,

$$k_{72} = k_1[H_2O] + k_2[OImNH] + k_3[OH^-] \simeq k_1[H_2O] \qquad (2.31)$$

Since the rate constants k_{23} and k_{32} in Scheme 9 govern the transfer of the amine proton rather than the imidazole proton, a unique evaluation is required. The acid dissociation constant of the amine proton in the species M–OImNH is defined by $K_{a4} = k_{23}(H^+)/k_{32}$. The value of K_{a4} is estimated to be less than 7×10^{-9} M, by comparison with the species $(NH_3)_5Co{-}OOCCH_2NH_3$ discussed in the introduction, and k_{32} is $\simeq 10^{-10}$ M. The terms in equation (2.31) can now be evaluated in the manner described previously. In this analysis, $k_1[H_2O] = k_{-1}K_{a4}$ and since $k_{-1} \simeq 10^{-1}$ s^{-1}, it follows that $k_1[H_2O] \simeq 10^{-10}$ M s^{-1}. Since $k_2K_{a1} \simeq 2 \times 10^{-4}$ M s^{-1}, and $k_{21} \simeq 10^4$ s^{-1}, it is easily shown that $k_{21} > k_{23}$ in the pH range of this study.

where $|A|$ is the determinant of the coefficient matrix A, (equation (C-7)) and $(cof)_{51}$ is the cofactor of the element a_{51} (fifth row; first column) in the matrix A.

The cofactor consists of the elements in rows 1,2,3,4 and columns 2,3,4,5 of A. Expansion of equation (C-13) gives an expression of the general form-

$$\frac{[M]}{M_t} = \frac{a^2 + bs + c}{s^2 + ps + q} \equiv \frac{(s+\alpha)(s+\beta)}{(s+\gamma)(s+\delta)} \qquad (C\text{-}14)$$

From a table of transforms and originals,[1] equation (C-14) can be expressed as

$$\frac{[M]}{M_t} = f_1 + f_2\, e^{-\gamma t} + f_3\, e^{-\delta t} \qquad (C\text{-}15)$$

where f_1 and f_2 and f_{32} are constants, and γ and δ are the roots of the quadratic equation in the denominator of (C-14).

Comparison of equations (C-13) and (C-14) shows that the expressions for γ and δ require the solution of the determinant of A. The complete expressions for a, b and c in equation (C-14) were determined with the aid of the computer program *REDUCE2,[2,3] and are shown on the following page.

118

The ligand species $[H_2L]$, $[HL]$ and $[L]$ in equation (C-36) of Appendix C are defined by

$$[H_2L] = \frac{(H^+)^2}{A} L_t \quad , [HL] = \frac{K_{a1}(H^+)}{A} L_t \quad , [L] = \frac{K_{a1}K_{a2}}{A} L_t \qquad (2.33)$$

where $A \equiv \{K_{a1} + (H^+)\}\{K_{a2} + (H^+)\}$. With these definitions, and for k_{21} to k_{23}, equations (C-35) and (C-36) can be rewritten to give

SCHEME 8

$$k_f = \frac{\left\{\frac{k_{35}K_{a1}}{(k_{35}+k_{34}+k_{32})}\left\{\frac{k_{87}K_{a3}}{k_{78}K_{a1}} k_{32}K_{a4} + k_{43}K_{a2}(H^+)\right\} + \frac{(k_{78}+k_{72})}{k_{78}k_{72}} K_{a3}\left(k_{12}k_{32}K_{a4} + k_{21}k_{43}K_{a2}\right)\right\}}{\{K_{a1}+(H^+)\}\{K_{a2}+(H^+)\}\left\{(H^+) + \frac{k_{21}(k_{78}+k_{72})}{k_{78}k_{72}} K_{a3}\right\}} \qquad (2.34)$$

SOLUTION FOR

and

$$k_r = \frac{k_{23}(k_{34}+k_{32})}{(k_{35}+k_{34}+k_{32})} \qquad (2.35)$$

Equations (2.35) and (2.34) combine to give the general expression

$$k_{exp} = \frac{\left\{P(1)(H^+) + P(2)\right\}L_t}{\{K_{a1}+(H^+)\}\{K_{a2}+(H^+)\}\{P(4)+(H^+)\}} + P(5) \qquad (2.36)$$

A least-squares fit of the data in Table 18 to equation (2.36) gave "best-fit" values of the parameters as listed in columns C and D of Table 19. Substitution of the result of detailed balancing ($k_{87}K_{a3}/k_{78} = k_{12}K_{a1}/k_{21}$) shows that equation (2.34) predicts $P(1) = P(2)/P(4)$. If the lower limits on $P(1)$ and $P(4)$ are 1.0×10^{-9} M and 6.0×10^{-7} M respectively, and if $P(2) < 9.0 \times 10^{-17}$ M^2, then $P(1) > 1.0 \times 10^{-9} \times 1.5 \times 10^{-10}$ or $P(2)/P(4)$.

It is concluded that equation (2.34) is inconsistent with the experimental results in Table 18, and therefore Scheme 9 is eliminated as a possible mechanism for the reaction of bisdiimidato NiII(oxalate)$_2^{+2}$.

All of the reactions studied in this present work follow an experimental rate law of the form

$$\frac{[M]}{M_t} = B\, e^{\{-k_{exp}\, t\}} \qquad \text{(C-20)}$$

It will be assumed that the observed rate coefficient k_{exp} corresponds to the smaller root γ, and thus $k_{exp} = c/b$. The validity of the binomial approximation will be considered later in this appendix, after the expressions for a, b, and c have been simplified.

Noting that the rate constants mc, md, and mf are dependent on the concentrations of the ligand

The expressions for γ and δ in equation (C-14) are given by

$$\gamma = \frac{-b + (b^2 - 4ac)^{\frac{1}{2}}}{2a} \qquad \text{(C-16)}$$

$$\delta = \frac{-b - (b^2 - 4ac)^{\frac{1}{2}}}{2a} \qquad \text{(C-17)}$$

If $4ac/b^2 << 1$, then equations (C-16) and (C-17) can be simplified by the binomial approximation to give

$$\gamma \simeq \frac{c}{b} \qquad \text{(C-18)}$$

$$\delta \simeq -\frac{b}{a} - \frac{c}{b} \simeq -\frac{b}{a} \qquad \text{(C-19)}$$

The third mechanism to be considered for the reaction of histidine with $NiTRI(OH_2)_3^{+2}$ is shown in Scheme 10.

Scheme 10

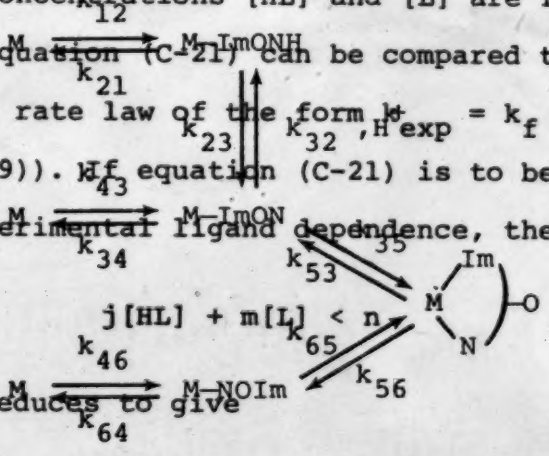

The ligand concentrations [HL] and [L] are functions of L_t, so equation (C-21) can be compared to the experimental rate law of the form $k_{exp} = k_f L_t + k_r$ (equation (2.9)). If equation (C-21) is to be consistent with the experimental ligand dependence, then

$$j[HL] + m[L] < n \qquad \text{(C-22)}$$

and (C-21) reduces to give

$$\frac{c}{b} = \frac{d[HL] + f[L] + g}{n} \qquad \text{(C-23)}$$

The symbols $_{ImONH}$ and ImON represent the histidine species IV and V shown previously.

Further simplification of the expressions for d, f, g and h requires estimates of the magnitudes of the individual rate constants. An interchange of symbols is appropriate for the following discussion, since these estimates refer specifically to Scheme 8 rather than to the general Scheme C-1.

As noted in the introduction to Chapter II, the S_NIP mechanism places definite upper limits on the rates of substitution reactions involving water as the leaving group. Specifically, for the reactions governed

terms in equation (2.14) as previously described, with $k_1[H_2O] = k'_1$, $k_{-1} = k'_{-1}$, and k_{a4} in Scheme 8 it is expected that the $k_{23} = k_3[OH^-] \gtrsim 200\ s^{-1}$ in the experimental pH range. It follows that $k_{21} \lesssim k_{23}$ in Scheme 10.

The kinetic analysis of Scheme 10, as described in Appendix C, leads to equations (C-43) and (C-44), which can be rearranged to give

$$k_f = \frac{\left(\frac{k_{12}k_{35}K_{a4}}{k_{21}} + k_{46}K_{a2}\right)K_{a1}(H^+) + \frac{(k_{43}+k_{46})k_{35}K_{a2}K_{a1}}{k_{21}}}{\{K_{a1}+(H^+)\}\{K_{a2}+(H^+)\}\left(\frac{k_{35}K_{a4}}{k_{21}}+(H^+)\right)} \qquad (2.38)$$

and

$$k_f = \frac{\left(\frac{k_{53}K_{a4}}{k_{21}}\right)K_{a1}(H^+) + k_{64}K_{a1}K_{a2}}{\{K_{a1}+(H^+)\}\{K_{a2}+(H^+)\}} + \frac{k_{56}(H^+)}{\left(\frac{k_{35}K_{a4}}{k_{21}}+(H^+)\right)} \qquad (2.39)$$

Equations (2.38) and (2.39) may be slightly simplified to give the general equation

$$k_{exp} = \frac{P_1(H^+) + P_2}{\{K_{a1}+(H^+)\}\{K_{a2}+(H^+)\}} + \frac{P_3(H^+)}{\{K_{a1}+(H^+)\}\{K_{a2}+(H^+)\}} + P_4(H^+) \qquad (2.40)$$

Comparison of equation (2.40) with (2.38) and (2.39) shows that

in the main text, it is likely that $k_{23} \simeq k_{32} \simeq k_{34}$. These

By k_{-1}, k_{a4}, and k_{46} in Scheme 8 it is expected that the outer sphere formation constants will be less than 1 M^{-1}.

Since the rate constant for water exchange on $NiTRI(OH_2)_3^{+2}$ is $3.8 \times 10^4\ s^{-1}$, an upper limit of $\sim 4 \times 10^4\ M^{-1}s^{-1}$ is predicted for k_{12}, k_{43} and k_{46} from the product $K_{os}k_{ex}$. Previous results[4,5] for reactions of $Ni(OH_2)_6^{+2}$ with unidentate ligands indicate that $k_{12} \simeq 5 \times 10^3\ M^{-1}s^{-1}$, and $k_{43} \simeq k_{46} \simeq 10^4\ M^{-1}s^{-1}$. The rate constants k_{35} and k_{65} may be as large as the water exchange rate constant and still be consistent with a dissociative mechanism. However, steric or entropy effects might inhibit chelate ring-closure, thus decreasing k_{35} and k_{65}.[4]

Hoffman[6] has observed a correlation between $k_t = pK_a$ of certain carboxylic acid ligands and the rates of decomposition of their respective nickel(II) complexes. These results predict $k_{21} \simeq k_{34} \simeq 10^4\ s^{-1}$. The rate constant k_{56} may be slightly smaller than k_{34} due to chelation effects, whereas k_{53} and k_{64} will likely have much lower values of $\sim 5\ s^{-1}$ as found for the decomposition of the imidazole complex of nickel(II).[5]

From these approximations, the rate constants in Scheme 8 are predicted to have magnitudes in the order $k_{21} \simeq k_{34} \simeq k_{56} \simeq k_{35} \simeq k_{65} \gtrsim k_{43} \simeq k_{46} \simeq k_{12} \gtrsim k_{64} \simeq k_{53}$. In addition, as shown

estimates allow simplification of the complete computer-derived expressions to give

$$P(2) = \left(k_{12}k_{35}K_{a4} + k_{46}K_{a2}\right) K_{a1} \qquad (2.41)$$

$$P(2) = \frac{(k_{43} + k_{46})\, k_{35}K_{a4}}{k_{21}}\, K_{a1}K_{a2} \qquad (2.42)$$

$$P(4) = \frac{k_{36}K_{a4}}{k_{21}} \qquad (2.43)$$

$$P(5) = k_{53} + k_{46}\left((k_{23} + k_{21})(k_{35} + k_{34}) + k_{32}k_{21}\right)[L] + (k_{64}k_{56} + k_{65}k_{53})\left(k_{34}(k_{23} + k_{21}) + k_{32}k_{21}\right) \qquad (2.44)$$

The results obtained by fitting the data in Table 18 to equation (2.40) are summarized in column E of Table 19. As found for the similar fit to equation (2.36), the value of P(2) is poorly defined, and the results show that P(2) < P(1)(H$^+$) over most of the pH range of the data. Substitution of equation (2.43) into (2.41) and (2.42) gives

$$P(1) = \left(k_{12}P(4) + k_{46}K_{a2}\right) K_{a1} \qquad (2.45)$$

and

$$P(2) = (k_{43} + k_{46})\, K_{a1}K_{a2}P(4) \qquad (2.46)$$

If the second term on the right-hand side of equation (2.45) dominates, then $k_{46} = P(1)/K_{a1}K_{a2} = 2.9 \times 10^6 M^{-1}s^{-1}$. This value is much greater than the estimate determined in Appendix C, and thus is inconsistent with the S_N1IP mechanism. On the other hand, if $P(1) = k_{12}P(4)\, K_{a1}$,

Evaluation of a, b and c using the estimates of the rate constants confirms that $4ac/b^2 << 1$ as assumed previously.

then $k_{1a} = (3.2 \pm 0.4) \times 10^3 M^{-1} s^{-1}$. This value is in good agreement with the predicted value in Appendix C.

From equation (2.46), a value of $(k_{43} + k_{46}) = (5.3 \pm 4) \times 10^4 M^{-1} s^{-1}$ can be calculated from the parameter P(2). This result is also consistent with the estimates in Appendix C.

If $k_{35} = 4 \times 10^4 s^{-1}$, $k_{2cd} = 5 \times 10^{-1}$, and $K_{a4} = K_{a2}$, then P(4) has a predicted value of $4 \times 10^{-6} M$. The experimental value of $5.2 \times 10^{-6} M$ is consistent within the error limits of the estimate. Likewise, the result that $k_{53} = 0.37\ s^{-1}$ is in reasonable agreement with the estimate in Appendix C.

It is apparent from this analysis that the kinetic data for the reaction of $NiTRI(OH_2)_3^{+2}$ with histidine can be successfully interpreted by Scheme 10, since the parameters obtained are consistent with each other and with expectation. However, the uncertainty in P(2) implies that the k_{43} and k_{46} paths contribute very little to k_{exp}. This observation, along with the results of the nmr study to be presented later, prompted a reappraisal of the data in terms of the modified mechanism shown in Scheme C-II.

Scheme 9

Scheme 9 can be written in the general form shown in Scheme C-II.

Scheme C-II

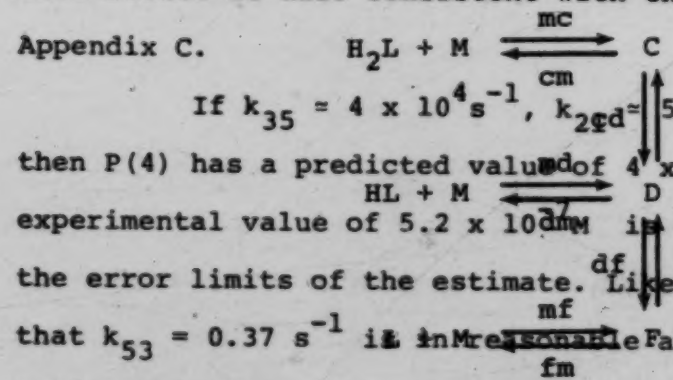

The kinetic analysis of this scheme is completely analogous to the previous treatment of Scheme C-I. The coefficient matrix A in equation (C-7) must be modified for application to Scheme C-II, using equations (C-27) to (C-33).

$$L1 = -(S + dm + dc + df) \quad \text{(C-29)}$$

$$L4 = -(fm + fd + fp) \quad \text{(C-30)}$$

$$L5 = -(S + pf) \quad \text{(C-31)}$$

Scheme 11

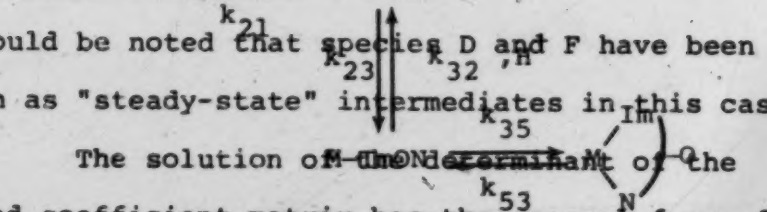

It should be noted that species D and F have been chosen as "steady-state" intermediates in this case.

The solution of the determinant of the revised coefficient matrix has the general form of equation (C-14), and thus the smaller root $\gamma = c/b$. The complete computer-derived expressions for a, b, and c are shown on the following page.

By analogy with the previous estimates of the rate constants in Scheme 8, the rate constants in Scheme 9 can be placed in the order $k_{12} \approx k_{23} \approx k_{35} > k_{32} \approx k_{53} \approx k_{34} \approx k_{35} > k_{43} \approx k_{12} \approx k_{87} > k_{53}$. From the discussion in the main text $k_{21} \approx k_{53}$ and thus $k_{27} \approx k_{73}$, whereas $(H^+) >> K_{a4}$ and so $k_{32} >> k_{23}$. With these estimates of the rate constants in Scheme 9, the complete computer-derived expressions for a, b and c simplify to give

$$k'_{12} = k_{12}[\text{ImONH}] = \frac{k_{12}K_{a1}t}{K_{a1} + (H^+)} \qquad (2.48)$$

Equation (2.48) is valid since $(K_{a2} + (H^+)) \approx (H^+)$ in the pH range of the kinetic study. The denominator of (2.47) is analogous to equation (C-43) derived for Scheme 10,

$$b = (k_{35} + k_{34})\left((k_{78} + k_{72})(k_{23} + k_{21}) + k_{27}k_{78}\right) \qquad (C\text{-}35)$$

except that the ligand dependent terms present in the complete expression (see computer output) have been dropped in the derivation of equation (C-43) because they do not appear in the experimental rate law. However,

$$+ k_{32}\left((k_{78} + k_{72})k_{21} + k_{27}k_{78}\right)$$

and

$$k_{exp} = \frac{k_{12}k_{23}k_{35}\{k_{32}k_{53} + k_{34}k_{43} + k_{34}k_{53} + k_{43}k_{53}\} + k_{12}k_{21}k_{53}\{k_{35} + k_{34} + k_{43}\}}{k_{32}k_{12} + k_{21}k_{53} + k_{35}k_{12} + k(H^+) + k_{a3}} \qquad (2.47)$$

where

$$k_{27} = k_{35}k_{53} + k_{34}k_{43} + k_{34}k_{53} + k_{43}k_{53} \qquad (C\text{-}32)$$

$$k_{21} = k_{35}k_{53} + k_{34}k_{43} + k_{34}k_{53} + k_{43}k_{53} \qquad (C\text{-}33)$$

$$k_{32} = k_{35}k_{53} + k_{34}k_{43} + k_{34}k_{53} + k_{43}k_{53} \qquad (C\text{-}34)$$

evaluation of k'_{12} with $k_{53} = 3 \times 10^3 M^{-1} s^{-1}$, $L_t < 2 \times 10^{-3} M$, $pK_{a1} = 6.2$ and $6 < pH < 7$ shows that k'_{12} is comparable to the expected value of k_{21}. Since the prior analysis gave $k_{53} = 0.37\ s^{-1}$, then it is likely that $k'_{12} > k_{53}$. Evaluation described previously indicated that $k_{23} \simeq k_3[OH]$, and therefore $k_{23} > k'_{12}$ for $6 < pH < 7$. With these approximations, equation (2.48) can be reduced and rearranged to give

SOLUTION FOR SCHEME 9

$$k_{exp} = \frac{k'_{12}\left(1 + \frac{k_{53}(H^+)}{k_{35}K_{a4}}\right) + \frac{k_{21}k_{53}(H^+)}{k_{35}K_{a4}}}{\left(\frac{k'_{12} + k_{21} + k_{53}}{k_{35}K_{a4}}\right)(H^+) + 1} \qquad (2.49)$$

A consideration of Scheme 11 shows that the second term in the numerator of equation (2.49) can also be written as

$$\frac{[M\text{—ImONH}^+]}{\left[M\text{—}\overset{\overset{Im}{|}}{N}\text{—O}\right]} = \frac{k_{53}(H^+)}{k_{35}K_{a4}} = F \qquad (2.50)$$

Since [M—ImONH] >> [M-ImONP], the ratio F indicates the completeness of ring-closure. In the analysis of Scheme 10, it was implicitly assumed that F<<1 (i.e. complete ring-closure). The nmr results to be discussed later imply that ring-closure may not be complete in some of

the systems under discussion. In addition, note that F increases with decreasing pH, implying that ring-closure is less favorable at low pH. These considerations indicate that equation (2.49) is likely to give a more meaningful interpretation of the kinetic behavior than was obtained from equations (2.38) and (2.39).

$$c = k_{35}\left\{k_{87}k_{72}k_{23}[H_2L] + k_{12}k_{23}(k_{78}+k_{72})[HL] + k_{43}\left[(k_{78}+k_{72})(k_{23}+k_{21}) + k_{27}k_{78}\right][L]\right\} + k_{53}\left\{(k_{34}+k_{32})(k_{78}+k_{72})k_{21} + k_{27}k_{78}\right\} \qquad \text{(C-36)}$$

A computer fit of the results in Table 18 to equation (2.49), with $pK_{a1} = 6.18$, gave $k_{12}=(3.41\pm0.5)\times 10^{2}$ $M^{-1}s^{-1}$, $k_{21}=35\pm4\ s^{-1}$, $k_{35}K_{a4}=(2.00\pm0.1)\times 10^{-8}$ M s and $k_{53}=0.29\pm0.1\ s^{-1}$. The error estimates are approximate 95% confidence limits. With these "best-fit" parameters, equation (2.49) gives calculated rate coefficients, k_{cald}, which are compared to the experimental values in Table 18. The results given above are similar to those of the previous analysis by equation (2.40), except that k_{21} has now been evaluated separately. The value of $k_{21} = 35\ s^{-1}$, although reasonable, is larger than was predicted in Appendix C. This explains why the k_{12} term in the denominator of equation (2.49) was not observed in the experimental rate law.

Evaluation of a, b and c using the estimated rate constants confirms that $4ac/b^2 << 1$, and thus $k_{exp} \cong c/b$.

The reaction of $NiTRI(OH_2)_3^{+2}$ with 3-methylhistidine

Scheme 10

The observed pseudo-first-order coefficients (k_{exp}) for the reaction of $NiTRI(OH_2)_3^{+2}$ with 3-methylhistidine (VI) are listed in Table 20.

Scheme 10 has the same general form as Scheme C-I, so equations (C-1) to (C-5) are applicable. However, a consideration of the nature of the bonds formed in Scheme 10 leads to a different choice of "steady-state" intermediates. In Scheme 10, k_{21} and k_{34} are expected to be considerably smaller than their counterparts in Scheme 8. Also, the amine proton is much less acidic than the imidazole proton. Therefore, for the kinetic analysis of Scheme 10, the "steady-state" approximation will be applied to the species M—ImON and M—NOIm, which correspond to D and F in Scheme C-I. The coefficient matrix in equation (C-7) must then be modified by replacing equations (C-7) and (C-10) with

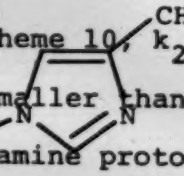

VI

$$L2 = -(s + cd + ep) \qquad \text{(C-37)}$$

$$L4 = -(fm + fp) \qquad \text{(C-38)}$$

The complete computer-derived expressions for b and c which result from this revised analysis are completely identical to those given previously for Scheme 8. However, the expression for a is now given by

$$a = dmfp(dp+dc+dm) + ep(fp+fm+dp+dc+dm) \qquad \text{(C-39)}$$

The similarity in the structure and pK_a values of 3-methylhistidine and histidine should lead to a similarity in their mechanisms, and comparison of the k_{exp} values in Tables 18 and 20 supports this proposal. The data for VI give linear plots of k_{exp} *versus* total ligand concentration (L_t) at fixed pH values of ~6.25, ~6.42, and ~6.75, with intercepts of about 0.1 s^{-1} as observed for histidine.

A computer fit of the data in Table 20 to equation (2.40) with K_{a1} fixed at 1.62×10^{-6} M gives $P(1) = 2.65 \pm 0.3 \times 10^{-9}$ M s^{-1} and $P(2) \leq 5 \times 10^{-17}$ M^2 s^{-1}. The error limits on the latter parameter show that it is not significantly different from zero. This

Table 20

Observed Rate Coefficients for the Reaction of $NiTRI(OH_2)^{+2}$ with 3-methylhistidine

pH	$10^2 L_t$, M	k_{exp}, s^{-1}	k_{cald}[b], s^{-1}
The ligand species HL and L in Scheme (C-III)			
5.61	1.85	0.728±.04	0.728
5.82	1.85	1.20±.07	1.16
6.01[c]	6.80	5.73±.3	5.13
6.05	1.85	1.96±.07	1.89
6.14	1.99	2.40±.2	2.38
6.24[c]	6.80	7.01±.3	8.16
6.26	0.920	1.36±.05	1.47
6.27	1.84	2.75±.2	2.78
6.41[c]	6.80	11.8±.3	10.8
6.42	0.920	1.76±.08	1.83
6.43	1.84	3.43±.08	3.51
6.51	1.99	4.54±.2	4.16
6.75	0.920	2.47±.1	2.52
6.75	1.84	4.94±.3	4.89
6.75[c]	6.80	14.8±.5	16.4
6.76[c]	6.80	18.8±.8	16.5
6.94[c]	6.80	19.6±.7	19.1
7.01	1.99	6.40±.3	6.23

In Scheme 10, the rate constants are expected to have values in the order $k_{35} \simeq k_{65a} > k_{43} \simeq k_{46} \simeq k_{12} > k_{64} \simeq k_{56} \simeq k_{53}$ by analogy with the discussion of the rate constants in Scheme 8. Estimates of k_{32}, k_{23}, k_{21} and k_{34} are discussed in the main text.

The ligand species HL and L in Scheme (C-III) are related to L_t by

$$[HL] = \frac{K_{a1}(H^+)L_t}{(K_{a1}+(H^+))(K_{a2}+(H^+))} \quad \text{(C-40)}$$

and

$$[L] = \frac{K_{a1}K_{a2}L_t}{(K_{a1}+(H^+))(K_{a2}+(H^+))} \quad \text{(C-41)}$$

With the approximations and substitutions given above, the complete computer-derived expressions for a, b and c appropriate to Scheme 10 can be simplified and rearranged to give

$$a = k_{65}(k_{32} + k_{35}) \quad \text{(C-42)}$$

$$b = k_{65}(k_{23}k_{35} + k_{32}k_{21}) \quad \text{(C-43)}$$

Table 20 (cont'd)

$$c = \frac{k_{65}}{(K_{a1} + (H^+))(K_{a2} + (H^+))}\Big(k_{12}k_{23}k_{35}K_{a1}(H^+) + k_{46}(k_{23}k_{35} + k_{32}k_{21})K_{a1}K_{a2} + k_{65}k_{53}k_{32}k_{21}\Big)$$

(a) The value of k_{exp} reported is the average of at least 9 identical runs at 25°. I= 0.10M($LiClO_4$). Error limits given are one standard deviation. [NiTRI] = (0.8-2.0) x 10^{-4}M after mixing. Bromothymol blue (BTB)(2.5 x 10^{-5}M) and PIPES buffer (6 x 10^{-4}M) were used unless otherwise stated.

(b) Calculated using equation (2.49) and the "best-fit" values given in the text.

(c) No buffer included.

(C-44)

Evaluation of a, b and c using the estimates of the rate constants confirms that $4ac/b^2 << 1$, and thus $k_{exp} = c/b$.

References

1. R.C. Weast (Editor) *"Handbook of Chemistry and Physics"*, 49th Ed., The Chemical Rubber Co., Cleveland, Ohio, 1968, p A234.
2. A.C. Hearn, *"A Program Designed for General Algebraic Manipulations"*, *REDUCE2, on file at the Univ. of Alberta, Edmonton, Alta. (see Computing Services memo M278)
3. A.C. Hearn, *REDUCE2 User's Manual, 2nd Ed., Univ. of Utah, Salt Lake City, Utah.
4. K.Kustin and J. Swinehart, *Prog.Inorg.Chem.*, 13, 107 (1970).
5. R.G. Wilkins, *Acc.Chem.Res.*, 3, 408 (1970).
6. H. Hoffman, *Ber.Bunsenges.Phys.Chem.*, 73, 432 (1969).